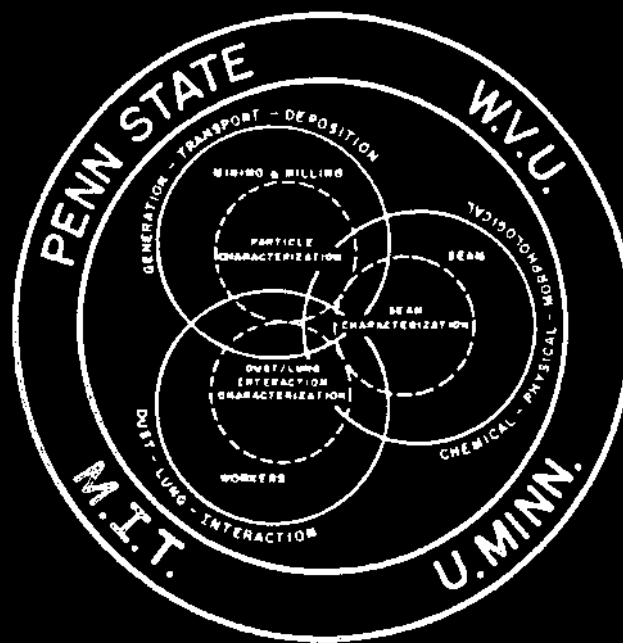


GENERIC MINERAL TECHNOLOGY CENTER FOR RESPIRABLE DUST

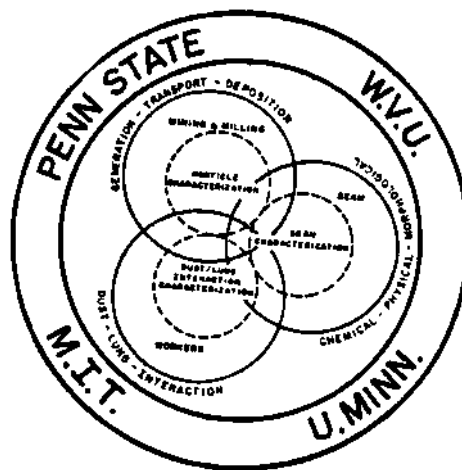
Edited by
Robert L. Frantz
Raja V. Ramani



PUBLICATIONS
1985

GENERIC MINERAL TECHNOLOGY CENTER FOR RESPIRABLE DUST

The Pennsylvania State University
West Virginia University
University of Minnesota
Massachusetts Institute of Technology



PUBLICATIONS 1985

Submitted To
Office of Mineral Institutes
U.S. Bureau of Mines
Washington, D.C.

June 30, 1988

PUBLICATIONS

PRODUCED IN

THE GENERIC MINERAL TECHNOLOGY CENTER FOR RESPIRABLE DUST

IN THE YEAR

1985

Edited by
Robert L. Frantz
Raja V. Ramani

PENNSTATE



WEST VIRGINIA UNIVERSITY



Published Volumes of the Respirable Dust Center

VOLUME 1	Status Report, 1984-1988
VOLUME 2	Report to the Committee on Mining and Mineral Resources Research, 1987
VOLUME 3	Publications, 1984
VOLUME 4	Publications, 1985
VOLUME 5	Publications, 1986
VOLUME 6	Publications, 1987
CONFERENCE PROCEEDINGS	Coal Mine Dust Conference West Virginia University Morgantown, West Virginia October 1984
CONFERENCE PROCEEDINGS	Respirable Dust in the Mineral Industries: Health Effects, Characterization and Control The Pennsylvania State University University Park, Pennsylvania October 1986

CONTENTS

	Page
Foreword	vi
National Plan	viii
Advisory Council Members	ix
I. Control of Dust and Particulate Matter Generation	1
1. Characterizing Fracture Types of Rock/Coal Subjected to Quasi-Static Indentation Using Acoustic Emission Technique	3
<i>A. Wahab Khair</i> , Department of Mining Engineering, College of Mineral and Energy Resources, West Virginia University, Morgantown, WV 26506. Presented at the Second International Conference on Acoustic Emission, Morgantown, WV, 1985, pp. 1-6. (WV-1)	
2. Correlation of Fragment Size Distribution and Fracture Surface in Coal Cutting Under Various Conditions	9
<i>A. Wahab Khair and W. M. DeVilder</i> , Department of Mining Engineering, West Virginia University, Morgantown, WV 26506, pp. 1-47. (WV-1)	
3. Coal Fracture Analysis Using Two Simultaneous Wedge Indicators and Laser Holographic Interferometry	68
<i>Richard D. Begley</i> , Fairmont State College, Division of Technology, Fairmont, WV 26554, and <i>A. Wahab Khair</i> , Department of Mining Engineering, College of Mineral and Energy Resources, West Virginia University, Morgantown, WV 26506. Presented at the 4th International Congress on Applications of Lasers and Electro Optics, San Francisco, CA, November 10-14, 1985, pp. 10-8. Sponsored by the Laser Institute of America. (WV-1)	
4. The Effect of In-Situ and Operating Parameters on Fragmentation of Coal	68
<i>A. Wahab Khair and Nagendra P. Reddy</i> , Department of Mining Engineering, College of Mineral and Energy Resources, West Virginia University, Morgantown, WV 26506. Presented at the 26th U.S. Symposium on Rock Mechanics, South Dakota School of Mines and Technology, Rapid City, SD, June 26-28, 1985, pp. 1-27. (WV-1)	
5. Mechanisms of Respirable Dust Generation by Continuous Miner	94
<i>A. Wahab Khair and M. K. Qutub</i> , Department of Mining Engineering, College of Mineral and Energy Resources, West Virginia University, Morgantown, WV 26506. Presented at the SME-AIME Fall Meeting, Albuquerque, New Mexico, October 16-18, 1985, pp. 1-14. (WV-1)	

CONTENTS

	Page
II. Dilution, Dispersion, and Collection of Dust	109
6. Behavior of Dust Clouds in Mine Airways	111
<i>R. Bhaskar and R. V. Ramani, Department of Mining Engineering, The Pennsylvania State University, University Park, PA 16802. Presented at the SME-AIME Annual Meeting, New York, NY, February 124-28, 1985, pp. 1-10. (PS-2)</i>	
III. Dust Characterization	123
7. Suppression of Inhaled Particle Cytotoxicity by Pulmonary Surfactants and Re-Toxication by Phospholipase--Distinguishing Properties of Quartz and Kaolin	125
<i>W. E. Wallace, Engineering Sciences, West Virginia University, Morgantown, WV 26506 and M. J. Keane, V. Vallyathan, P. Hathaway, E. D. Regad, V. Castranova, and F. H. Y. Greene, Appalachian Laboratory for Occupational Safety and Health Division of Respirable Disease Studies, National Institute for Occupational Safety and Health, Inhaled Particles VI - Proc. of an International Symposium organized by the British Occupational Hygiene Society, Cambridge, England, September 1985, pp. 1-19. (WV-12)</i>	
8. In Vitro Biologic Toxicity of Native and Surface-Modified Silica and Kaolin	144
<i>W. E. Wallace, Jr., V. Vallyathan, M. J. Keane, and V. Robinson, National Institute for Occupational Safety and Health, Morgantown, WV 26505 Journal of Toxicology and Environmental Health, 16:415-42224, 1985, Hemisphere Publishing Corporation. (WV-12)</i>	
IV. Dust Lung Interaction	155
9. Evaluation of the Size Distribution of Large Aerosols in an Animal Exposure Chamber	157
<i>F. Pisano, M. McCawley, D. Hinton, C. Stanley, and R. C. Lantz, West Virginia University, Morgantown, WV 26505. (WV-5)</i>	

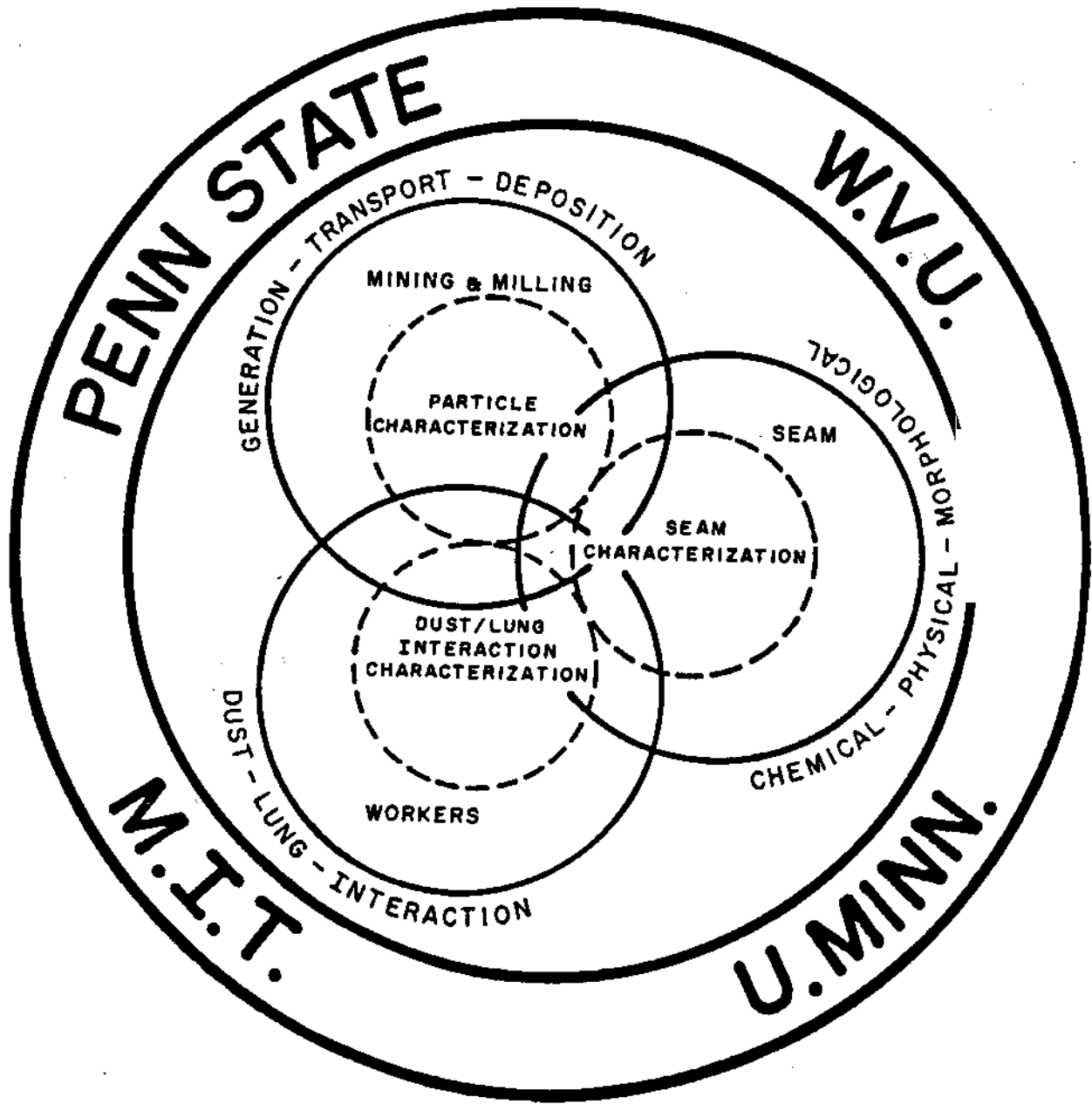
CONTENTS

	Page
V. Relationship of Mine Environment, Geology and Seam Characteristics to Dust Generation and Mobility	165
10. Coal Mine Respirable Dust	167
<i>Christopher J. Bise and Jan M. Mutmansky, Department of Mineral Engineering, The Pennsylvania State University, University Park, PA 16802. Published in Earth and Mineral Sciences, Volume 54, No. 4, Summer 1985, pp. 43-45. (PS-5)</i>	

INDEX	171
--------------	------------

Cumulative Author Index	173
Cumulative Subject Index	173

THE RESPIRABLE DUST CENTER



The Respirable Dust Center

FOREWORD

This volume contains publications resulting from respirable dust research performed in the Generic Mineral Technology Center for Respirable Dust by faculty, staff and graduate students at The Pennsylvania State University, West Virginia University, University of Minnesota, and Massachusetts Institute of Technology. These publications have appeared in scientific journals, proceedings of the national and international symposiums and meetings. Complete citations of the publications can be found in the text. The Generic Mineral Technology Center for Respirable Dust is funded by the U.S. Bureau of Mines through the Mining and Mineral Resources Research Institute Program. The opinions and conclusions expressed in the papers are those of the authors alone and do not represent the opinions of the Generic Mineral Technology Center for Respirable Dust, the Mining and Mineral Resources Research Institute Program or the U.S. Bureau of Mines. Citation of manufacturers' names in the papers were made for general information purposes, and do not imply endorsement of the products by the authors.

All of the publications in this volume are on research that has been supported by the Department of the Interior's Mineral Institute program administered by the Bureau of Mines through the Generic Mineral Technology Center for Respirable Dust under allotment grant number G1135142 or G1175142.

In addition to these papers, a dust conference was organized by the Center and held at West Virginia University in October 1984. The conference was co-sponsored by ACGIH, MSHA, NIOSH and USBM. Proceedings from this conference are available in the publication, Coal Mine Dust Conference, 1984. The generic center maintains a reference center that serves as a clearinghouse for technical information for the generic area and supplies reports on generic center accomplishments.

The support from the United States Congress for the Generic Mineral Technology Center for Respirable Dust is gratefully acknowledged. We also acknowledge and appreciate the support and inputs from USBM, NIOSH, MSHA, the Research Advisory Council, and the Committee on Mining and Mineral Resources Research which have significantly contributed to the activities of the Generic Mineral Technology Center for Respirable Dust.

Respectfully submitted,

Robert L. Frantz
Co-Director, Generic Mineral
Technology Center for Respirable Dust
Co-Editor

R. V. Ramani
Co-Director, Generic Mineral
Technology Center for Respirable Dust
Co-Editor

THE RESPIRABLE DUST CENTER
Excerpted From The

1988 UPDATE TO THE NATIONAL PLAN
FOR
RESEARCH IN MINING AND MINERAL RESEARCH

Report to:

December 15, 1987

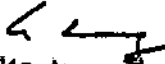
The Secretary of the Interior
The President of the United States
The President of the Senate
The Speaker of the House of Representatives

Section 9(e) of Public Law 98-409 of August 29, 1984, (98 Stat. 1536 et seq.) mandates that the Committee on Mining and Mineral Resources Research submit an annual update to the National Plan for Research in Mining and Mineral Resources: "Improving Research and Education in Mineral Science and Technology through Government-(Federal, State and Local), Industry, and University Cooperation."


Respirable Dust (centered at Pennsylvania State U. and West Virginia U., with affiliates at U. of Minnesota and Massachusetts Institute of Technology): brings together experts concerned with particles causing potentially disabling or fatal diseases, including pneumoconiosis ("black lung"), silicosis, and asbestosis, the latter of deep concern not just to workers in the mineral sector of the economy but also to the general populace.

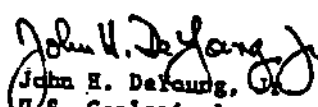
SIGNED:



Carl K. Randolph
Mining Industry

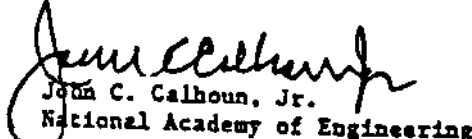

Win Aung
National Science
Foundation

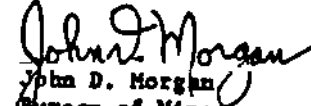

Don L. Warner
University Administrator

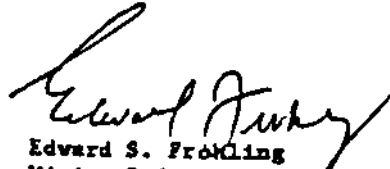

Walter R. Hibbard, Jr.
National Academy of
Sciences

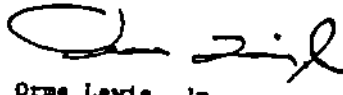

John H. DeYoung, Jr.
U.S. Geological
Survey

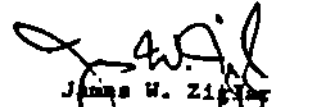

Joseph N. Crowley
University Administrator


John C. Calhoun, Jr.
National Academy of Engineering


John D. Morgan
Bureau of Mines


Edward S. Frothing
Mining Industry


Orme Lewis, Jr.
Conservation Community
COCHAIR


James W. Ziegler
Assoc. Secretary-
Water & Science
U.S. Department of
the Interior
COCHAIR

THE RESPIRABLE DUST CENTER

Generic Mineral Technology Center For Respirable Dust

RESEARCH ADVISORY COUNCIL MEMBERS

Dr. John A. Breslin
Senior Staff Physical Scientist
U.S. Bureau of Mines
2401 E Street, N.W.
Columbia Plaza
Washington, D.C. 20241
(202) 634-1220

Dr. Ronald Munson
Director, Office of Mineral
Institutes - MS 1020
U.S. Department of the Interior
2401 E Street, N.W.
Washington, D.C. 20241
(202) 634-1328

Dr. Lewis Wade
Research Director
Twin Cities Research Center
U.S. Bureau of Mines
5629 Minnehaha Avenue, S.
Minneapolis, MN 55417
(612-725-4610

Dr. John A. Campbell
Director, Engineering and
Technology Support
Kerr-McGee Corporation
P.O. Box 25861
Oklahoma City, OK 73125
(405) 270-3778

Mr. John Murphy
Research Director
Pittsburgh Research Center
U.S. Bureau of Mines
P.O. Box 18070
Pittsburgh, PA 15236
(412-675-6601

Dr. James L. Weeks, C.I.H.
Deputy Administrator for
Occupational Health
United Mine Workers of
America
900 15th Street, N.W.
Washington, D.C. 20005
(202) 842-7300

Mr. Robert E. Glenn
Director, Division of Respiratory
Disease Studies - NIOSH
944 Chestnut Ridge Road
Morgantown, WV 26505
(304) 459-5978

Dr. Kandiah Sivrajah
State Toxicologist
Room 825--Health and Welfare
Building
Harrisburg, PA 17108
(717) 787-1708

Dr. Jerome Kleinerman
Department of Pathology
Cleveland Met. General Hospital
3395 Scranton Road
Cleveland, OH 44109
(216) 459-5978

Dr. Pramod Thakur
Research Group Leader
CONOCO, Inc.
R & D Division
Route #1, Box 119
Morgantown, WV 26505
(304) 983-2251

PAST RESEARCH ADVISORY COUNCIL MEMBERS

Mr. Darrel Auch
Senior Vice President
Northern West Virginia Region
Consolidation Coal Company
P.O. Box 1314
Morgantown, WV 26507
(304) 296-3461

Dr. Thomas Falkie
President
Berwind Natural Resources
Company
Centre Square West
1500 Market Street
Philadelphia, PA 19102
(215) 563-2800

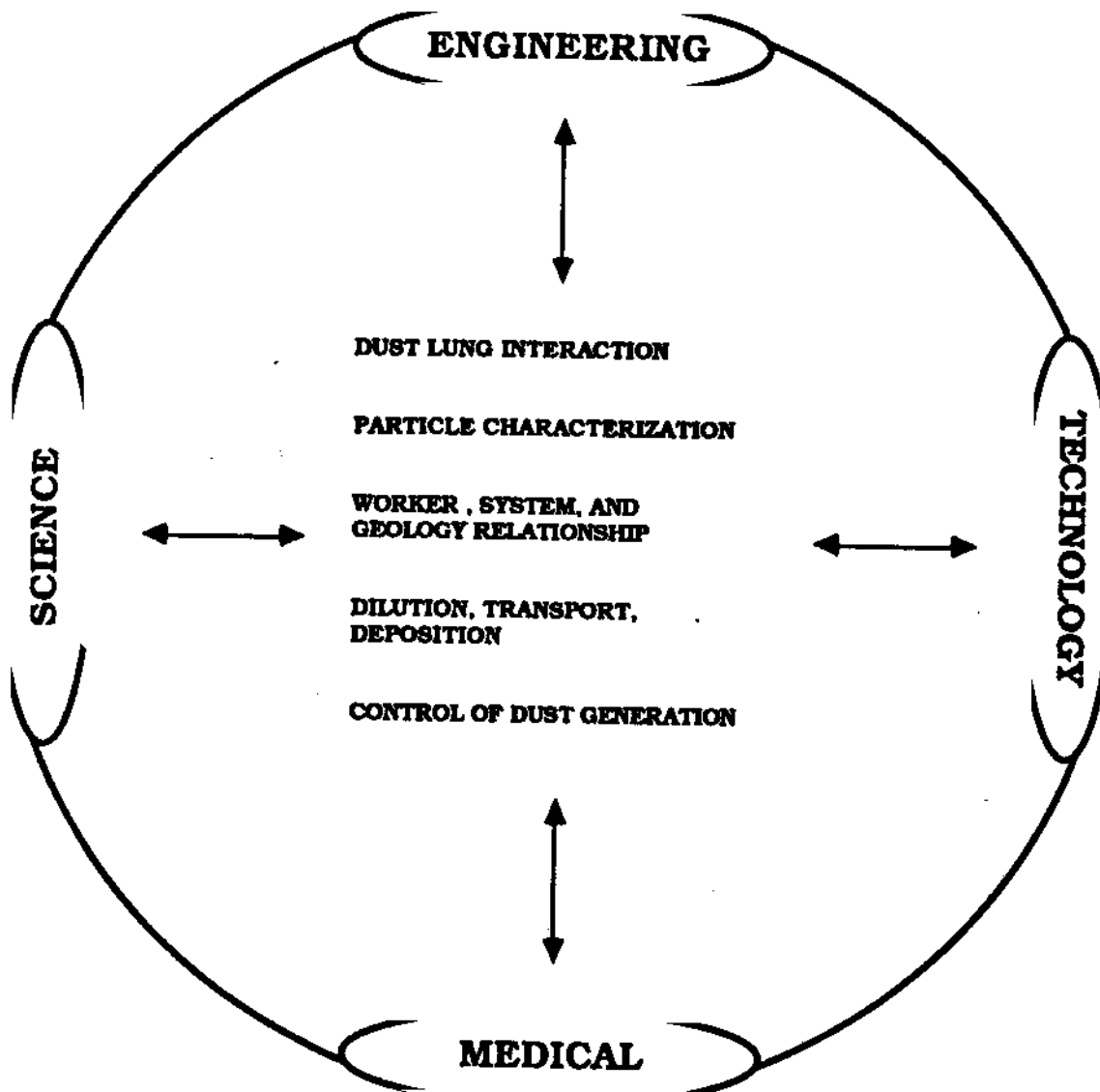
Mr. C. Wesley McDonald
Senior Vice President
(Mining)
Northern West Virginia
Region
Consolidation Coal Company
P.O. Box 1314
Morgantown, WV 26505
(304) 296-3461

Dr. J. Harrison Daniel
Program Manager, Mining
Research
Health and Safety
2401 E Street, N.W.
Washington, D.C. 20241
(202) 634-1253

Dr. Fred Kissell
Research Supervisor
Pittsburgh Safety Research Center
U.S. Bureau of Mines
4800 Forbes Avenue
Pittsburgh, PA 15213
(412) 675-6679

Dr. Donald Reid
Deputy Secretary for Public
Health Programs
Department of Health
Health and Welfare Building
P.O. Box 90
Harrisburg, PA 17108
(717) 783-8804

THE RESPIRABLE DUST CENTER



THE RESPIRABLE DUST CENTER

RESEARCH



CONTROL OF GENERATION

- Amount
- Fracture

**DILUTION,
TRANSPORT
AND
DEPOSITION**

- Concentration
- Size Consist
- Modeling

**MINE WORKER,
MINING SYSTEM,
SEAM GEOLOGY**

- Seam Sections
- Silica
- Trace Elements
- System Configuration
- Worker Location



- Coal Data Bank
- Mine Samples

**SUITE OF
GENERATED
RESPIRABLE
DUSTS**

- Anthracite
- Medium Volatile Bituminous
- High Volatile Bituminous
- Silica
- Fireclay
- Rock Dust



CHARACTERIZATION

- Size/Shape/Composition
- Surface/Functional Groups
- Particle Interaction

**DUST LUNG
INTERACTION**

- Medical/Cellular
- Medical/Animal
- Medical/Human
- Medical/Engineering



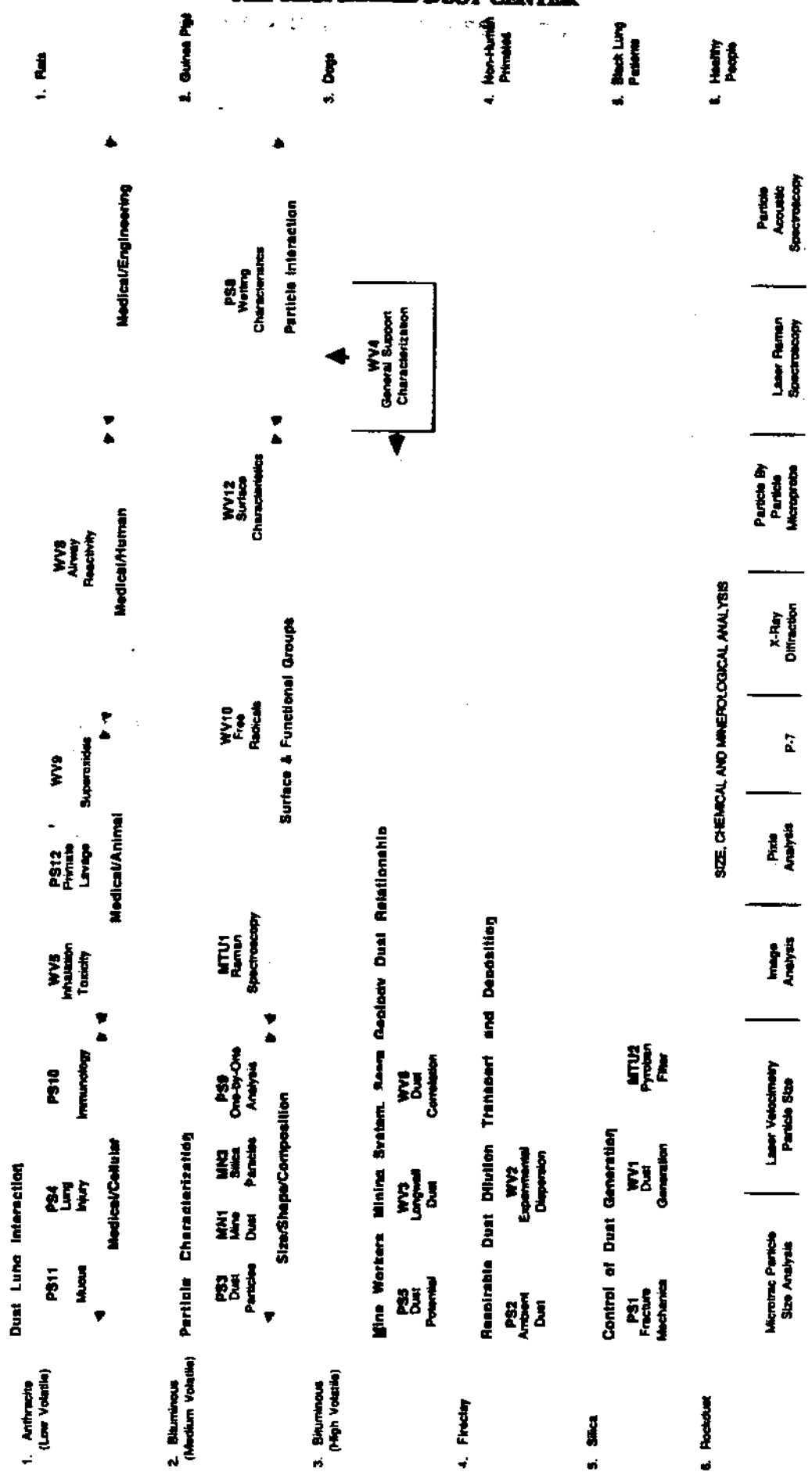
TRAINING

SUITE OF CHARACTERIZED DUST SAMPLES

SAMPLING AND DUST GENERATION METHODS



SUITE OF MEDICAL TESTS



THE RESPIRABLE DUST CENTER

The Generic Mineral Technology Center for Respirable Dust

SUITE OF CHARACTERIZED DUST SAMPLES	SAMPLING AND DUST GENERATION METHODS	SUITE OF MEDICAL TESTS
1. Anthracite (Low Volatile)	Dust/Lung Interaction	1. Rats
2. Bituminous (Medium Volatile)	Particle Characterization	2. Guinea Pigs
3. Bituminous (High Volatile)	Mine Workers. Mining System. Seam Geology Dust Relationship	3. Dogs
4. Fireclay	Respirable Dust Dilution. Transport and Deposition	4. Non-Human Primates
5. Silica	Control of Dust Generation	5. Black Lung Patients
6. Rockdust		6. Healthy People

**SIZE, CHEMICAL AND
MINEROLOGICAL ANALYSIS**

Statement of Goal

The primary goal of the Generic Mineral Technology Center for Respirable Dust is to reduce the incidence and severity of respirable dust disease through advancing the fundamental understanding of all aspects of respirable dust associated with mining and milling and the interaction of dust and lungs.

I

**Control of Dust and
Particulate Matter Generation**

CHARACTERIZING FRACTURE TYPES IN ROCK/COAL SUBJECTED TO QUASI-STATIC
INDENTATION USING ACOUSTIC EMISSION TECHNIQUE

A. Wahab Khair

Associate Professor
Mining Engineering Department
West Virginia University
Morgantown, WV 26506

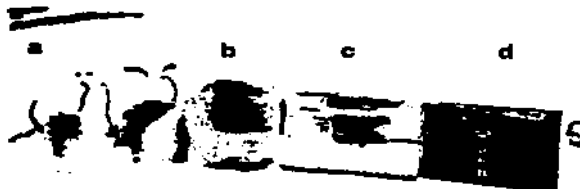
INTRODUCTION

Geologic materials emit transient noises when stressed /1/. The rate and pattern of these transient noises or acoustic emissions (A.E. hereafter) depend on the stages of deformation of the material /2/. It has been demonstrated that rock/coal fracture processes under stress consist of three distinctive stages--crack initiation, propagation and ultimate fracture--and that coalescence of numerous cracks leads to ultimate failure rather than the propagation of a single crack /2,3/. This paper presents an analysis of fracture formation in rock/coal specimens subjected to straight wedge indentors using A.E. technique.

EXPERIMENTAL STUDY

The effect of specimen geometry, wedge indenter angle, confining pressure, and material anisotropy on fracture type (tension, extension, and shear crack), fracture length, and fracture intensity were studied. Two types of material mainly Berea sandstone and Coal Berg No. 2 coal were used in this study. Prior to the experiment the mechanical properties of both sandstone and coal were determined using rectangular specimen (Figures 1 a) in standard compression tests and are given in Table 1. In this study cylindrical and rectangular specimens

Table 1. Mechanical Properties of the
Rock/Coal Materials
(1 psi = 6.89 KPa)



Material	Compressive Strength (psi)			Young's Modulus (10 ⁶ psi)			Poisson's Ratio		
	σ_x	σ_y	σ_z	ν_x	ν_y	ν_z	μ_x	μ_y	μ_z
Rock	7500	7500	9488	2.04	2.04	2.23	0.07	0.07	0.15
Coal	4688	3234	7400	0.88	1.16	0.50	0.33	0.28	0.47

x, y, and z indicates the directions perpendicular to the bedding, face cleat, and butt cleat planes, respectively.

Fig. 1. Instrumented specimens.

were first prepared to proper dimensions of 2 in. x 1.5 in. and 3 in. x 1.5 in. x 1.5 in. (5.08 cm x 3.81 cm and 7.62 cm x 3.81 cm), respectively and then instrumented with SR-4 strain gages as shown in Figure 1. The instrumented specimens were then tested under four distinct load boundary conditions as illustrated in Figure 2. During a typical experiment the instrumented specimen was placed in a specially designed loading jig (Figure 3) where a predetermined

Presented at the Second International Conference on
Acoustic Emission, Morgantown, W. Va., 1985.

THE RESPIRABLE DUST CENTER

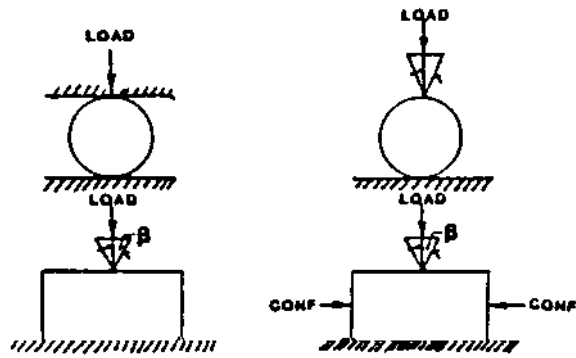


Fig. 2. Test specimens and load boundary conditions.



Fig. 3. Confining chamber and failed specimen.

lateral pressure was applied mechanically to the specimen by adjusting the inner plate of the confining chamber via screw while monitoring strains in the specimen. Using rock/coal elastic constants and measured strains, a predetermined lateral pressure was applied to the specimen. Then a vertical load was applied by the straight edge of a wedge indenter attached to the upper platen of the universal loading machine via ball and socket arrangement (Figure 4). The arrangement allowed uniform application of load in a straight line manner on the surface of the specimen. During the test a number of parameters namely strains, load and A.E. rates were recorded (Figures 5a-b).

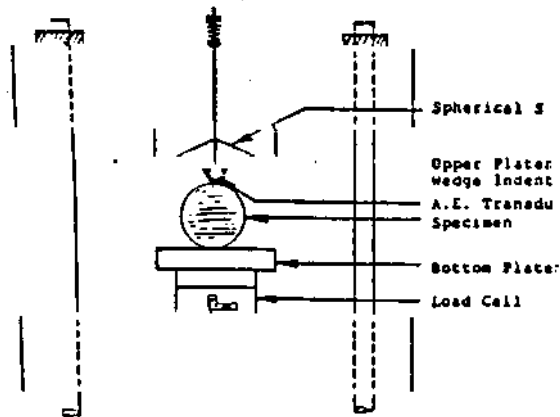


Fig. 4. Experimental setup.

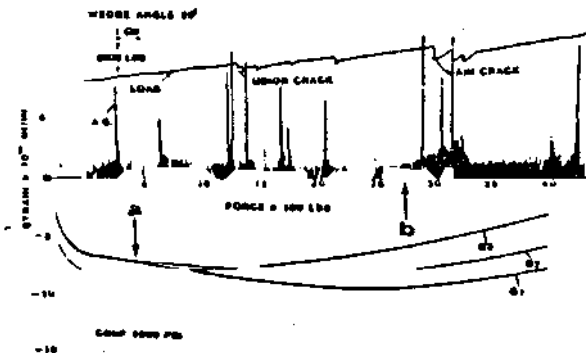


Fig. 5. a. Force-strain curve;
b. Load-A.E. rate curve.

Results

Figure 5a illustrates deformation characteristics (strains-load history) of specimen during test where gage G1 located at the edge of the specimen close to the wedge indenter and gage G3 indicates strain at the center of the specimen (Figure 1b-c). Figure 5b indicates fracture formation in the specimen as depicted by the A.E. rate (load is 2000 lb/division (907 kg/division), A.E. rate 999 counts/0.25 sec. at 68 db, chart speed is 4 cm/min). Fracture initiation and extension are exhibited by the higher rate of A.E. By adjusting the offset due to the super imposition of recorder's pens, the higher rate of A.E. coincides with drop in magnitude of load, indicating fracture propagation.

CHARACTERIZING FRACTURE TYPES IN COAL/ROCK

The larger the fracture the larger the drop in load level can be observed and that coincides with the higher rate of A.E. Rock/coal chip formation were associated with crack development in the specimen and the sizes of these chips were directly proportional to the sizes of the cracks, and therefore to the rate of A.E. A higher A.E. activity at a lower rate was indicative of micro-size crack development in the test specimen lead to the formation of fine particles (crushed material). These facts were substantiated by visual observations and photographs of the tested specimen.

The results of tests on cylindrical specimen indicated that the mode of failure in the specimen is affected by the load boundary condition. Under flat wedge ($\beta = 90^\circ$) it is called diametrical compression test (Brazilian test) where failure of the specimen predicted by the elastic theory initiates from the center of the specimen due to the development of high tensile stress and fracture propagates toward the edges (loading platens). The magnitude of tensile stress is maximum at the center and decreases toward the edges. This fact has been substantiated by the magnitude of the strain in the specimen as depicted by the strain gages (Figure 6A-a). Fracture formation in the specimen is characterized with less activity and lower rate of A.E. prior to failure (Figure 6A-b). Decreasing the wedge angle ($\beta = 60^\circ, 45^\circ, 20^\circ$) changes load boundary condition, consequently changing the mode of failure in the specimen from pure tension to mixed-mode tension-extension. Figure 6B-a illustrates deformation history of a cylindrical specimen under 20° wedge indenter. Gage (G1) in Figure 6B-a indicated compressive strain at early stage of loading and increasing higher tensile strain rate prior to failure and contrary to the behavior exhibited in Figure 6A-a. However, magnitude of tensile strain was highest at the center of the specimen, indicating tension and at the edge (under the indenter) was extension. A.E. pattern exhibited higher activity prior to the failure of the specimen indicative of localized crushing of the specimen due to high stress concentration under the wedge indenter (Figure 6B-b).

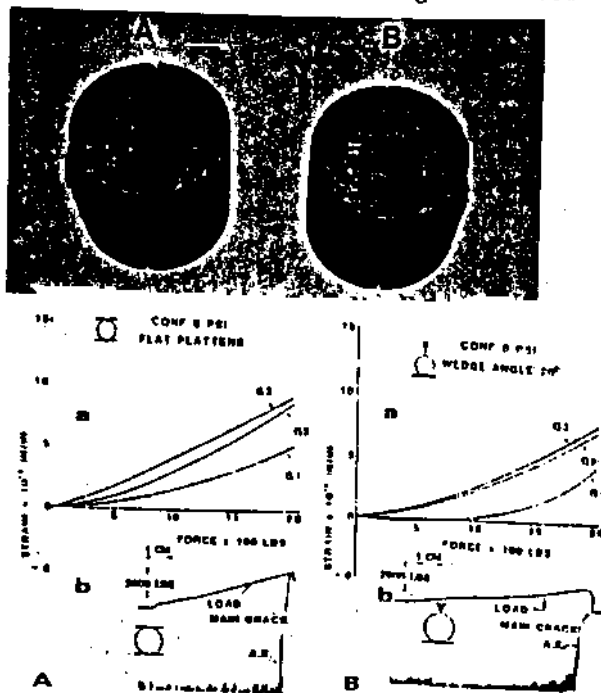


Fig. 6. Force-strain (a) and Load-A.E. rate curve (b); A - Brazilian Test; B - Indentation Test.

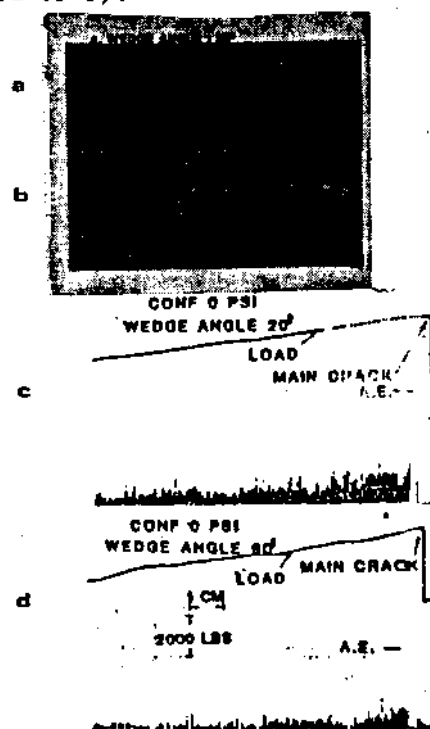


Fig. 7. Failed specimens (a. $\beta = 20^\circ$, b. $\beta = 60^\circ$) and Load-A.E. rate curves (c. $\beta = 20^\circ$, d. $\beta = 60^\circ$).

THE RESPIRABLE DUST CENTER

The result of the tests on rectangular specimen of Berea sandstone indicated that the type of fracture formation (intensity and sizes) and mode of failure in the specimen is a function of wedge indenter angle (β) and lateral confining pressure. At zero lateral confining pressure failure of the specimen under indentation loads ($\beta = 20^\circ, 45^\circ, \text{ and } 60^\circ$) were in extension mode and characterized by a major fracture preceeding high A.E. activity (Figure 7a-d). However, A.E. activity was higher using smaller wedge angle ($\beta = 20^\circ$) than the larger one ($\beta = 60^\circ$). This fact is probably associated with micro-crack formation due to high stress concentration under 20° wedge, while under larger wedge ($\beta = 60^\circ$) surface crushing of the specimen may occur. Increasing lateral confining pressure altered mode of failure in the specimen, and consequently affected the type of fractures. Generally at lower confining pressure failure of the specimen was characterized by a single major crack more or less parallel to the direction of the indentation load and failure mode was in extension. As the lateral confining pressure increased minor and major fractures preceded failure of rock and resulted in rock chip formation (Figure 8a-h). The chip formation caused by tension cracks while failure of the specimen were in shear mode. The magnitude of chip formation in the tested specimen decreased prior to failure as wedge indenter angle β increased. This fact is evident if comparison between failed specimens and their associated A.E. rate characteristics were made (see Figures 8, c-d and g-h).

The effect of anisotropic properties of material on fracture formation was analyzed by testing coal specimens where the indentation load and confining pressure were applied perpendicular to the face/butt cleats and the strains were measured on the bedding planes of the specimen. Some typical measured parameters and associated tested specimens are presented in Figures 9A-B. Fracture formation in the tested coal specimen was similar to rock specimen at zero lateral confining pressure and failure in the specimen were in extension mode. However, the rate of A.E. during fracture formation was higher than in the case of rock specimens (Figures 9A a-b). This fact could be due to the existence of micro-crack, discontinuities and flaws within the coal specimens, lower rate of loading and higher gain set (70 db). Chart speed in this experiment was kept at 16 cm/hour. The presence of cracks, flaws, material inhomogeneity and stress concentration within the specimen were identified using holography /4/. The existence of these micro-cracks has affected the strain distribution within the specimen especially under higher confining pressures, where erratic behavior is exhibited by the strain gages (Figures 9A c-e). The coal specimens were instrumented with five strain gages where G2 was positioned at the edge of the specimen under the wedge indenter and G1 at the side of G2 and G3, G4 and G5 were below G2. All gages were perpendicular to the direction of indentation load except G5 which was parallel (Figure 1d). The effect of wedge angle (β) on fracture formation in tested coal specimen was similar to those results described in the case of rock specimens. Wedge indenter with larger angle (β) produced larger crush zone in the specimen during fracture formation, which was accompanied by higher A.E. activity prior to the failure of the specimen (Figure 9A c-e). Failure characteristics of coal specimen under indentation load and lateral confining pressures were different than the rock specimens tested. Failure of coal specimens was accompanied with less minor cracks and more of crushing and the mode of failure was extension. At high lateral confining pressures failure of the specimen preceded higher degree of crushing and it was in extension mode (Figures 9A e-f), however the failure plane was perpendicular to the direction of indentation load, along the bedding plane. Type of fracture, intensity, and length of fractures are obvious from the observation of failed specimen (Figure 9B a-f). The characteristics associated with these fractures are well demonstrated by the A.E. rate and patterns as illustrated in Figures 9A a-f.

CHARACTERIZING FRACTURE TYPES IN COAL/ROCK

2000-10-10 10:00 AM

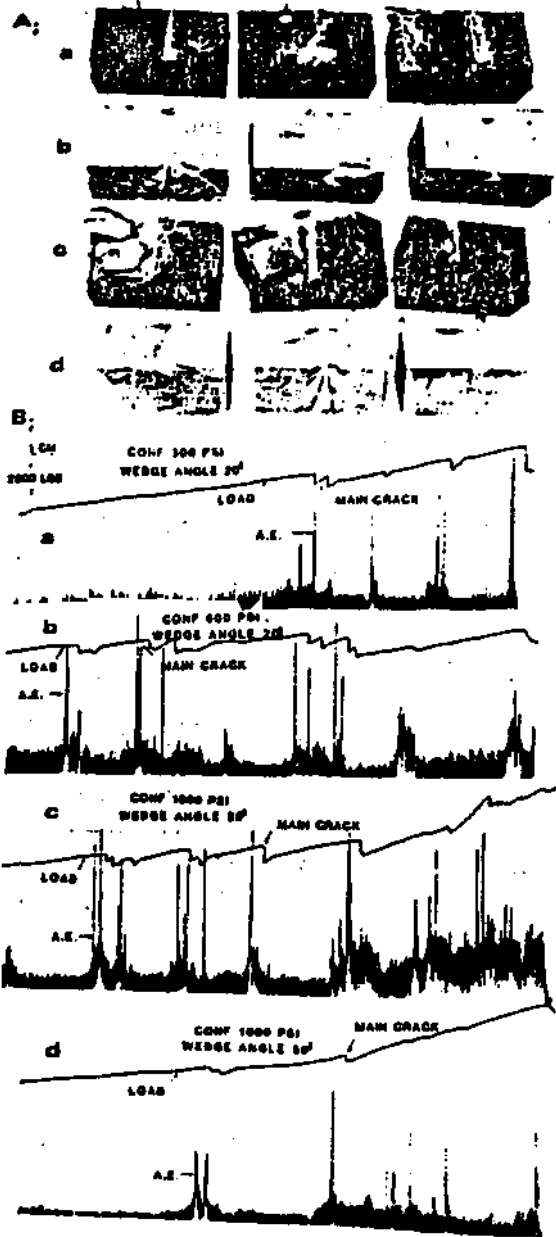


Fig. 8. A. Failed specimens, B. Load-A.E. rate curves for different wedge indentors at various confining pressures (1 psi = 6.89 KPa, 1 lb = 0.453 kg).



Fig. 9. A. Strains-A.E. rate for coal specimen using various wedge angle and confining pressures; B. Typical failed coal specimens (1 psi = 6.89 KPa).

CONCLUSIONS

The results of tests indicated that A.E. technique is a very useful method to characterize fracture formation, type, intensity and failure modes in rock/coal specimens subjected to different load boundary conditions. Very high rate of A.E. indicated major crack formation whereas high A.E. activity indicated the intensity of fracture formation resulting in production of chip or larger fragment sizes. A lower A.E. rate accompanied by high activity indicated localized crushing of the specimen which lead to the production of fine size particles.

THE RESPIRABLE DUST CENTER

ACKNOWLEDGMENTS

The author acknowledges the assistance of S. Jung, a graduate student in the Mining Engineering Department. This project was supported by funds from the Generic Center associated with Respirable Dust, sponsored by the U. S. Bureau of Mines under Grant Number G1135142.

REFERENCES

1. Hardy, H. R., Jr. and Leighton, F. W., eds., 1977 and 1980, First and Second Conferences on A.E./M.A. in Geologic Structures and Materials, respectively, Pennsylvania State University, Trans. Tech. publ.
2. Khair, A. W., 1981, "Acoustic Emission Pattern: An Indicator of Mode of Failure in Geologic Materials as Affected by Their Natural Imperfections," Third Conference on A.E./M.A. in Geologic Structures and Materials, Hardy, H. R., Jr. and Leighton, F. W., eds., Trans. Tech. Publ., October, 22 pp.
3. Peng, S. S. and Ortiz, C., 1972, "Crack Propagation and Fracture of Rock Specimens Loaded in Compression," Proc. Int. Conf. Dynamic Rock Propagation, Lehigh University, July, 17 pp.
4. Khair, A. W., 1984, "Study of Fracture Mechanisms in Coal Subjected to Various Types of Surface Traction Using Holographic Interferometry," Proc., 25th U. S. Rock Mechanics Symposium, Northwestern University, June, Society of Mining Engineering, AIME, 12 pp.

Correlation of fragment size distribution and fracture surface in coal cutting under various conditions

A. WAHAB KHAIR and W. M. DEVILDER

Department of Mining Engineering, West Virginia University, Morgantown, WV. 26506

ABSTRACT

This paper presents an analysis of fragment size distribution and characteristics of fracture surface in coal cutting using a rotary coal cutting simulator. Coal cutting by a drum type continuous miner was simulated in the laboratory. A series of tests along both the face and butt cleat direction of coal under different operating and in-situ conditions were performed. In each experiment the cut surface was photographed microscopically and the coal cuttings were collected and sized. Data were used to show how and to what extent various parameters effect size distribution of the coal cutting and how this correlates with the characteristics of the fracture surface. This study resulted in establishing a number of distinct correlations between the size distribution and fracture surface. These correlations were primarily based on the degree of interaction between adjacent bits and the amount of bit-coal interaction taking place on the cutting path. Some of the major results of this study are as follows:

Zones of bit-coal interactions proved vital toward understanding the effect the conical bit has on the fragmentation process. This in turn led to the identification of areas which are responsible for the production of fines and generation of respirable dust.

The various parameters employed in the coal cutting experiments which showed a strong effect on the coal fragment size distribution were: bit type, bit spacing, depth of cut, in-situ stresses, and cleat orientation. Bit angle and cutting head velocity exhibited the least effect and no correlation was established.

From this study it is obvious that the key to achieving efficient coal fragmentation is to limit the degree of bit-coal interaction that takes place throughout the bit path while causing maximum interaction between adjacent bits. Accomplishing this not only increases the percentage of large fragments produced but limits the amount of secondary crushing that takes place in the bit path thus resulting in decreasing fines and consequently, the amount of respirable dust generated.

INTRODUCTION

Over 2,000 continuous mining machines (introduced in the 1950's) equipped with conical bits or point attach bits account for well over half of the United States' production from underground coal mines. Today, competition in the coal industry has increased, due mainly to coal market conditions and legal restrictions, thus placing an emphasis upon increasing production, efficiency and health/safety of the workers. Mine operators are always interested in finding the most efficient performance of continuous mining machinery to produce the largest amount of size of coal at the lowest cost. An increase of fine material sent to the cleaning plant can seriously overload the plant to the extent that plant efficiencies deteriorate significantly (1). Also, the difficulty and expense of cleaning very small particles often cannot be done economically and thus, thousands of tons of coal are sent to the refuse pile because of costly or ineffective cleaning facilities. It has been said, "the efficient extraction of coal or rock implies breakage into a size range that contains a minimum quantity of very small sizes" (2). All known fragmentation theories concur that more fragmentation requires more energy (3). So, the importance of reducing fines is already evident from an outlook upon efficiency.

THE RESPIRABLE DUST CENTER

Now, let's consider another view point, dust generation.

The Federal Coal Mine Health and Safety Act of 1969, with revisions in 1977, was enacted to insure more healthful and safer working conditions for miners. The Act of 1969 established initially the respirable dust standard for coal mining operation as 3.0 mg/m^3 . The 1969 Act further reduced this standard to 2.0 mg/m^3 in 1973. The impact of respirable dust on miners health and economy of the coal industry is obvious. Since 1970 the federal government has paid over \$11.7 billion to more than 470,000 miners with black lung diseases and their survivors (4). Also, the coal mining industry considers respirable dust to be the greatest obstacle to achieving the full-production potential of current mining equipment. The following was stated: "it has been concluded that the amount of dust produced is approximately in proportion to the degree of fragmentation and to reduce the production of respirable dust, the fragmentation process must be better understood" (5). Accordingly, it is most important to develop extraction technology that reduces the production and release of particles in the small size, even though only a small fraction of the fine particles produced by coal cutting become airborne.

By better understanding the coal fragmentation process and how various parameters effect this process, it may be possible to reduce unwanted fines and respirable dust generation. This may be accomplished by shifting the size distribution to a higher percentage of larger fragments, thus reducing the percentage of fines. If the top sizes of coal are low, it is generally true that the portion of extremely small sizes is correspondingly high (2). By reducing the amount of fines, this will tend to shift the size distribution, improving cutting efficiency, thus reducing bit and machine related costs and those associated with handling, and cleaning those unwanted fines. This will also aid in decreasing the amount of respirable dust generated.

Considerable effort has been expended in the last 30 years on laboratory experiments and in the mine investigations of the cutting process applied to coal and rock cutting machines. Most of the early work by many authors has been summarized by Rad and provides a good reference (6). From these studies, inconsistencies and discrepancies were revealed. Some of the most basic studies done try to understand the fracturing process involved in indentation of a rigid wedge or bit into a brittle material (7,8,9,10). With the continuing development of more sophisticated mining equipment, the need to understand the fragmentation process was becoming more important. This led to the undertaking of many more research projects to evaluate the effect of operating, in-situ and geologic parameters on the cutting process in hopes of aiding in the design of more efficient mining machinery, reducing dust generation and improving the overall fragmentation process.

There are three basic types of research which have been done to evaluate the effects of various parameters in coal cutting. The three types are: 1) linear cutting in the laboratory using single or multiple bits; 2) rotary laboratory or in the mine cutting using single or multiple bits; and 3) in the mine tests on actual production equipment. Investigators for the U.S. Bureau of Mines have done and are currently doing extensive work in all three areas. In the Bureau of Mines Research Plan for Coal Mine Health and Safety during fiscal years 1979-83, the most important study area was fragmentation (5). A detailed review of the above three types of research and the work done prior to 1980 is given some place else (11), due to relevant interest of this paper emphasis will be on rotary type coal cutting.

Recent review of research on the measurement and control of respirable dust prior to 1980 concluded the following (5): "It has long been recognized that deep cutting coal mining machines produce larger fragments and less respirable coal mine dust than do machines that take only shallow cuts. Apart from this general observation,

FRAGMENT SIZE DISTRIBUTION AND FRACTURE SURFACE

however, significantly diverse experience exists on the effects of cutting speed and cutting-pick or bit design. This situation is clear evidence that the mechanics of fragmentation are not understood adequately. It has been concluded that these disparities reflect the incomplete nature of many experiments. It has been also concluded that such questions and similar questions related to cutting speed, pick design, and other cutting parameters as well as dust generation, can only be answered by cutting experiment in which more attention is given to the actual process of fragmentation." No tests were available that completely evaluated the point-attack bit so broadly accepted by the U.S. mining industry; in fact most published cutting research has been done using chisel-type tools. Most of the past work with rotary cutting machines was done in the area of rock cutting (12). However, to better understand the process of rotary cutting and the factors that effect the fragmentation of coal and dust generation process a unique rotary coal cutting simulator was designed and developed at West Virginia University (13). Correlation of the fragment size distribution and characteristics of fracture surface in coal cutting under various parameters is a part of the research program entitled "An Experimental and Analytical Approach to Study the Mechanisms of Respirable Dust Generation and Entrainment in Underground Coal Mining" sponsored by the U.S. Bureau of Mines through the Generic Center for Respirable Dust to be presented here. It is believed that a major source of respirable dust is the intensely crushed material produced at the tip of the cutting tool (5,14). Therefore this paper emphasizes microscopic analysis. Using microscopic photographs to better analyze the area of bit-coal interaction (bit path analysis) for better understanding the effect of the conical bit on the coal fragmentation process in relation to areas that contribute to the production of fines and generation of dust.

BACKGROUND

A continuous mining machine removes coal from the seam by a fracturing process consisting of forcing a conical bit into the coal face. In the removal of coal and rock from the face, tensile and/or shear failure is induced by the cutting machine, through the compressive action of the bit as it is forced into the coal. This compressive stress, which is transmitted primarily through the carbide tip, produces a high degree of crushing or pulverizing of the material at the bit tip which leads to the generation of a very fine dust. This compressive stress initiates fracture propagation into an area where the combination of tensile or shear stress fields and existing cracks creates the most favorable conditions for fracturing; thus failure of the material results and a chip or fragment is produced. As the strength of the coal or rock increases, so does the compressive stress required to initiate failure; the fragments are released more explosively from the face, causing greater dispersion of the crushed material and hence higher entrainment (3,5,6,14,15).

The major portion of the primary dust generated occurs in the crushed zone around the tip of the tool. This portion of primary dust generation doesn't vary with depth, but does vary with bit geometry (16). The total dust will increase with the depth of cut, but the increase is small compared to that produced in the crushed zone and will vary as the fracture length to the free surface varies (17). However, under deeper cut more material is broken per bit and the amount of dust produced becomes a smaller proportion of the total product removed (18). Investigators are in complete agreement with the fact that the amount of fines and airborne dust is directly proportional to the amount of specific energy used in cutting the coal (2,19,20,21,22). Increasing the depth of the cut reduces the specific energy used to fragment the coal.

If the broken coal is not cleared from the cutting element, the material will become subjected to secondary degradation by the bit in the bit path. Also, if insufficient interaction occurs between adjacent bits the coal boundary between them may be left

THE RESPIRABLE DUST CENTER

intact. If this occurs excessive crushing and grinding action will be present between the bit body and the coal surface causing dust generation and entrainment. It is very important to break the coal boundary and remove the chips bounded before energy is wasted grinding and regrinding the chips, fragments and the sides of the bit path (3,5,14,21,23). By increasing the depth of cut the spacing can be increased and still maintain breakage of the coal boundary. The optimum spacing to depth of cut ratio falls in the range of 0.5 to 0.3 (2,3,21,24).

The crescent-shaped cutting action is a significant part of the dust problem. When the top cutters start to recover coal, all the broken coal must be transported through the remaining arc of the drum. The transport of already recovered coal through the cutting zone of the rotary head makes it also a rotary grinder. The potential effect on dust generation by this secondary grinding may be at least as much as that produced by primary fragmentation (17).

Any time fractures propagate through the coal dust is produced. However, the amount of dust which is produced along fracture lines is very small as compared to that generated by the cutting tool. By breaking off larger fragments this will reduce the total surface area produced and thus the dust created along fracture lines (3,21).

Another area where dust is generated during the cutting process is that of crushing action by the drum and bit blocks. This regrinding or rubbing action can arise from several sources. First, if the cut material is not removed from this area it may be forced into the cutting head causing regrinding of the material. Another cause is if the coal isn't broken between bit paths the bit blocks may come into contact with the solid coal generating dust. Any time the coal isn't removed from the cutting area there will be excessive fragmentation in one form or another in this area. Due to the motion of cutter head, dust is more likely to become airborne (14,21,25).

EXPERIMENTAL PROGRAM

The overall objectives of this research program are to study the mechanisms of respirable dust generation and entrainment in underground coal cutting by continuous miner and how these mechanisms will be affected by important factors such as operating parameters, coal properties and in-situ stresses. However, this paper deals with the analysis associated with bit-coal interaction and coal cutting size distribution as affected by the above mentioned factors. Therefore, a number of monitoring facilities and experimental procedures will be described here which may not be directly related or essential to carry out the segment of research which is the subject of this paper.

Laboratory Facilities

A thorough discussion of coal cutting and monitoring facilities used in the current studies is given elsewhere (13,26). Therefore, only a brief outline of the facilities will be discussed here.

The main component of the testing facilities is an automated rotary coal cutting simulator (ARCCS) as shown in Figure 1. The ARCCS was designed with the capability to study the different machine and in-situ parameters that influence the fragmentation of coal and the resulting dust generation. The ARCCS operates under simulated mining conditions with equivalent in-situ horizontal and vertical stresses applied to a coal block of 18 in. x 15 in. x 6 in. (45.7 cm x 38.1 cm x 15.2 cm) located in a specifically designed confining chamber (Fig. 1a). The cutting drum (8 inches in diameter and 12 inches wide) has the capability of rotating from 1 to 50

FRAGMENT SIZE DISTRIBUTION AND FRACTURE SURFACE

however, significantly diverse experience exists on the effects of cutting speed and cutting-pick or bit design. This situation is clear evidence that the mechanics of fragmentation are not understood adequately. It has been concluded that these disparities reflect the incomplete nature of many experiments. It has been also concluded that such questions and similar questions related to cutting speed, pick design, and other cutting parameters as well as dust generation, can only be answered by cutting experiment in which more attention is given to the actual process of fragmentation." No tests were available that completely evaluated the point-attack bit so broadly accepted by the U.S. mining industry; in fact most published cutting research has been done using chisel-type tools. Most of the past work with rotary cutting machines was done in the area of rock cutting (12). However, to better understand the process of rotary cutting and the factors that effect the fragmentation of coal and dust generation process a unique rotary coal cutting simulator was designed and developed at West Virginia University (13). Correlation of the fragment size distribution and characteristics of fracture surface in coal cutting under various parameters is a part of the research program entitled "An Experimental and Analytical Approach to Study the Mechanisms of Respirable Dust Generation and Entrainment in Underground Coal Mining" sponsored by the U.S. Bureau of Mines through the Generic Center for Respirable Dust to be presented here. It is believed that a major source of respirable dust is the intensely crushed material produced at the tip of the cutting tool (5,14). Therefore this paper emphasizes microscopic analysis. Using microscopic photographs to better analyze the area of bit-coal interaction (bit path analysis) for better understanding the effect of the conical bit on the coal fragmentation process in relation to areas that contribute to the production of fines and generation of dust.

BACKGROUND

A continuous mining machine removes coal from the seam by a fracturing process consisting of forcing a conical bit into the coal face. In the removal of coal and rock from the face, tensile and/or shear failure is induced by the cutting machine, through the compressive action of the bit as it is forced into the coal. This compressive stress, which is transmitted primarily through the carbide tip, produces a high degree of crushing or pulverizing of the material at the bit tip which leads to the generation of a very fine dust. This compressive stress initiates fracture propagation into an area where the combination of tensile or shear stress fields and existing cracks creates the most favorable conditions for fracturing; thus failure of the material results and a chip or fragment is produced. As the strength of the coal or rock increases, so does the compressive stress required to initiate failure; the fragments are released more explosively from the face, causing greater dispersion of the crushed material and hence higher entrainment (3,5,6,14,15).

The major portion of the primary dust generated occurs in the crushed zone around the tip of the tool. This portion of primary dust generation doesn't vary with depth, but does vary with bit geometry (16). The total dust will increase with the depth of cut, but the increase is small compared to that produced in the crushed zone and will vary as the fracture length to the free surface varies (17). However, under deeper cut more material is broken per bit and the amount of dust produced becomes a smaller proportion of the total product removed (18). Investigators are in complete agreement with the fact that the amount of fines and airborne dust is directly proportional to the amount of specific energy used in cutting the coal (2,19,20,21,22). Increasing the depth of the cut reduces the specific energy used to fragment the coal.

If the broken coal is not cleared from the cutting element, the material will become subjected to secondary degradation by the bit in the bit path. Also, if insufficient interaction occurs between adjacent bits the coal boundary between them may be left

THE RESPIRABLE DUST CENTER

intact. If this occurs excessive crushing and grinding action will be present between the bit body and the coal surface causing dust generation and entrainment. It is very important to break the coal boundary and remove the chips bounded before energy is wasted grinding and regrinding the chips, fragments and the sides of the bit path (3,5,14,21,23). By increasing the depth of cut the spacing can be increased and still maintain breakage of the coal boundary. The optimum spacing to depth of cut ratio falls in the range of 0.5 to 0.3 (2,3,21,24).

The crescent-shaped cutting action is a significant part of the dust problem. When the top cutters start to recover coal, all the broken coal must be transported through the remaining arc of the drum. The transport of already recovered coal through the cutting zone of the rotary head makes it also a rotary grinder. The potential effect on dust generation by this secondary grinding may be at least as much as that produced by primary fragmentation (17).

Any time fractures propagate through the coal dust is produced. However, the amount of dust which is produced along fracture lines is very small as compared to that generated by the cutting tool. By breaking off larger fragments this will reduce the total surface area produced and thus the dust created along fracture lines (3,21).

Another area where dust is generated during the cutting process is that of crushing action by the drum and bit blocks. This regrinding or rubbing action can arise from several sources. First, if the cut material is not removed from this area it may be forced into the cutting head causing regrinding of the material. Another cause is if the coal isn't broken between bit paths the bit blocks may come into contact with the solid coal generating dust. Any time the coal isn't removed from the cutting area there will be excessive fragmentation in one form or another in this area. Due to the motion of cutter head, dust is more likely to become airborne (14,21,25).

EXPERIMENTAL PROGRAM

The overall objectives of this research program are to study the mechanisms of respirable dust generation and entrainment in underground coal cutting by continuous miner and how these mechanisms will be affected by important factors such as operating parameters, coal properties and in-situ stresses. However, this paper deals with the analysis associated with bit-coal interaction and coal cutting size distribution as affected by the above mentioned factors. Therefore, a number of monitoring facilities and experimental procedures will be described here which may not be directly related or essential to carry out the segment of research which is the subject of this paper.

Laboratory Facilities

A thorough discussion of coal cutting and monitoring facilities used in the current studies is given elsewhere (13,26). Therefore, only a brief outline of the facilities will be discussed here.

The main component of the testing facilities is an automated rotary coal cutting simulator (ARCCS) as shown in Figure 1. The ARCCS was designed with the capability to study the different machine and in-situ parameters that influence the fragmentation of coal and the resulting dust generation. The ARCCS operates under simulated mining conditions with equivalent in-situ horizontal and vertical stresses applied to a coal block of 18 in. x 15 in. x 6 in. (45.7 cm x 38.1 cm x 15.2 cm) located in a specifically designed confining chamber (Fig. 1a). The cutting drum (8 inches in diameter and 12 inches wide) has the capability of rotating from 1 to 50

FRAGMENT SIZE DISTRIBUTION AND FRACTURE SURFACE

rpm and can be stopped after a predetermined number of revolutions or a certain depth of cut. The bits can be mounted on the drum at four different angles 15, 30, 45, and 60 degrees and spacings of 1.5 in. (3.81 cm) to 3 in. (7.62 cm). A maximum of seven bits can be mounted on the drum in an echelon pattern. The ARCCS can be controlled manually or automatically through the use of a programmable control unit (Fig. 1b). Figure 1 also shows some of the testing and monitoring facilities used in this research. They are sonic testing unit (Fig. 1c) to measure fracture extension, acoustic emission (A.E.) monitoring unit (Fig. 1d) to measure fracture propagation and fracturing characteristics, microscope and attached camera unit (Fig. 1e) for analysis of fractured surface, 6-stage cascade impactors (Fig. 1f) for collecting airborne dust, hood and air generating unit (Fig. 1g), and data acquisition and recording unit (Fig. 1h). In addition to this, linear variable differential transformers (LVDTs), pressure transducers, flow meters, flow controls and drum rpm indicator were some of the other monitoring devices. LVDTs were used to monitor the displacement of the coal block as well as the depth of cut. Pressure transducers were used to monitor the changes in pressure both due to the thrust and due to the intermittent cutting nature of the rotary cutting. Flow controls were used to run the drum at a particular rpm and to provide a specific rate of advance. U.S. sieve series/ASTM specification E-11-61 was used in conjunction with the Ro-Tap Testing sieve shaker to size the fragments (settled) from 0.742 in. (1.885 cm) to -0.0015 in. (-0.0038 cm) or -400 mesh (-37 microns). Allen Bradley Sonic Sifter, model L3P, Series A was used to size the product from 37 microns to -10 microns.

Experimental Procedure

Large blocks of coal were obtained from a surface mine in the Waynesburg coal seam. The coal blocks were then cut in the laboratory to an approximate dimension of 16 in. x 13 in. x 6 in. (40.0 cm x 33.0 cm x 15.2 cm) with respect to the intended cutting direction (i.e. against face or butt cleat). The specimen was molded into plaster of paris mixture to a perfect dimension of 18 in. x 15 in. x 6 in. (45.7 cm x 35.6 cm x 15.2 cm) which was essential to avoid stress concentrations in the specimen when confining pressures were applied. The molded specimens were allowed to dry a week before testing. The molded specimen was placed in the confining chamber, the test conditions were set, and the in-situ and operating parameters were marked on the mold at the top of the specimen. Using the following nomenclature: #41-test number, III-bit type, 7-number of bits, 30-bit attack angle, 1.5-bit spacing (inches), 1/32-depth of cut per revolution (inches), 25-cutting head velocity (rpm), F-face cleat (B-butt cleat), S_v and S_h - equivalent vertical and horizontal in-situ stresses (confining pressures). Note if S_v and S_h are not specified, the confining pressures are negligible. A sonic test was done by which the stress wave travel time through the coal sample was recorded. Then predetermined confining pressures (equivalent in-situ stresses) were applied to the coal block. Some of the tests were done without any significant confining pressures; however, a small amount of pressures were used to keep the specimen in the confining chamber. The confining pressures were applied through the use of two sets of hydraulic jacks consisting of two jacks in a set (one set for horizontal pressure and one set for vertical pressure) each connected in parallel to a hand pump. A 1.0 inch (2.54 cm) thick steel plate was positioned between the sample and hydraulic jacks in order to distribute the pressure uniformly over the whole surface of the specimen. Before the test, the operating parameters such as velocity of the cutting drum and advance rate were adjusted to predetermined values. Then bit blocks of specific attack angle were mounted at a particular spacing and pattern. Conical bits of a specific make were inserted into the bit block and kept in position by a screw in a way as to allow symmetric bit wear. An acoustic emission transducer was mounted on top of the specimen on the mold. Then a canvas was hooked to the main frame of the machine and a plastic sheet was spread on it to

collect the coal fragments after each experiment. Six-stage cascade impactors were prepared (according to the instruction manual provided by Anderson Samplers, Inc.). A set of four impactors were then mounted on the specially designed arms at fixed positions with respect to the rotating drum. The number of rotations by the cutting head was set in the counter unit in the control module and then the machine was started to execute the program in continuous or counter mode. The counting of the number of rotations started when the hydraulic pressure was increased, due to the cutting process, or when the cutting head traveled to a preset distance measured mechanically and by the LVDT. After the execution of the predetermined number of rotations, the cutting head retreated and stopped. After each experiment the canvas was unhooked and the coal fragments were collected in the Ziploc bags and the vacuum bag with the help of a vacuum cleaner. This product was sieved into different sizes. A standard square root of 2 series was used from 0.742 in. (1.885 cm) to 0.187 in. (0.475 cm), then the screens were used alternatively, meaning that the previous screen size was divided by square root of 2 to get the net size. From 0.187 in. (0.475 cm) to 0.0029 in. (0.0074 cm) every other sieve size was used or a ratio of 2 between screen sizes. The -0.0029 in. (-0.0074 cm) sizes were screened with the square root of 2 series again. This method of screening was used to reduce the number of screens, thus reducing the amount of fines lost in the 0.187 in. (0.475 cm) to 0.0029 in. (0.0074) range. This method also distributes irregularities at both ends of the size range. After the screening was completed, the material retained on each screen size was weighed. Then the percent of weight retained on each screen was plotted on three-cycle, semi-log graph paper at the corresponding opening size. In general, there are two dips that appear in the size distribution curve that are due to the transition from screens in the square root of 2 series to those of the 2 series and back. The dips occur because the screens that start the change in a series receives more material than it would have in a straight series. The bump occurring at the 0.0015 in. (0.0038 cm) or 400 mesh size is natural and is characteristic of the material and not related to screening. The sizing from 400 mesh (37 microns) to -10 microns was done by the sonic sifter. All the sized products were then weighed up to 0.1 gm by Sartorius Type 2351, mechanical balance with analog readout and the percent weights retained were then calculated.

Following the completion of the tests, the tested coal block was removed from the confining chamber. It was photographed using a Nikon 35 mm camera and auxiliary lights to give overall pictures of the fractured surface of each test specimen. The bit paths were then photographed using a camera attached to an optical microscope. The pictures were taken of the center bit path approximately 1 inch from the bit entry, middle of the coal block, and 1 inch from the bit exit. In general, these pictures were taken using 0.66 and 1.5 zoom settings, given a total magnification of 3.5 and 8 times, respectively. In some instances more detailed pictures of the bit path and the particles trapped in this area were taken in order to understand what happens in the zone of bit-coal interaction. These pictures were used to help categorize and correlate the fracture surface characteristics with the size distribution and other parameters involved in the coal cutting process.

RESULTS AND DISCUSSION

Most of the coal used in this study is part of the Waynesburg coal seam. Presently, only limited tests have been completed on the Pittsburgh coal seam. The physical and mechanical properties of the Waynesburg coal were determined in the laboratory and are presented in Tables 1 and 2. However, the properties of the Pittsburgh coal seam are not available at the present time. There have been a total of 43 individual tests completed and detailed analysis has been presented elsewhere (11). However, only brief analysis of the results will be discussed here. It should be noted that due to the extended scope of the study and involvement of a large number of parameters/factors a limited number of tests have been documented under

FRAGMENT SIZE DISTRIBUTION AND FRACTURE SURFACE

a specific set of parameters. Therefore, if the results may not be clear it is probably due to the inhomogeneous nature of the coal.

To compare the size distribution results of different tests, it is first necessary to define the size limits used in this study. Two types of particle analysis were made. The first type includes the settled particles and the second type is airborne particles. In the first type, large fragments are defined as fragments greater than 0.0937 in. (0.238 cm), fine fragments between 0.0937 in. (0.238 cm) and 0.0015 in. (0.0038 cm) or 400 mesh, and dust is defined as the material below 0.015 in. (0.038 cm). In the second type particle size distributions were made based on the standard sizes associated with cascade impactor.

This paper deals with the analysis of the appearance of fracture surface after a test has been completed. An optical microscope was used (Fig. 2) to investigate the area of the bit path and to determine what happens in the area of contact between the bit and coal from the resulting traces left on the fracture surface by the bit. The four different types of conical or point attack bits used in this study are shown in Fig. 3a. The corresponding manufacturer's specifications giving bit dimensions and angle of carbide tip (degree of sharpness) are shown in Fig. 3b. The bit types are known as: pencil bit with medium carbide tip, Type II; plumbob with large carbide tip, Type III; sharp/slender bit with fins to aid in bit rotation and sharp carbide tip, Type IV; plumbob bit with medium carbide tip, Type V. Tests conducted to evaluate the effects of bit spacing, depth of cut, bit angle, drum velocity confining pressure, and face/butt cleat direction of cutting were all done using the Type IV bits.

Bit Path Analysis

In analysis of zone of bit-coal interaction, it was found that there are two extreme cases. Test #10 and Test #41 are typical tests that represent Case 1 and Case 2, respectively shown in Fig. 4. In Case 1 fracture surface shows only interaction of the carbide tip and the coal surface as evident by a shiny line in the center of the bit path. However, the Case 2 fracture surface involves not only interaction of the carbide tip but also that of part of the bit body and the coal surface. The zone of interaction of the carbide tip and coal surface was formed to have the same general characteristics in all tests, although, the size and shape were found to vary with bit type.

To characterize interaction of bit-coal, it is necessary to define the zones of the bit which correspond to distinct zones in the bit path. Figure 5 illustrates three distinct Zones 1, 2, and 3, which correspond to the carbide tip, transition between the carbide tip and the bit body (appears as an offset or gap), and the bit body, respectively. The corresponding zones in the center of the bit path are indicated in Fig. 6 while for the top (one inch from the bit entry) in the same bit path are shown in Fig. 7. Within these three zones, there are three notable microscopic fractures (denoted by A, B, and C). Feature (A) representing the shiny or black areas, Feature (B) the light brown areas, and Feature (C) areas of solid intact coal which have not been scared by bit action. Feature (A) is formed as the bit passes through the bit path causing excessive crushing or grinding of loose and/or intact material between the bit and the solid coal surface along the bit path. Frictional heat generated by the abrasive action between the bit (body and carbide tip) and coal surface tend to liquify part of the crushed material causing it to fuse together leaving a shiny almost metallic looking surface with small microscopic ridges on its surface (Fig. 8a). These ridges ran parallel to the direction of the bit travel. This shiny surface tended to break in a platy fashion. Along the breakage, small dust size particles of irregular shape were produced. Further, breakage of the platy particles resulted in a production of very fine dust size particles thus giving the

THE RESPIRABLE DUST CENTER

area shown in Fig. 8b. Further analysis indicated that beneath this shiny surface at Zone 1 a pocket of crushed material was trapped. The size, shape and depth of this pocket varied with the size/shape of the carbide tip with typical depth of approximately between 1/64 and 1/16 of an inch. It was noticed that the shiny surface and associated crushed material appeared to be charged (or became active by a chemical or electro static means) because it was attracted to the metal tool and any other metallic object (knife, tweezer). Crushing of these materials resulted in very small dust size particles of irregular shape which were attracted to each other and grouped in small clusters, agglomerated (see center of Fig. 8b). It should be noted that the material in Fig. 8b is from the side of the bit path and appears similar and exhibits the same characteristics of that in the center of the path (Fig. 8a). However, in general the shiny material on the sides of the bit path did not have quite as much crushed material beneath it. Speaking in relative terms, this suggests that more crushed material was produced by the carbide tip as opposed to the bit body. This can primarily be attributed to the high compressive stresses imposed on the coal by the carbide tip. The brown areas (Feature (B)) are where crushed material is slightly compacted and deposited (Fig. 7b). Note the large platy particles are from the black areas and the finer particles are from the brown areas. The intermittent shiny and dark areas (Feature (C)) represent freshly exposed intact coal.

Any or all of these features may be presented in any one zone. However, Zone 1 mainly consisted of a shiny or black surface that was produced from frictional contact with the carbide tip, also some brown deposits of crushed material may be present. Zone 2 consisted of freshly exposed intact coal and brown deposits of crushed material depending on the gap (offset) between the bit body and carbide tip. In general, the larger the gap (Zone 2) resulted in a clean fracture with little or no crushed material. Zone 3 consisted generally of all these features. The extent of each zone was largely dependent upon the degree of fracturing and the amount of frictional contact between the bit and solid coal. The particles deposited in the brown areas appear much larger than those produced by breakage of the black or shiny areas.

Effect of Bit Type

A series of tests were conducted, using seven bits mounted in an echelon pattern, to evaluate the effects of the four bit types. The test parameters used were: 30 degree attack angle, 1.5 inches bit spacing, 1/32 inches depth of cut per revolution, 25 rpm drum velocity, negligible confining pressure and cutting was made along the face cleat. Observation of the fracture surface indicated that all four tests were representative of Case 2. That is, there were traces left on the fractured surface by all three zones of the bit. The height of the coal boundary left between the bit path fell in the range of 3/4 to 1 inch for the specimen which were cut using bit Type III, V, and II and 1 to 1 1/2 inches using bit Type IV. In general, bit type seems to have no significant effect on the degree of breakage of the boundary between the bit paths. Although it was observed that for each bit type fracturing may initiate at different points in the bit path breaking material away from the bit as it proceeds through the coal. This tends to widen the groove but has little effect on the overall breakage of the coal boundary.

Figure 9 shows the corresponding microscopic photographs of the specimen using the above four types of bit. It is obvious that Zone 1 is the largest using Type III bit with the large carbide tip (Fig. 9a). Zone 1 is virtually the same size using Type V and Type II bits with a medium carbide tip, shown in Figs. 9b and 9c, respectively. The smallest of Zone 1 was produced using bit Type IV with sharp carbide tip (Fig. 9d). The relative size and shape of the pocket of crushed material using different types of bit is illustrated in Fig. 10. The depth of the crushed

FRAGMENT SIZE DISTRIBUTION AND FRACTURE SURFACE

material shown in Fig. 10 varied from approximately 1/64 to 1/16 of an inch. The intermittent brown areas in Zone 1 in essence did not change the general shape of the pocket of crushed material but where these areas occurred, the pocket was slightly deeper than indicated in Fig. 10. The Type III bit by far trapped the most crushed material, due to the bluntness of the carbide tip. This material was of uniform thickness throughout Zone 1 tapering off at the edges. Type IV bit trapped the least material because of the sharpness of the carbide tip. The trapped material was very shallow throughout Zone 1, whereas, Type V and Type II bits fell somewhere in between, trapping most of the crushed material at the edge of Zone 1 (due to offset of carbide tip and bit body). There was little material trapped directly under the carbide tip. Zone 2 is by far the largest for the Type II bit because of the large offset between the bit body and carbide tip. This offset provided a relief for fractures to propagate from Zone 1 to Zone 3, leaving a freshly exposed ridge of intact coal which was not scarred by bit action (Fig. 9c), whereas, Zone 2 for Types V and IV bits appeared as small thin ridges of exposed coal with intermittent dust pockets, brown areas (Figs. 9b and 9d). The transition between the bit body and carbide tip is gradual compared to Type II (small gap) leaving a small ridge across Zone 2. For the Type III bit, there is a small line which runs between Zone 1 and Zone 3 and represents the very small gap between the bit body and carbide tip (Fig. 9a). Zone 2 in Fig. 9a is mostly filled with fines; however, some small areas of exposed coal can be seen. For this type of bit, a smooth transition occurs between the bit body and carbide tip. Zone 3 consisted of a small band of shiny platy material with intermittent areas of compacted fines. The amount of crushed material trapped behind the areas of frictional contact (shiny areas) was less than that associated with Zone 1 for all bit types. Type II bit had by far the least amount of bit-coal interaction in Zone 3 as compared to the other bits. Zone 3 was much wider meaning more interaction, larger area of contact, occurred for the Type V bit as compared to Type II. The Type III and IV bits by far showed the most bit-coal interaction in Zone 3. In the case of the Type III bit, Zone 3 extends beyond that captured in the microscopic photograph (Fig. 9a) and is made up equally of black and brown areas. In other words, almost half of the total area has been subjected to frictional contact producing black areas, whereas, for the Type IV, Zone 3 was slightly wider as would have been expected because it had the highest coal boundary left between the bit path and almost entirely consisted of areas of frictional contact, black (shiny areas) with few areas of deposited fines (Fig. 9d).

An attempt was made to correlate bit-coal interaction with product size distribution. The results/correlation were obviously within certain ranges, however, in some ranges they became less conclusive. Figure 11 shows the fragment size distribution associated with the four bit types for Case 2 fracture surface. The fine range of the size distribution (-0.007 inches) is affected by the degree of bit-coal interaction in Zone 1, by the carbide tip. The Type III bit being the most blunt of the four bits produced the most crushed material in Zone 1, part of which is trapped by bit action and the remaining undoubtedly released during cutting. This pocket of crushed material which was produced by each pass of the bit will be released upon the next cutting cycle. Thus, the Type III bit produced the highest percentage of material in the fine range (-0.007 inches) of the size distribution. Next, the Type V and II bits which have the same size carbide tip produced virtually the same amount of crushed material in Zone 1, resulting roughly in the same percentage of fine material (-0.007 inches), whereas, the Type IV bit being sharper produced the least amount of crushed material in Zone 1 and reflected in the size distribution by having the lowest percentage of material in the fine range (-0.007 inches). The size distribution from 0.09 to 0.007 inches is affected by the degree of bit-coal interaction in Zone 2 and Zone 3. The larger area of frictional contact resulted in excessive crushing and grinding of loose material in the bit path as well as that of intact coal. For this reason, Type IV bit produced the highest percentage of fine material in the range of 0.09 to 0.007 inches of size distribution.

THE RESPIRABLE DUST CENTER

In contrast, the Type II bit had the least amount of frictional contact. Also, because fracturing occurred across Zone 2 (ridge remains due to offset to bit tip and bit body), the bit did not trap broken material. However, these ridges may be subjected to secondary crushing by the bit body in subsequent cycles and will reflect the production of dust size particles. Figure 11 shows that the Type II bit produced the lowest percentage of fines in the range of 0.09 to 0.007 inches. Zone 3 for the Type III bit was large but only partially had areas of frictional contact, thus accounting for a slightly higher percentage of fines than Type V bit for which Zone 3 was much narrower and had correspondingly less total area of frictional contact. To further evaluate the effect of bit type on fragment size distribution another series of experiments are presented here. The test parameters used were: four bits mounted in an echelon pattern, 30 degree attack angle, 1.5 inches bit spacing, 1/5 inch depth of cut per revolution, 15 rpm drum velocity, 512 psi vertical and 300 psi horizontal confining pressures and tested along the face cleats. The fractured surface of the tested specimen were representative of Case 1, indicating breakage occurring between bit paths and only the resulting trace left by the carbide tip (Zone 1) remains on the fractured surface. Furthermore Zone 1 had the same general size/shape and characteristics associated with it as in the previous tests. The size distribution for these experiments is presented in Fig. 12. Figure 12 shows that the Type IV bit produced the least percentage of fines and that the Type III bit produced the most. The Type IV bit had the sharpest carbide tip and produced the smallest frictional contact in Zone 1, whereas, the Type III bit having the largest carbide tip produced the largest frictional contact in Zone 1. Size distribution for the Type V and II bits fell between that of the Type III and IV bits mainly due to the size and shape of their carbide tips and associated frictional contact in Zone 1.

It is difficult to identify any correlation in the large range (+0.0937 in.) size distribution. Mainly, due to the bit type having no significant affect on breakage of the boundary between bit paths. Similarly on the dust range (-0.015 in.) there is no obvious correlation. The size distribution graph between 40 to 10 microns crossing each other at approximately 27 microns and has a natural dip at 20 microns (Fig. 13). Between 20 and 12 micron sizes, bit Type IV produced the highest percentage, but Type II second, bit Type V third and bit Type III the lowest. Furthermore the size distribution curves for bit Types V and II shows similar characteristics with crossing each other at 27 and 12 micron size, similar curves for Type V and III with only crossing each other at 27 micron size. This irregularity could be due to the characteristics of coal and bit-coal interaction and possibly may have been affected by the sieving process where further breakage of the fragments may have resulted in various production of dust size particles. An important feature to note in Fig. 13 is the sharp decline in size distribution curve for bit Type IV between 20 and 10 micron sizes, where the percentage weight retained at 10 microns is the lowest for bit Type IV than others indicating possibly the least production of respirable size dust.

Particle size distribution of the entrained dust sampled by 6 stage cascade impactors was plotted on log-probability graphs (Fig. 14). Most distribution functions like this require two parameters, one that identifies the location or center of the distribution and the other that characterizes the width or spread of the distribution. Location of center of the distribution here is identified by mass median diameter (MMD). MMD is defined as the diameter for which half the mass is contributed by particles larger than the MMD and half by particles smaller than the MMD. The geometric standard deviation (GSD) is a measure of the spread of the particle size distribution. It is defined as the ratio of MMD and the particle size at 16 percentile. If GSD = 1, all the particles are of the same size, i.e., the entrained dust is "monodisperse" (27). The MMD and GSD for bit Type V are 5.4 and 3.55, respectively. They are considerably different when compared to the bit Types III and IV for which the MMDs and GSDs are consistent between 9.2 and 9.4 and 2.16

FRAGMENT SIZE DISTRIBUTION AND FRACTURE SURFACE

and 2.38, respectively. Table 3 shows the weight and percent of respirable size mass divided into 10.0 x 6.0 microns and 6.0 x 6.6 microns. Table 3 confirms with the MMDs and GSDs where in the bit Type V produced 76.3 percent of the mass in the 6.0 x 6.6 micron size range while bit Types III and IV produced only 58.0 and 56.7 percent in the same size range respectively. At 10.0 x 6.0 micron size range the order of highest production reversed resulting in 23.7, 43.30, and 42.00 percent for bit Types V, IV, and III, respectively.

In analysis of bit coal interaction for these experiments, as it was described before, largest of Zone 1 and least of Zone 3 occurred by bit Type III opposed to the bit Type IV, and bit Type IV and bit Type V showed characteristics somewhat in between the two. This bit-coal interaction reflected in size distribution curves shown in Figs. 11-13. Geometrically bit Type V has somewhat common characteristics with both types of bits III and IV. Its plumbob shape, small head and large base make the bit body sharper than the Type III bit which has the largest of all three. Bit Type V has a smaller head than bit Type IV and has the smallest carbide tip of all three. This small carbide tip caused a rough surface feature on the bit and left a large gap around the carbide tip as the extension of the head (body) of the Type V bit. This gap provided a trap zone for the crushed material and left ridges (Zone 2) in the bit path (Fig. 10), which was further subjected to crushing and grinding in subsequent cutting cycle resulting in production of higher respirable dust sizes (Fig. 14 and Table 3). It was mentioned before, breakage of ridges and fine particles (shiny surface, black area, and agglomerated crushed material) produced dust size particles, therefore any bit type which produces rough surfaces and large percentage of fine particles, excessive fractured surface area, will also produce the larger percentage of respirable size dust. From Figs. 11-14 it could be concluded that the bit which has a carbide shape and tip-head arrangement of bit Type IV and the body of bit Type V is more effective in less production of fine and respirable dust size particles. A sharp and larger carbide tip for bit Type V would have given a smooth transition between the tip and body of the bit. This would improve the cutting efficiency of the bit by having least bit-coal interaction and resulting in less regrinding and frictional contact at all three zones, thus producing less respirable dust.

Effects of Bit Spacing

A series of experiments were run to study the effect of bit spacing on fragment size distribution and to see how this may relate to the overall and microscopic appearance of the fracture surface. The tests were conducted using 1.5 and 3 inch spacing. The appearance of the coal blocks after cutting for 1.5 inch spacing resembled Fig. 4 and for a typical test with 3 inch spacing is shown in Fig. 15a. Despite varying the cutting head velocity, bit type, bit attack angle and confining pressures within the depths of cut used in this study, the boundary walls between the bit paths remained intact with the least interaction between each bit. The fractured surface represented the extreme end of Case 2 indicating a high degree of bit-coal interaction and frictional contact as shown in Fig. 15b. For the reasons mentioned above, the 3 inch spacing produced, percentage wise, far less large size and more fine size particles than did the 1.5 inch spacing as shown in Fig. 16.

Effect of Depth of Cut and Cleat Orientation

A series of experiments have been performed both along the face and butt cleat direction keeping the other parameters constant while changing the depth of cut. Four tests representing general characteristics of this series of experiments are selected for discussion here. Tests #11 and #35 were performed along the face cleat, while #21 and #40 was performed along the butt cleat. Test #11 represents a 1/4

inch depth of cut per revolution with five bits mounted in an echelon pattern (Fig. 17a). Test #35 represents a 1/32 inch depth of cut per revolution with seven bits mounted in an echelon pattern (Fig. 18a). Test #11 indicates the breakage of the boundary wall between the adjacent bit paths. The height of the boundary lift is in the range of 0 to 1/2 inches (average of 1/4 inch) measured from the center of the bit path and the fractured surface here represents case 1. However, test #35 indicates a much lesser degree of interaction between the adjacent bit paths leaving a much larger boundary between them as shown in Fig. 18a. The height of the boundary is in the range of 1 to 1 1/2 inches (averaging 1 1/4 inches) and the fractured surface represents Case 2. In deep cut (Test #11) only a small trace of the carbide tip on the fractured surface lift (Fig. 17a) and indicating less bit-coal interaction as shown in Fig. 17b. However, shallow depth of cut caused excessive bit-coal interaction and frictional contact as shown in Fig. 18b.

Fracture initiates at the zone of highest stress concentrate or where the stress exceeds first the strength of material. In coal cutting fracture initiates under the bit tip. This feature continues to propagate as long as the above conditions are met or the fracture reaches to a free surface. Generally the depth or length of crack depends on the magnitude of stress at the time of fracture initiation. Increasing the depth of cut requires a higher stress level and causes more complete interaction between the bit paths; coal is broken away from the test specimen so the bit is not enclosed by the bit groove which causes the production of fines as shown in Fig. 19. When the depth of cut is increased, the cracks, which were produced from the compressive stresses induced on the coal by the bit, must propagate further to a free surface to allow breakage, thus causing larger fragments to be formed and more coal broken per pass. Not only were larger fragments produced with a deeper depth of cut per revolution but there was less contact between the carbide tip and coal surface in removing the same volume of material versus that of a shallow cut, thus reducing the amount of crushed material produced at the bit tip for the same volume of coal removed. When the depth of cut is decreased, the cracks have much less distance to travel to reach a free surface producing smaller fragments and allowing the boundary wall to be built up between the bit paths.

The fractured surfaces for the specimens tested along the butt cleats (tests #21 and #40) was much rougher and broke irregularly. The figure associated with these tests is not included here due to limited space. The cutting resistance along the butt cleat was much higher than those tested along the face cleat under the same set of parameters. This higher resistance attributed to a 5.2% higher compressive and 33% higher tensile strength of coal in the butt cleat direction (see Table 2). This in turn led to different failure characteristics in the butt cleat direction especially at deeper cuts. For example the average height of the boundary wall between the bit path for test #21 along the butt cleat was 3/4 inch which was much greater than that of test #11 along the face cleat direction (averaging 1/4 inch) for the depth of cut of 1/4 inch. This resulted in more bit-coal interaction and caused more frictional contact between the coal and bit for the case of cutting along the butt cleat. Comparing the same depth of cut, along the face and butt cleat, percentage-wise more larger size fragments and fewer fines are produced when cutting along the face cleat (Fig. 19). However, this difference became negligible when depth of cut was reduced (i.e., 1/32 inch) especially at the lower end of the fine size (dust). The latter claim was substantiated by the analysis of respirable dust collected by cascade impactors as shown in Fig. 20. In Fig. 20, respirable dust in both experiments having the same mass median diameter (MMD = 9.4) with less difference between their spread of the particle size distribution, GSD of 2.38 and 2.16 for face and butt cleat respectively. One of the reasons for this lack of difference in particle size distribution, when testing along face cleat versus butt cleat at very shallow depth of cut probably the characteristics of coal itself. Under shallow depth of cut, cutting stress will be very low, fracture length will be small,

FRAGMENT SIZE DISTRIBUTION AND FRACTURE SURFACE

consequently coal will break along its natural imperfection which is rather constant for these specimens (because of being all prepared from the same block of coal) and has not been affected by the cutting direction.

Effects of Cutting Head Velocity

During coal cutting the velocity of cutting head is not uniform rather it is cyclic due to the intermittent nature of the fracturing process. When cutting head exerts peak dynamic force on the coal its velocity reduces to its lowest value and meanwhile causes fracture initiation and propagation. During fracture propagation resistance offered by the coal is low and also due to the back up pressure the cutting head accelerates and its velocity reaches its peak value. In this period of the cycle the cutting head grades the cutting path. Higher peak dynamic stress causes longer/deeper fracture; however, it also increases the length of the grading surface. The higher the velocity of cutting head and resistance offered by the coal, the higher peak stress and more fluctuation is observed in the velocity of the cutting head, consequently increasing the grading period (26). The higher the cutting velocity the higher the required cutting force is observed as shown in Fig. 21. However, the specific energy might be the same because under a higher rpm the bit spends little time cutting coal. Analysis of both microscopic and overall appearance of the fractured surface for this series of tests showed no significant differences due to changing drum velocity. However, change in rpm of drum has been reflected on fragment size distributions as shown in Fig. 22a-b. The higher rpm produced a higher percentage of large and a lower percentage of fine size material. There is an exception where the size distribution curve for 15 rpm experiment lies between 35 and 25 rpm in range of 20-10 microns (Fig. 22b). This could be due to the characteristics of coal or due to the limited number of tests with orthotropic and nonhomogeneous material. Analysis of respirable dust for this experiment indicated similar results with less differences in production of respirable dust as shown in Table 4. However, the aerodynamic particle size is smaller for 35 rpm cutting head speed than 25 rpm as shown in Fig. 23.

Increasing the cutting head velocity under a constant depth of cut imposed more energy on the coal during dynamic loading (fracturing) producing more large and deep fractures in the coal resulting in more large and less fine fragments. The higher velocity will also tend to enhance crack propagation allowing a greater distance to be traveled before reaching a free surface, thus detaching a larger fragment. Increasing the velocity will increase the kinetic energy of the fragmented material which will help in removal from the bit path and reduce secondary degradation (reducing fines) but will undoubtedly increase dust entrainment. That is to say, it increases the airborne dust in expense of settled dust. Also coal is "weaker under a higher rate of loading (impact) making it easier to fracture, thus giving larger fragments (6). The only drawback for higher speed would be increasing grading period of cutting process and secondary fracturing of the crushed material due to high impact resulting in smaller size particles. Even though the total airborne dust might be less under the high speed cutting bit the total number of dust particles might be high as it is shown by the GSD of 2.79 for 35 rpm as compared to 2.38 for 25 rpm. This substantiates the possibility of increasing airborne dust in expense of settled dust under higher drum speed.

Effects of Bit Attack Angle

The point of contact for bits along the cutting path changes from entry to exit for any attack angle. At the entry of the cutting path the front portion of the bit tip will make contact mostly with the coal, at the center of the path almost the tip of the bit tip (depending on the angle of attack) and at the exit position the back of the bit tip as shown in Fig. 24. However, the tip of the bit is semispherical where

its curvature slightly changes from the tip to the sides which might affect the required force to cut the coal. Figure 25 shows the resultant forces (resultant of cutting and thrust forces) for the depth of cut for the four types of attack angles. Figure 25 shows that a 30 degree bit attack angle required the least force to cut the coal for a given depth of cut where a 15 degree attack angle required the highest. The fragment size distribution for these tests are shown in Fig. 26. From Fig. 26 it is obvious that a 30 degree attack angle is producing more large and less fines compared to the other three. However, the trend based on force requirement for a depth of cut for the other attack angles are not exhibited on fragment size distribution. This suggests that directional properties of coal highly influence the cutting force and fragment size distribution. That is to say coal breaks easily and produces larger size fragments when it has been cut at a certain angle. Analysis of the fractured surface indicated no significant apparent differences for the different bit attack angles and the bit traces were very similar. Eventhough the 30 degree attack angle which produced substantially more large fragments, it was expected that there may be more interaction between the bit paths but this was not evident. In fact, all four tests showed almost the same degree of interaction, leaving a very small boundary between the paths. However, the 30 degree attack angle may break off larger fragments during the cutting process which may not always be evident by the appearance of the fracture surface after cutting.

Effect of Confining Pressure

A series of tests were performed both along the face and butt cleat directions at various equivalent in-situ stresses. The fractured surface definitely has a different appearance than that of the unconfined situation. Along the face cleats the fracture surface was very rough and irregular in appearance as though the coal provided a very high cutting resistance. This was clearly indicated in resultant force required to cut a specific depth as shown in Fig. 27. The higher the equivalent in-situ stresses (horizontal stress = 1/3 vertical stress) the higher required cutting forces. Under the confining pressure, no longer was the splitting type fracture prominent between adjacent bit paths as was seen under no confining pressure. In a constrained situation, the fracture seemed to propagate in an angular almost unpredictable fashion seeking the path of least resistance giving a very rough appearance of the fractured surface. Increasing compressive strength of coal due to confining pressure makes it much more difficult for fractures to propagate directly to adjacent bit paths breaking the wall boundary of bit paths. Instead the confining pressures closes the joints causing the coal to act like a solid continuous material. When cutting the coal, crater shaped grooves were formed and ridges were left between them. In both directions (face and butt cleat), the coal offered more resistance to cutting, giving a rougher fractured surfaces. Microscopic photographs of these tests indicated that, in general, the only trace left by the bit was that due to the carbide tip, no excessive contact was evident. The trace left by the carbide tip was more intermittent than those tested without confining pressures. Larger gaps occurred between traces (shiny lines) left by the carbide tip through the bit path and are indicative of the harder cutting and irregular fracturing. Furthermore, fractures propagated in a step-like manner toward the coal face deviated by the confining pressure before breaking across the wall boundary of the bit path in an irregular fashion.

The effect of confining pressures on size distribution for the tests done (using 30° attack angle) is less conclusive as shown in Fig. 28. Increasing the confining pressure in the butt cleat direction resulted in a slight decrease in the percentage of fines and increased the percentage of large fragments in the upper end of the size distribution. However, it is not quite clear what effect the increasing pressure has on size distribution, when cutting along the face cleat. In a similar test conducted along the face cleat but at the other three attack angles (15, 45, 60), it

FRAGMENT SIZE DISTRIBUTION AND FRACTURE SURFACE

was found that the confining pressure decreased the percentage of large fragments and increased the percentage of fines as shown in Fig. 29. In general, confining pressure has the opposite effect while cutting along the face cleat than those of butt cleat. A possible explanation may be that the confining pressure may make the coal either easier or harder to cut, depending on the inherent characteristics of the coal in the face and butt cleat directions.

Effect of Coal Properties

A limited number of tests have been carried out on the Pittsburgh coal seam and for comparison an example is presented here. The apparent feature of the tested specimen is shown in Fig. 30. The fractured surface represents Case 2 indicating higher bit-coal interaction and frictional contact resulting in production of more percentage of fines and less of large fragments as exhibited in Fig. 31a-b. The analysis of airborne dust, collected by cascade impactor, indicated that smaller aerodynamic particles with higher particle size spread ($MMD = 9.0$, $GSD = 2.77$) were reproduced when coal specimen of Pittsburgh seam was tested under similar tests carried out on the Waynesburg seam. A comparison between the two coal seams in the dust size range is presented in Fig. 32 as well as in Table 5. Table 5 shows 61.70 percent of respirable mass having particle size in the range of 6.0×0.6 microns for the Pittsburgh seam as compared to 56.70 percent for the Waynesburg seam.

CONCLUSIONS

Only a limited number of tests have been performed at a specific condition on the two types of coal to evaluate the effect of various parameters on coal cutting. However, the results of this study have yielded many distinct conclusions which can be summarized as follows:

The depth of cut and bit spacing seem to have by far the most affect on the breakage of the coal boundary between the bit paths. The results indicate that increasing the cutting head speed increased the percentage of large sized fragments and reduced the percentage of fine material produced. Of the four attack angles tested, the 30 degree, clearly gave the highest percentage of large material and the fewest fines. The effect of in-situ stresses seems to depend on the cutting direction as well as the physical and mechanical properties of the coal, thus confining pressure may shift the size distribution depending upon other factors. Under the same testing conditions cutting along the butt cleat produced more fines and less large fragments as opposed to the face cleat. Also, under the same testing conditions bit type appears to only have an offset on the percentage of fines and amount of dust produced in the area of the bit path. It is evident that each coal has its own fragmentation characteristics, thus reflecting its product size distributions. More fines and dust were produced in cutting Pittsburgh coal than Waynesburg coal.

For most of the parameters studied, an apparent relationship between the size distribution and the fractured surface characteristics exist. These parameters include: bit type, bit spacing, depth of cut, in-situ stresses (confining pressure), cleat orientation and coal type the only exceptions being bit attack angle and cutting head velocity. In many cases from the apparent characteristics of the fracture surface, one can tell how the fragmentation process has taken place with respect to the size distribution and resulting dust generation.

It appears that the key to achieving efficient coal fragmentation is to limit the degree of bit-coal interaction that takes place in the bit path while causing maximum breakage of the coal boundary (wall) between the paths. By increasing the degree

of breakage of the coal boundary, it not only increases the percentage of large fragments produced but limits the amount of secondary crushing that takes place in the bit path which results in decreasing fines and consequently the amount of dust. Cutting bits having proper (carbide tip and body) shape, size and geometry (stream lined shape) will enhance further reduction of dust.

ACKNOWLEDGMENTS

This project was funded by the Generic Center for the Respirable Dust Research sponsored by the U.S. Bureau of Mines under Grant No. G1135142.

FRAGMENT SIZE DISTRIBUTION AND FRACTURE SURFACE

REFERENCES

1. Leonard, J.W.: Coal Preparation, pp. 6-19. Port City Press, Inc., Baltimore, Maryland (1979).
2. Pomeroy, C.D.: Mining Applications of the Deep Cut Principle. *The Mining Engineer* 20(6):506-517 (1968).
3. Warner, E.M.: Machine and Cutting Element Design. *Mining Congress Journal* 56(8):35-43 (1970).
4. Newmeyer, G.E.: Cost of Black Lung Program. *Mining Congress Journal* 67(11):74-75 (1981).
5. National Materials Advisory Board (NMAB): Measurement and Control of Respirable Dust in Mines, pp. 1-25. National Academy of Sciences, Washington, DC (1980).
6. Rad, P.F.: Mechanical Properties and Cutting Characteristics of Coal, 66 pp. U.S. Department of the Interior, Bureau of Mines, IC 8585 (1973).
7. Evans, I. and S. Murrell: Conference on Mechanical Properties of Nonmetallic Brittle Materials, pp. 432-450. Butterworths, London (1958).
8. Hartman, H.L.: Basic Studies of Percussion Drilling. *Mining Engineering* 11(1):68-75 (1959).
9. Paul, B. and D.L. Sikarskie: Preliminary Theory of Static Penetration by a Rigid Wedge into a Brittle Material. *Transactions, Society of Mining Engineers* 233(2):372-383 (1965).
10. Lawn, B.R. and M.V. Swain: Microfracture Beneath Point Indentations in Brittle Solids. *Manual of Materials Science* 10, 22(8):113-122 (1975).
11. Devilder, W.M.: Correlation of Fragment Size Distribution and Fracture Surface in Coal Cutting Under Various Conditions, 117 pp. M.S. Thesis, Department of Mining Engineering, West Virginia University (1986).
12. Barker, J.S.: A Laboratory Investigation of Rock Cutting Using Large Picks. *International Journal of Rock Mechanics* 1:519-534 (1964).
13. Khair, A.W.: Design and Fabrication of a Rotary Coal Cutting Simulator. *Proceedings of the Coal Mine Dust Conference*, pp. 190-197. Department of Mining Engineering, West Virginia University (1984).
14. Daniel, H.J.: Respirable Dust Control Research—The Bureau of Mines Program. *Proceedings of the Coal Mine Dust Conference*, pp. 1-8. Department of Mining Engineering, West Virginia University (1984).
15. Niewiadomski, G.: Improving Dust Control Technology for U.S. Mines. *Proceedings Symposium on Control of Respirable Coal Mine Dust*, pp. 41-73. Beckley, WV (1983).
16. Roepke, W.W., D.P. Lindroth and T.A. Myren: Reduction of Dust and Energy During Coal Cutting Using Point Attack Bits, 53 pp. U.S. Department of the Interior, Bureau of Mines, RI 8185 (1976).

THE RESPIRABLE DUST CENTER

17. Roepke, W.W., C.F. Wingvist, B.D. Hanson and L.L. Sundae: Research on Reducing Generation of Primary Respirable Dust in Cutting Coal. Proceedings of the Coal Mine Dust Conference, pp. 37-44, Department of Mining Engineering, West Virginia University (1984).
18. Hamilton, R.J.: Principles of Machine Design and Operation Related to Dust Production and Control with Particular Reference to Longwall Mining in the United Kingdom. Proceedings Symposium on Respirable Coal Mine Dust, pp. 160-178. Washington, DC (1969).
19. Roepke, W.W. and B. D. Hanson: New Cutting Concepts for Continuous Miners. Coal Mining and Processing 16(10):62-67 (1979).
20. Roepke, W.W.: U.S. Bureau of Mines Coal-Cutting Research for Dust and Energy Reduction. Proceedings of the European Economic Community Symposium on Reduction of Dust in Coal Mining, pp. 12-23. Luxemburg (1983).
21. Fuh, G.F.: On the Determination of Cutter Bit Spacing for Optimum Coal Mining. Proceedings 24th U.S. Symposium on Rock Mechanics, pp. 703-712 (1983).
22. Black, S., B.V. Johnson, R.L. Schmidt and B. Banerjee: Impact of Deeper Depths of Cut on Coal Mining Machines and Respirable Dust, pp. 161-179. U.S. Bureau of Mines Unofficial Report (1976).
23. Friedman, M. and L.M. Ford: Analysis of Rock Deformation and Fractures Induced by Rock Cutting Tools Used in Coal Mining. Proceedings 24th U.S. Symposium on Rock Mechanics, pp. 713-723 (1983).
24. Strebis, K.C. and H.W. Zeller: Effect of Depth of Cut and Bit Type on the Generation of Respirable Dust, 16 pp. U.S. Department of the Interior, Bureau of Mines, RI 8042 (1975).
25. Arentzen, R.F.: Machine Design: State of the Art. Proceedings Symposium on Respirable Coal Mine Dust, pp. 178-183. Washington, DC (1969).
26. Khair, A.W. and M.K. Quinn: Mechanisms of Respirable Dust Generation by Continuous Miner. Preprint No. 85-413, 14 pp., presented at the SME-AIME Fall Meeting, Albuquerque (1985).
27. Hinds, C.W.: Particle Size Statistics. Aerosol Technology, Properties, Behavior, and Measurement of Airborne Particles, Chapter 4, pp. 69-103. John Wiley and Sons, New York, New York (1982).

FRAGMENT SIZE DISTRIBUTION AND FRACTURE SURFACE

Table 1
Physical Properties of Waynesburg Coal

Moisture %	Ash %	Sulfur %	Rank	HGI*	Sp.Gr.
0.0-1.5	13.5-13.7	2.03-2.06	hbBv**	50.43	1.42

*Hardgrove Grindability

**High Volatile B Bituminous

THE RESPIRABLE DUST CENTER

**Table 2
Mechanical Properties of Waynesburg Coal**

Cleat/Bedding Plane Orientation	Compressive Strength psi (kPa)	Young's Modulus psi (kPa)	Poisson's Ratio	Indirect Tensile Strength psi (kPa)	Direct Shear Strength psi (kPa)
Face Cleat	3289 (473.6)	5.1×10^5 (7.3×10^4)	0.25	154 (22.2)	204 (29.4)
Butt Cleat	3459 (498.1)	4.7×10^5 (6.8×10^4)	0.31	205 (29.5)	180 (25.9)
Bedding Plane	4912 (707.4)	4.6×10^5 (6.6×10^4)	0.32	146 (21.0)	80 (11.5)

FRAGMENT SIZE DISTRIBUTION AND FRACTURE SURFACE

Table 3
Respirable Mass Fraction Sampled by Impactors While Cutting with Different Bit Types (Face Cleat)

Bit Type	Concentration	Particle Size (μm)	
		10.0 x 6.0	6.0 x 0.6
III	A. Weight* (mg)	7.69	10.61
	N. Weight ⁺ (mg)	8.35	11.53
	Percent	42.00	58.00
IV	A. Weight* (mg)	8.61	11.28
	B. Weight ⁺ (mg)	8.61	11.28
	Percent	43.30	56.70
V	A. Weight* (mg)	2.95	9.45
	B. Weight ⁺ (mg)	4.72	15.17
	Percent	23.70	76.30

*Actual weight sampled

⁺Normalized with the highest weight in series

THE RESPIRABLE DUST CENTER

Table 4
Respirable Mass Fraction Sampled by Impactors While Cutting at Different
Drum Speeds (Face Cleat)

Drum RPM	Concentration	Particle Size (μm)	
		10.0 x 6.0	6.0 x 0.6
25	A. Weight* (mg)	8.61	11.28
	N. Weight [†] (mg)	8.76	11.47
	Percent	43.30	56.70
35	A. Weight* (mg)	8.99	11.24
	B. Weight [†] (mg)	8.99	11.24
	Percent	44.40	55.60

*Actual weight sampled

[†]Normalized with the highest weight in series

FRAGMENT SIZE DISTRIBUTION AND FRACTURE SURFACE

Table 5
Respirable Mass Fraction Sampled by Impactors While Cutting Different Types
of Coals (Face Cleat)

Coal Type	Concentration	Particle Size (μm)	
		10.0 x 6.0	6.0 x 0.6
Waynesburg	A. Weight* (mg)	8.61	11.28
	N. Weight+ (mg)	11.12	14.57
	Percent	43.30	56.70
Pittsburgh	A. Weight* (mg)	9.83	15.86
	B. Weight+ (mg)	9.83	15.86
	Percent	38.30	61.70

*Actual weight sampled

+Normalized with the highest weight in series

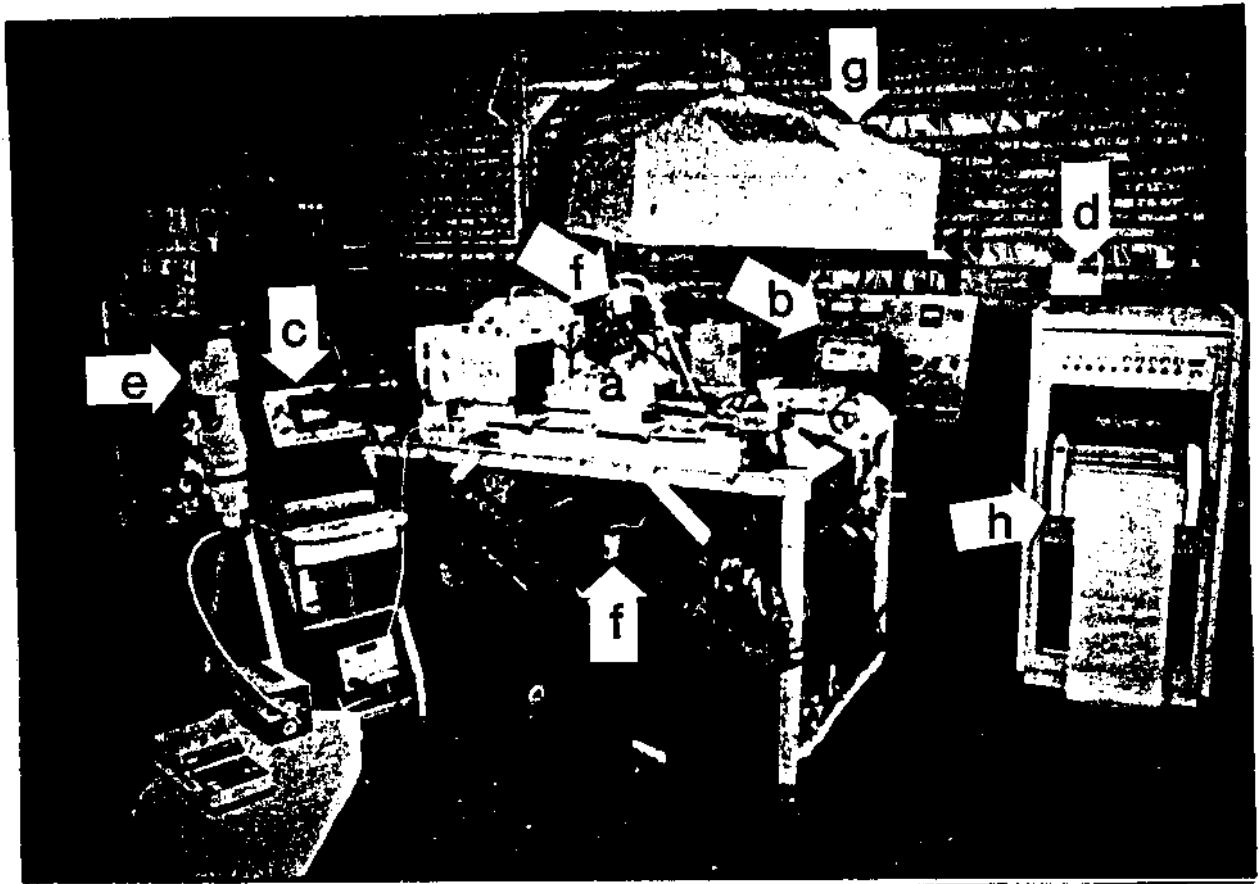


Figure 1. Test and monitoring equipment facilities (a) automated rotary coal cutting simulator, (b) programable control and monitoring unit, (c) sonic testing unit, (d) acoustic emission, (e) microscope and the attached camera unit, (f) cascade impactors, (g) hood and air current generating unit and (h) data acquisition and recording unit.

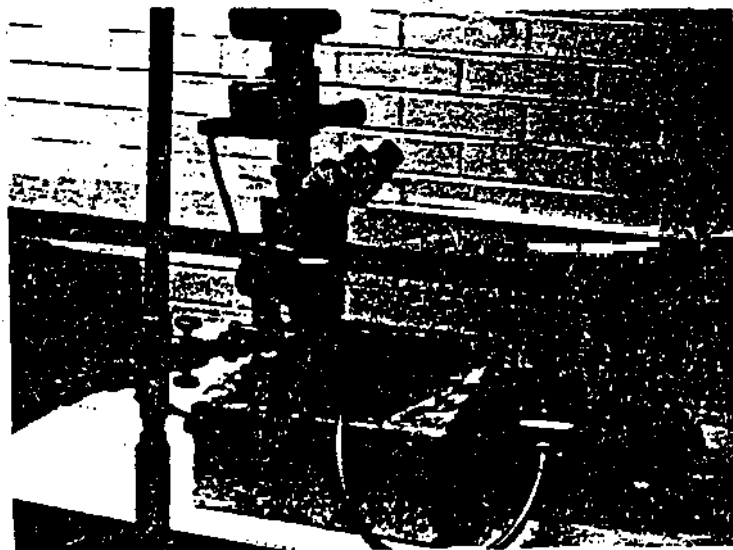


Figure 2. Illustrates facilities used in microscopic photography of the fractured surface of the tested specimen.

FRAGMENT SIZE DISTRIBUTION AND FRACTURE SURFACE

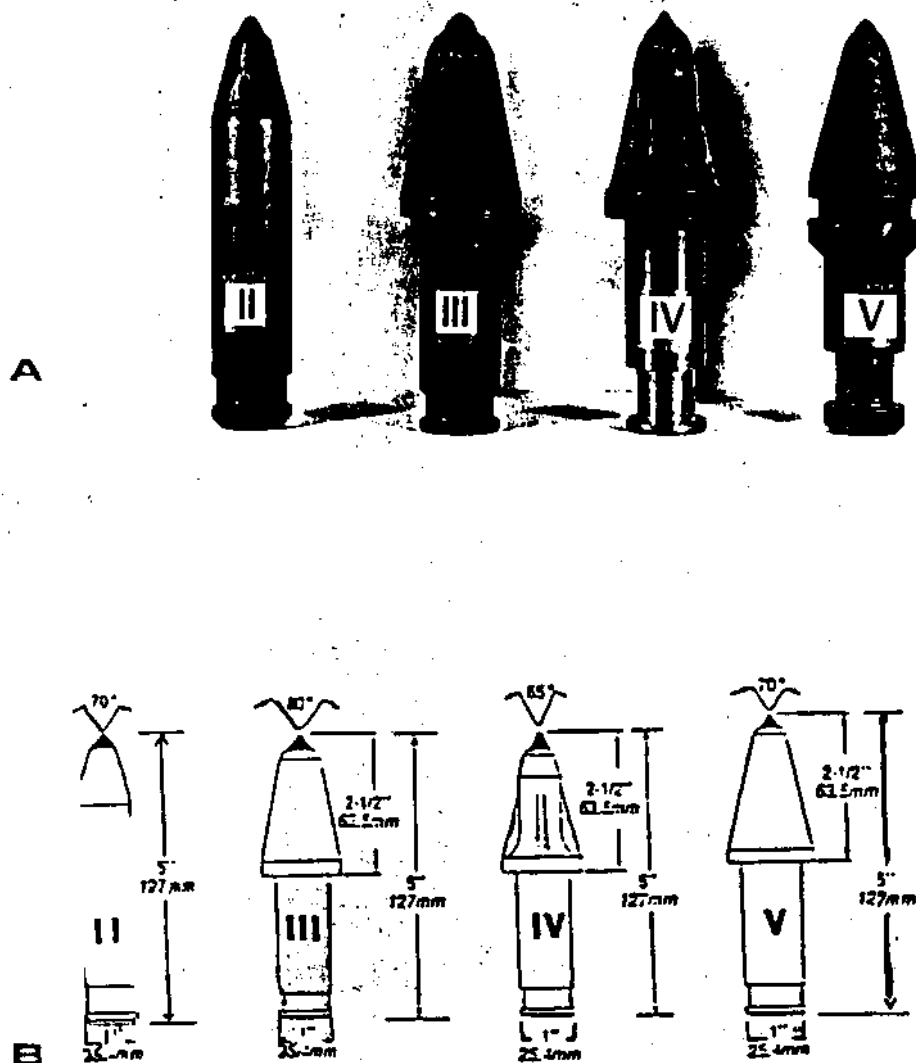


Figure 3. Illustrates four types of bits: (a) Type II, pencil bit with medium carbide tip; Type III, plumbob bit with large carbide tip; Type IV, sharp/slender bit with fins and sharp carbide tip; Type V, plumbob bit with medium carbide tip. (b) corresponding manufacturers specifications showing bit dimensions and angle of carbide tip.

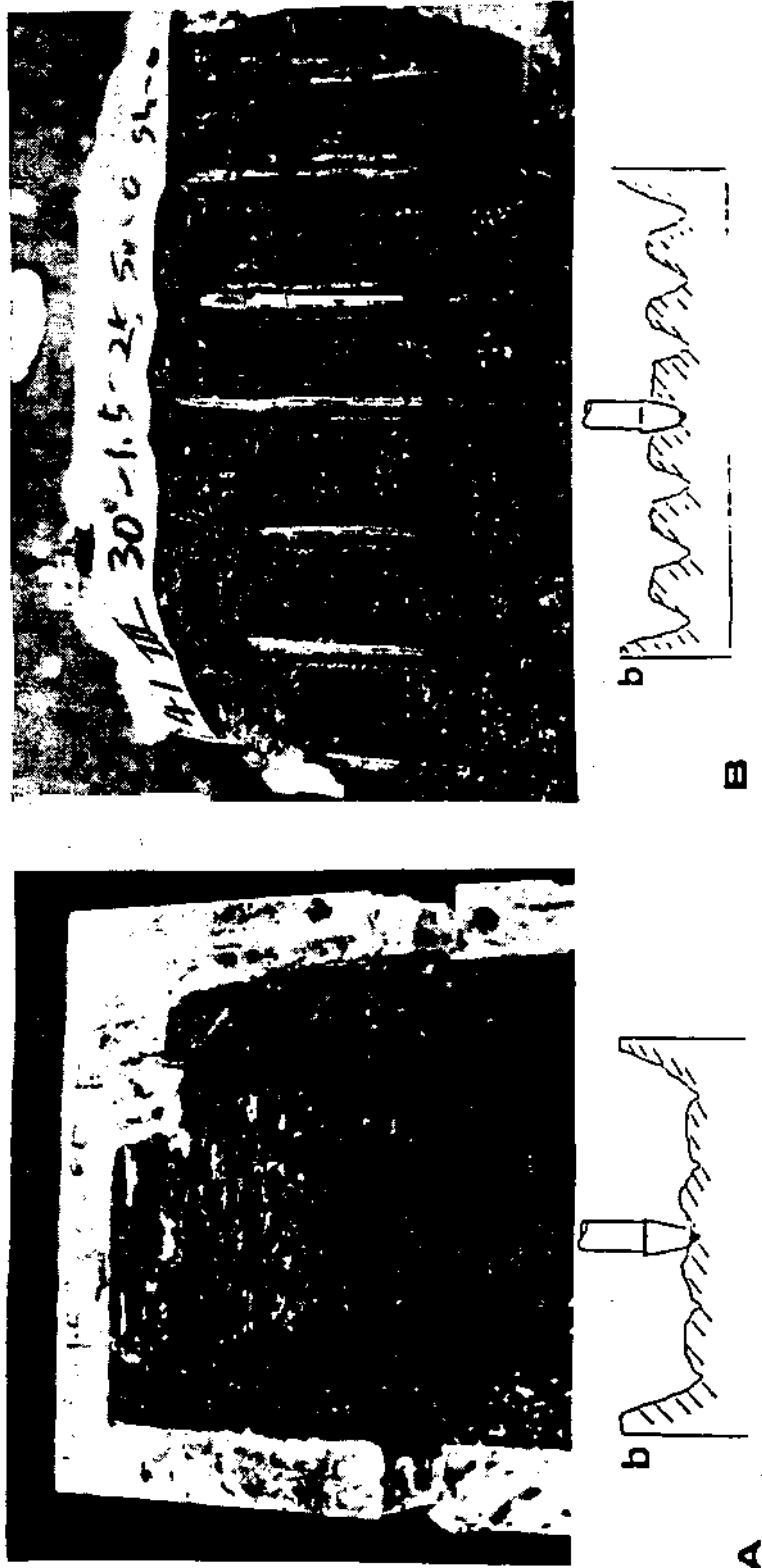


Figure 4. Illustrates two types of fractured surfaces: A - Case 1, B - Case 2 (a - photographs of typical test representing each case, b - general cross-section corresponding to each case).

FRAGMENT SIZE DISTRIBUTION AND FRACTURE SURFACE

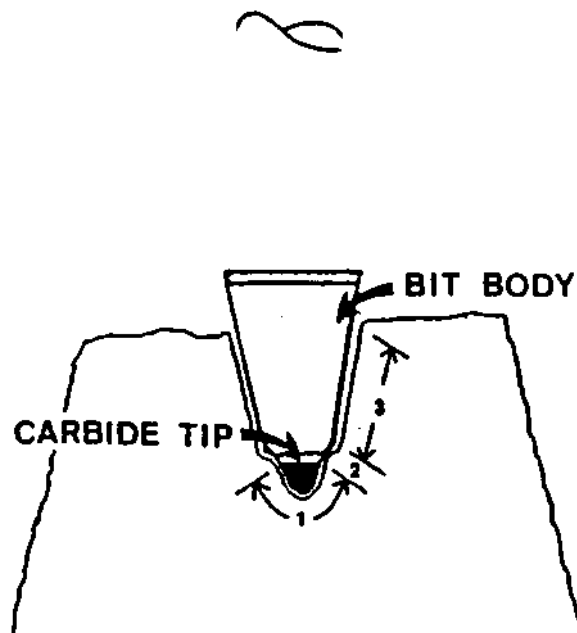


Figure 5. Shows the three zones of the bit which correspond to three distinct zones of the bit path.

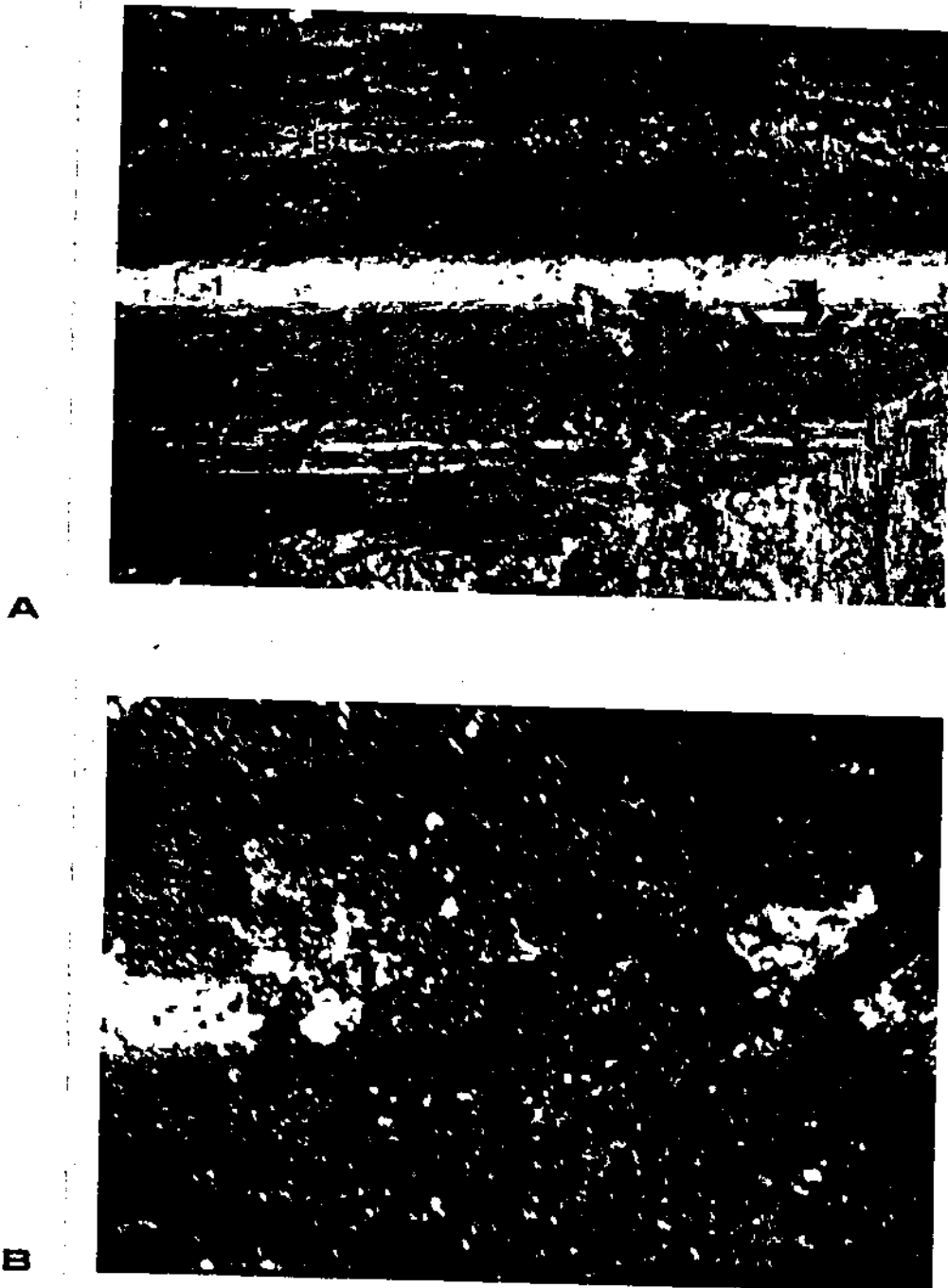


Figure 6. Microscopic pictures of the center bit path taken in the middle of the coal block (test #41). (a) Indicates the three zones of the bit path (1,2,3) and the three features within these zones (A,B,C) taken with a .66 zoom setting; (b) shows the same material created upon disturbing the shiny surface taken with a 1.5 zoom setting.

FRAGMENT SIZE DISTRIBUTION AND FRACTURE SURFACE

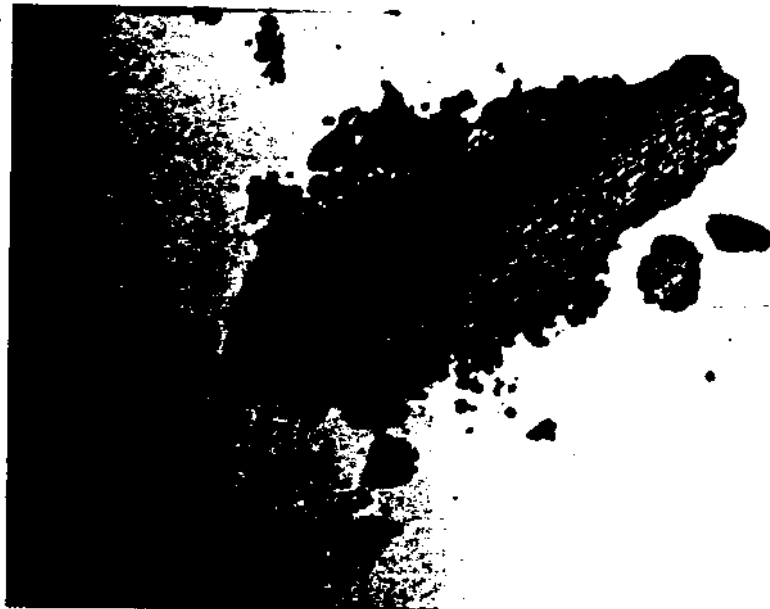


A

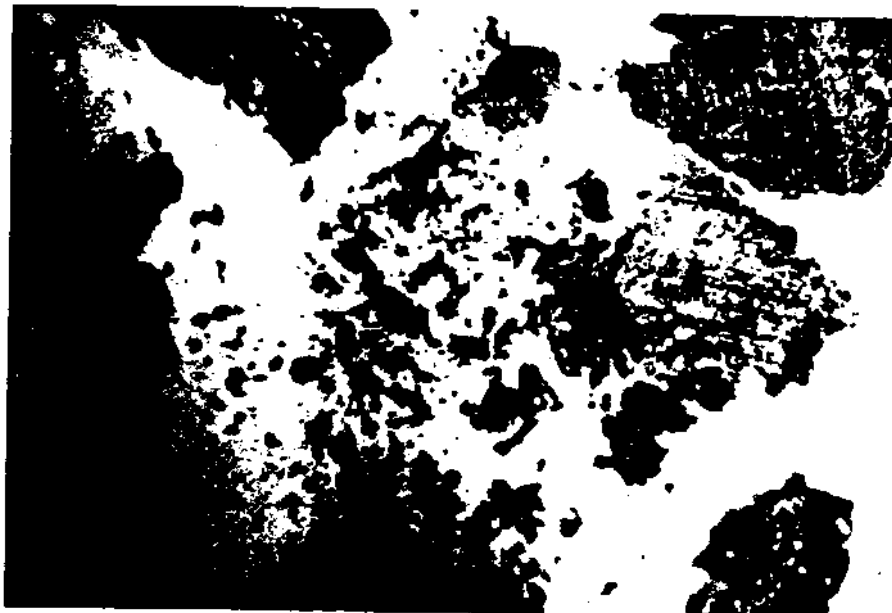


B

Figure 7. Microscopic pictures of Zone 3. (a) Indicates the three features (A,B,C) in Zone 3 taken with a .66 zoom setting; (b) shows Zone 3 after lightly brushing the surface.



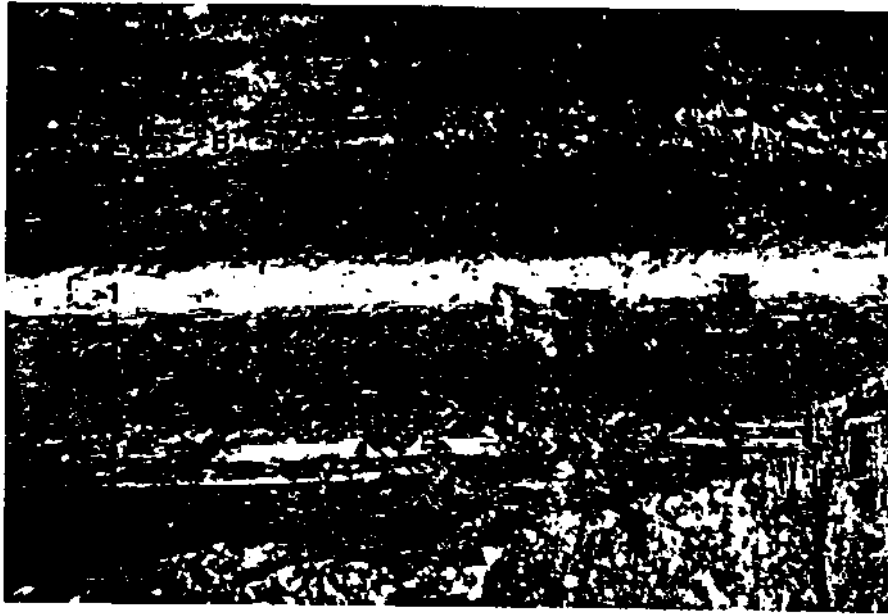
A



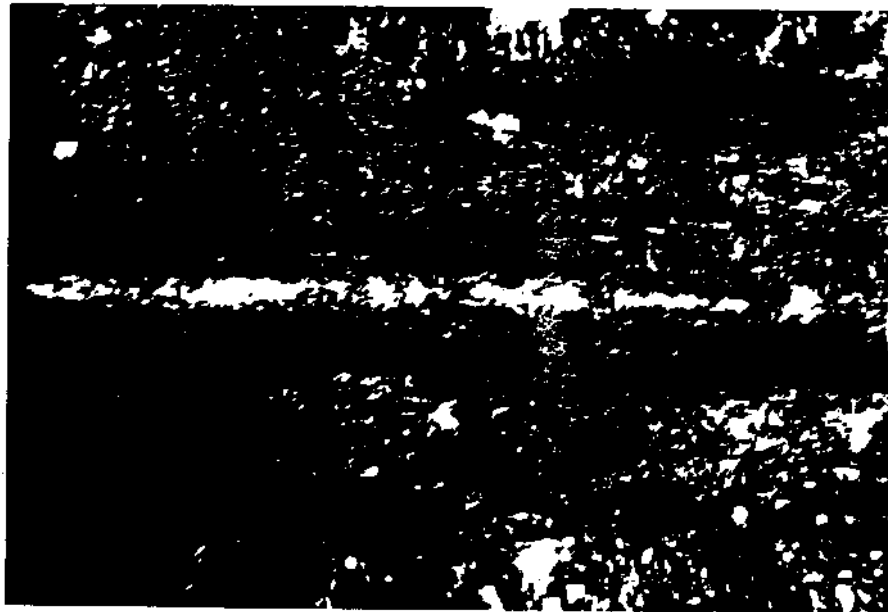
B

Figure 8. Microscopic pictures of the shiny surface and related material. (a) Typical piece of material removed from the area of contact with the carbide tip (Zone 1) and resulting pocket of crushed material beneath it; (b) typical piece of material removed from the side of the bit path (Zone 3) note the clustering of the very fine material, magnified 11 times.

FRAGMENT SIZE DISTRIBUTION AND FRACTURE SURFACE



A



B

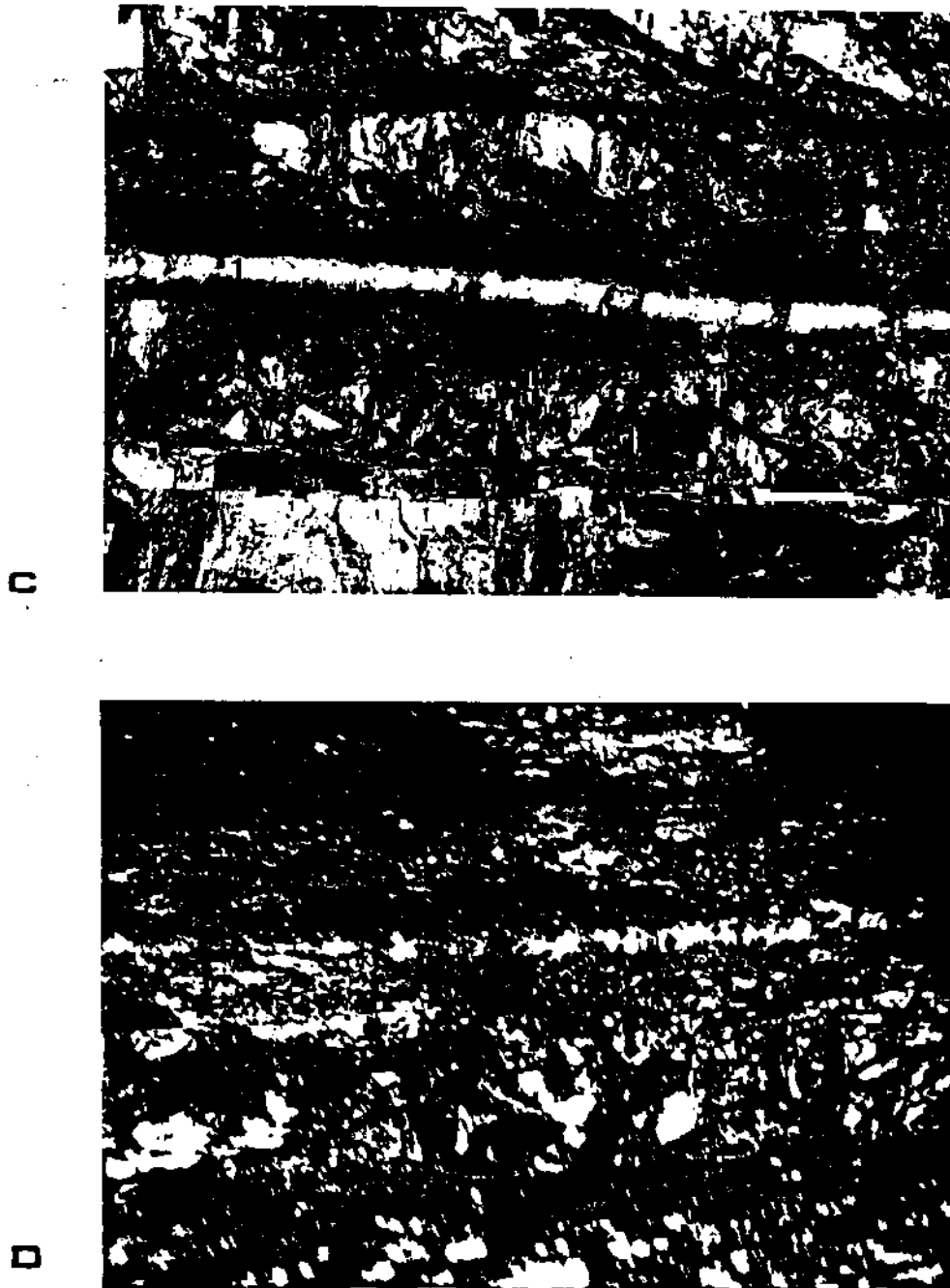


Figure 9. Shows the corresponding microscopic photographs in the center bit path taken with a .66 zoom setting in the middle of the coal block. The three zones (1,2,3) are appropriately labeled. (a) Test #41, Type III bit; (b) Test #43, Type V bit; (c) Test #36, Type II bit; (d) Test #35, Type IV bit.

FRAGMENT SIZE DISTRIBUTION AND FRACTURE SURFACE

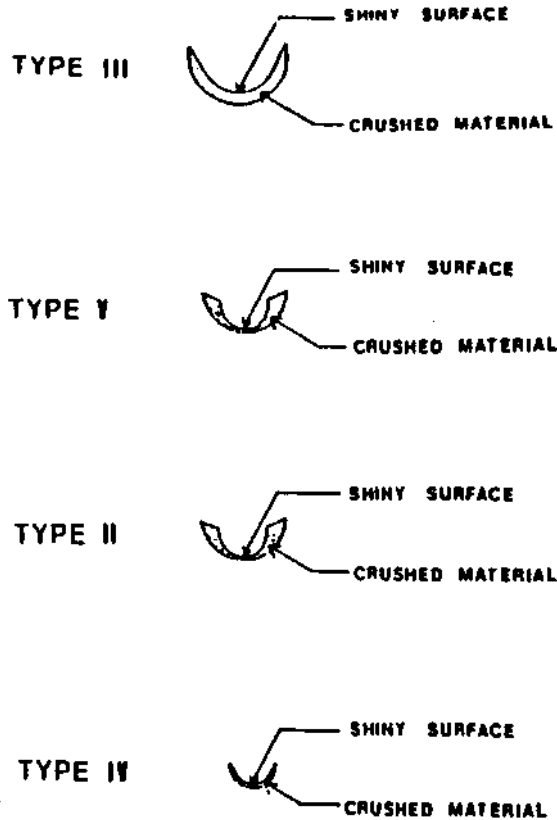


Figure 10. Shows the relative size and shape of the pocket of crushed material in Zone 1 for each bit type (not to scale).

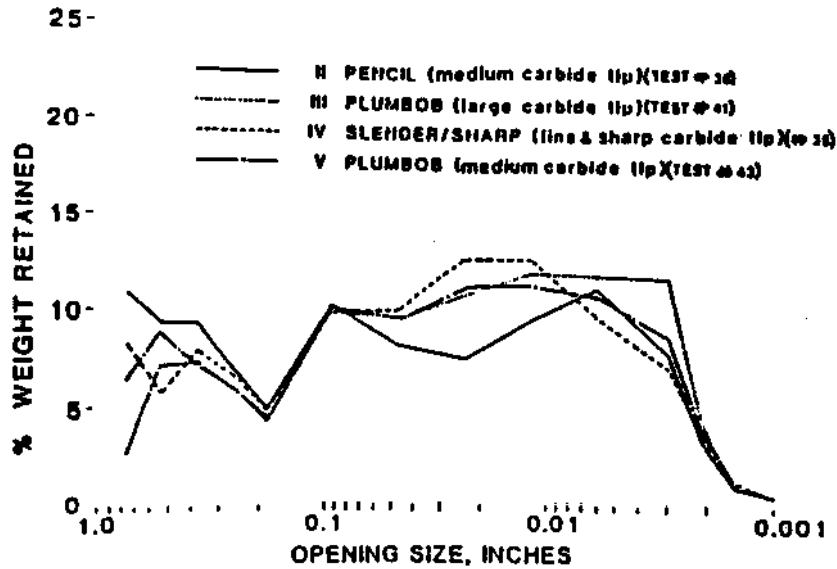


Figure 11. Opening size vs. percent of weight retained as a function of bit type when cutting against the face cleat (representative of the Case 2 fracture surface).

THE RESPIRABLE DUST CENTER

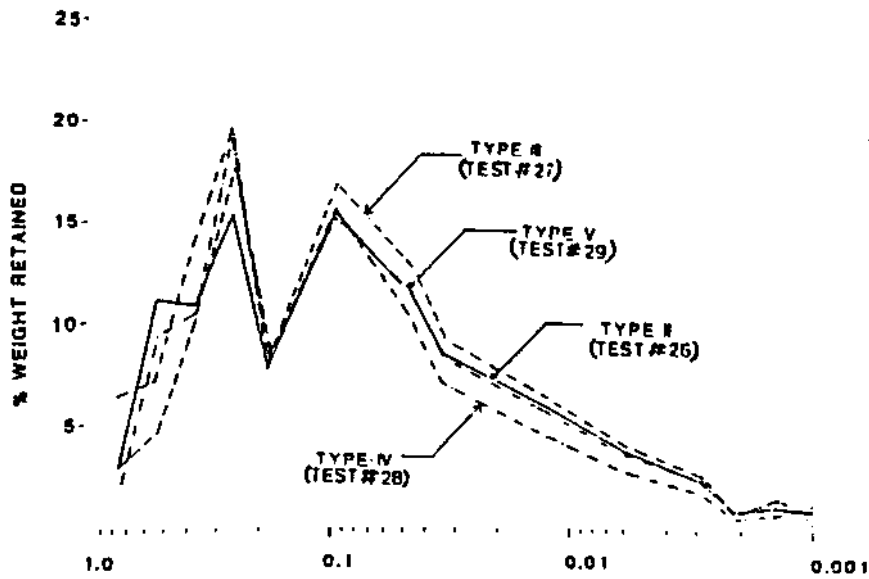


Figure 12. Opening size vs. percent of weight retained as a function of bit type when cutting against the face cleat (representative of the Case 1 fracture surface).

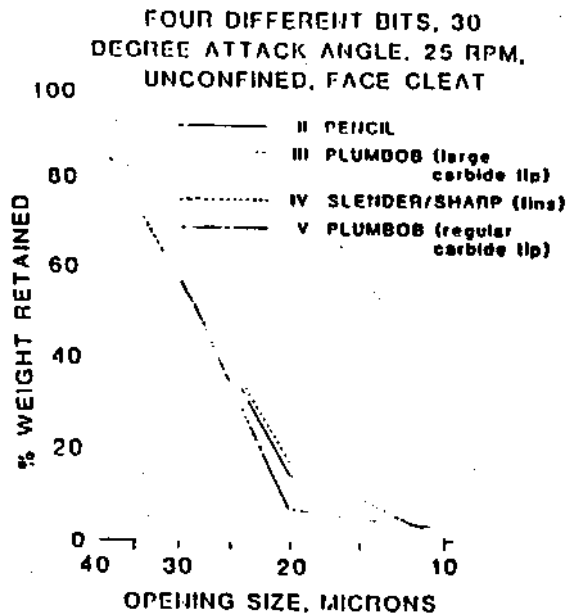


Figure 13. Mesh size versus percent of weight retained as a function of bit type, dust size distribution from 37 microns (400 mesh) to -10 microns.

FRAGMENT SIZE DISTRIBUTION AND FRACTURE SURFACE

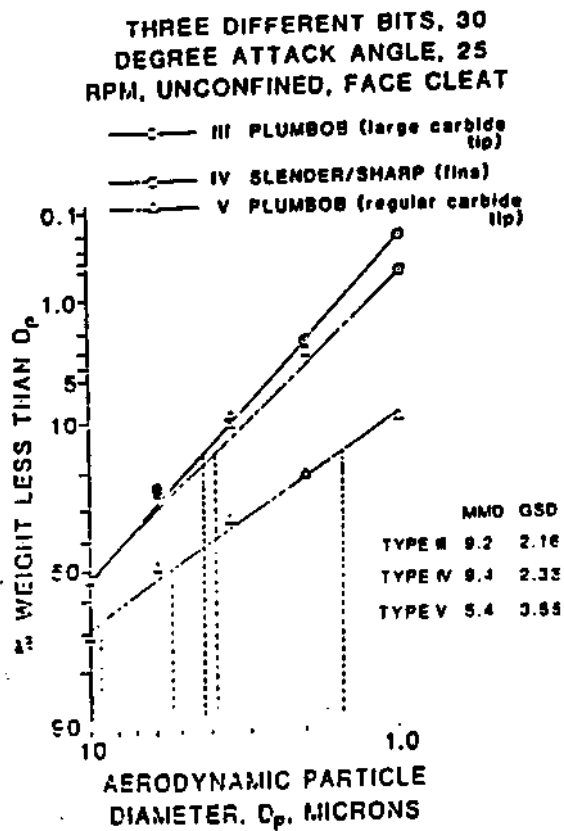


Figure 14. Particle size distribution of the respirable coal dust sampled by cascade impactors, while cutting coal with different types of bits.

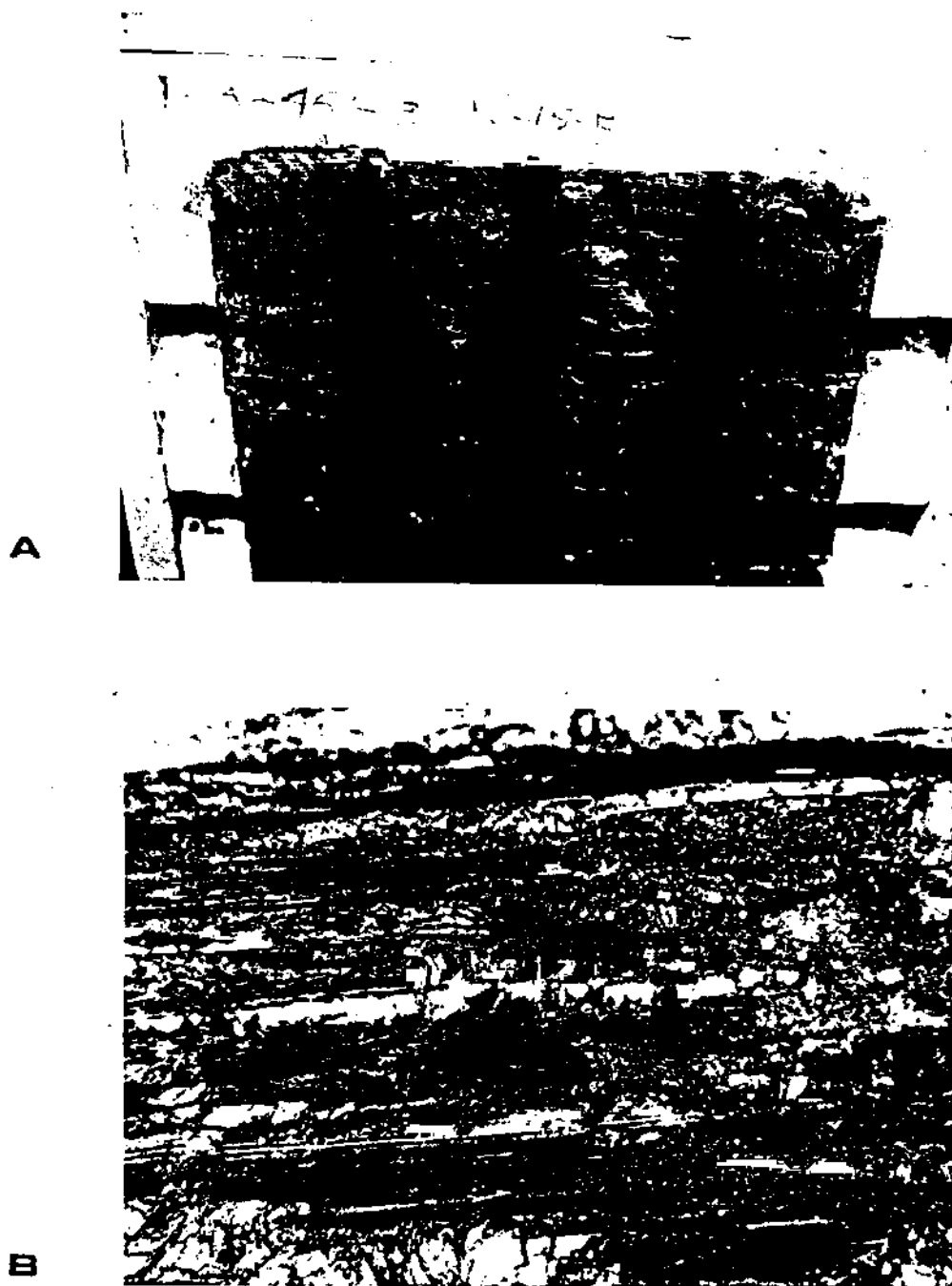


Figure 15. (a) Photograph of the coal block of test #3 after cutting against the face cleat; (b) microscopic photograph taken approximately 1.5 inches from the entrance of the center bit with .66 zoom setting.

FRAGMENT SIZE DISTRIBUTION AND FRACTURE SURFACE

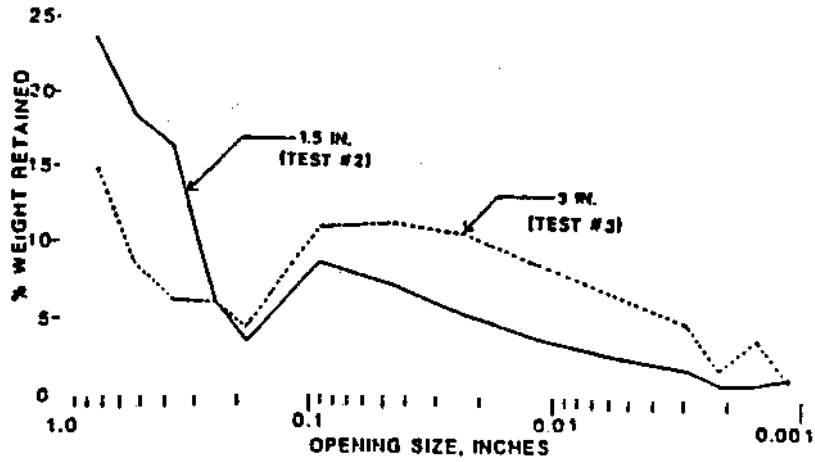


Figure 16. Opening size vs. percent of weight retained as a function of two different bit spacings when cutting against the face cleat.

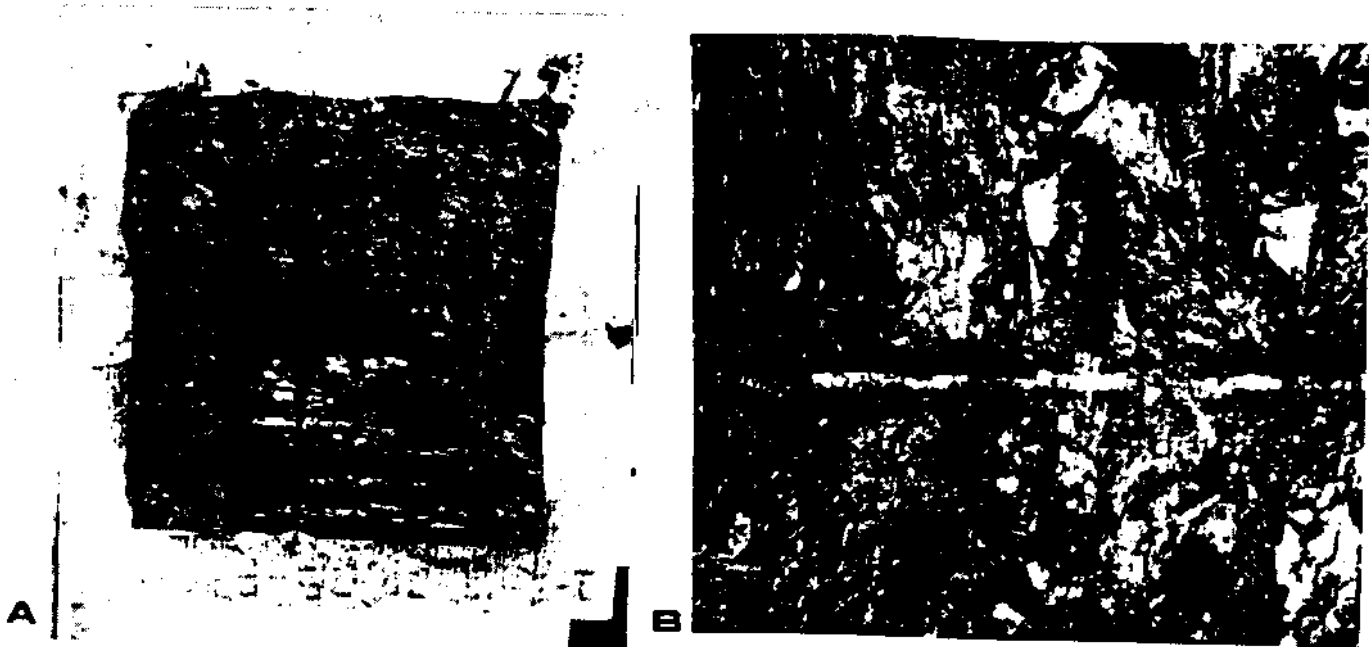


Figure 17. (a) Photograph of the coal block of test #11 after cutting along the face cleat; (b) microscopic photograph taken of the center bit path in the middle of the coal block with a .66 zoom setting.



A



B

Figure 18. (a) Photograph of the coal block of test #35 after cutting against the face cleat; (b) microscopic photograph of test #35 taken of the center bit path near the middle of the coal block with a .66 zoom setting.

FRAGMENT SIZE DISTRIBUTION AND FRACTURE SURFACE

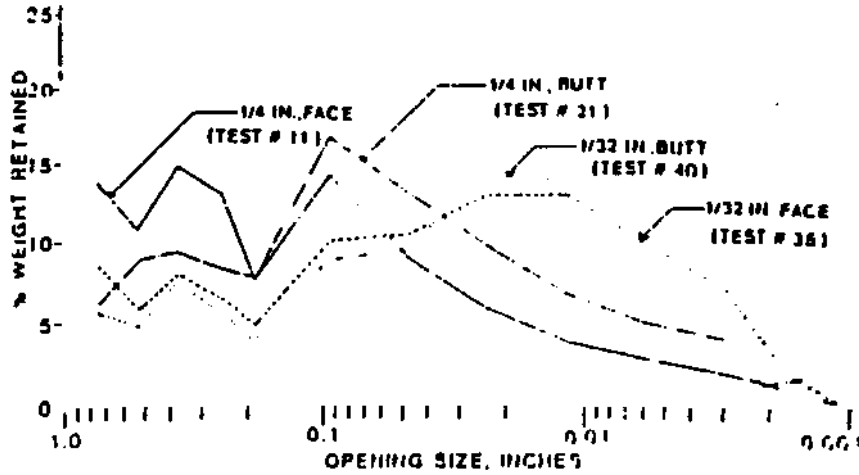


Figure 19. Opening size vs. percent of weight retained as a function of two different depths of cut per revolution and cleat directions.

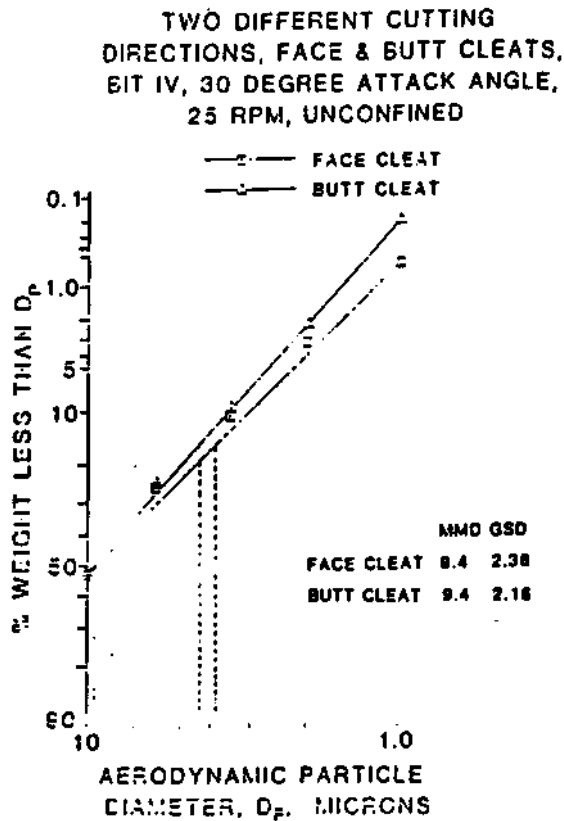


Figure 20. Particle size distribution of respirable coal dust sampled by cascade impactors while cutting coal with different cleat orientations.

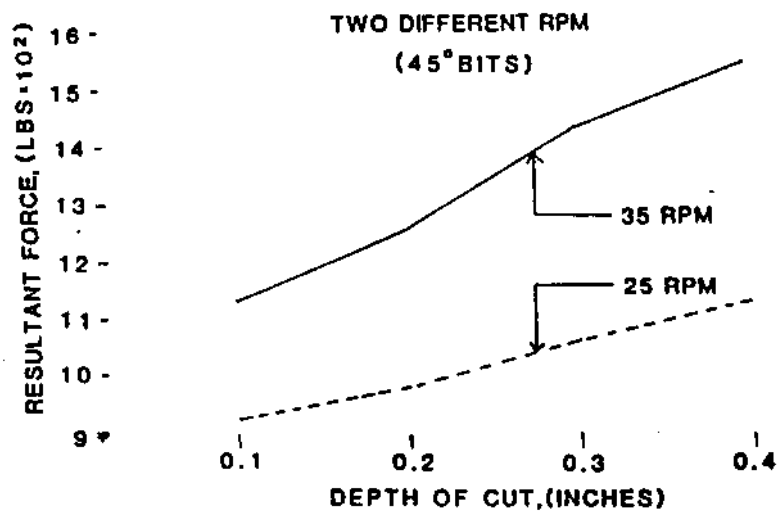
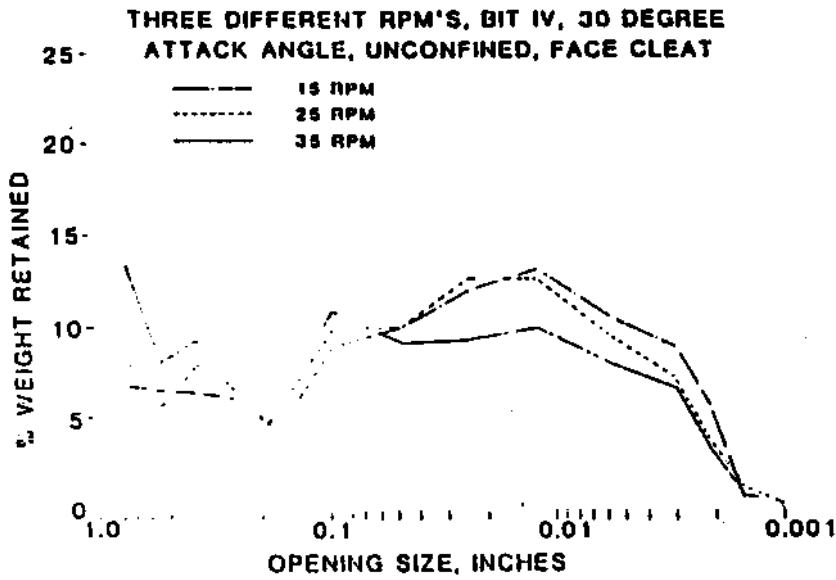
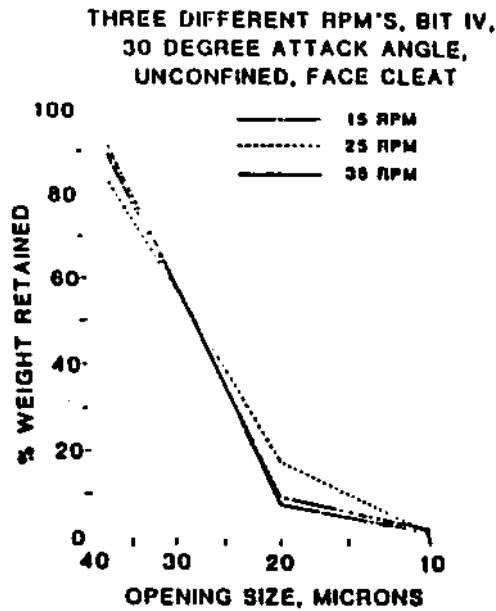


Figure 21. Resultant force vs. depth of cut as a function of rpm (face cleat direction).

FRAGMENT SIZE DISTRIBUTION AND FRACTURE SURFACE



A



B

Figure 22. Mesh size versus percent of weight retained as a function of cutting head speed (rpm) for face cleat orientation, (a) fragment size distribution from 1.885 cm (0.742 in.) to 0.0038 cm (0.0015 in.) or 400 mesh and (b) dust size distribution from 37 microns (400 mesh) to -10 microns.

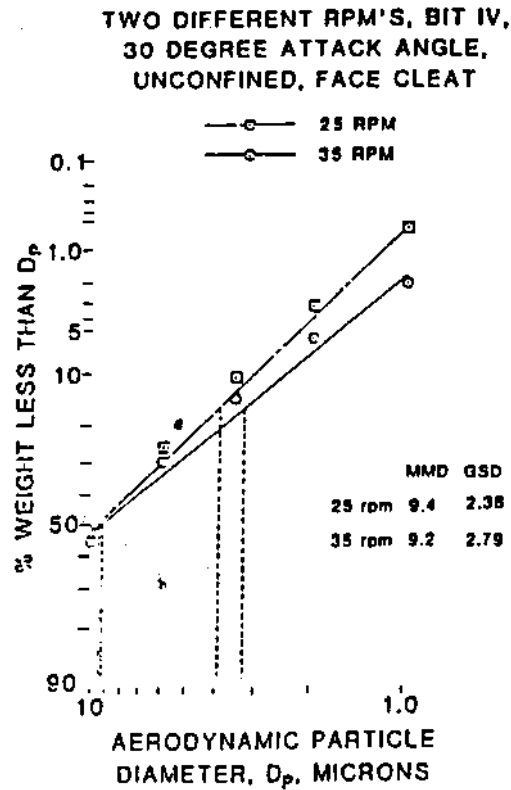


Figure 23. Particle size distribution of respirable coal dust sampled by cascade impactors while cutting coal with different cutting head speeds (rpm).

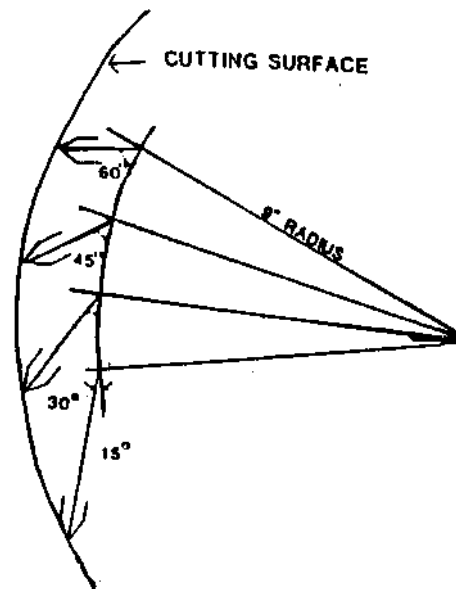


Figure 24. Illustrates the cutting surface and the area of contact between the cut surface and bits mounted at various attack angles on the cutting head.

FRAGMENT SIZE DISTRIBUTION AND FRACTURE SURFACE

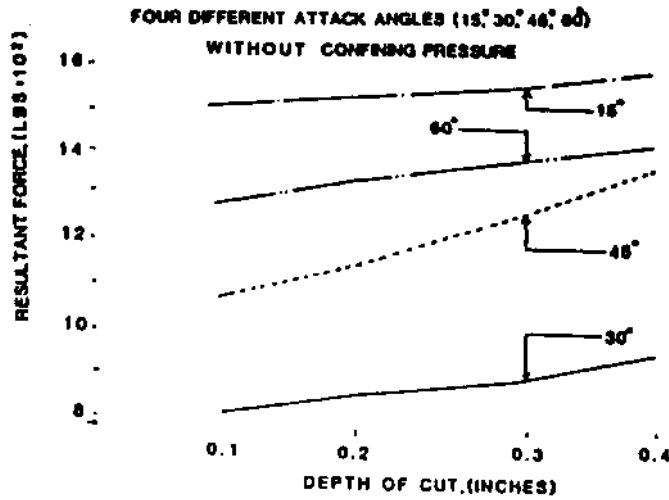


Figure 25. Resultant force vs. depth of cut as a function of bit attack angle (face cleat direction)(1 lb = 0.45 kg; 1 in. = 2.54 cm).

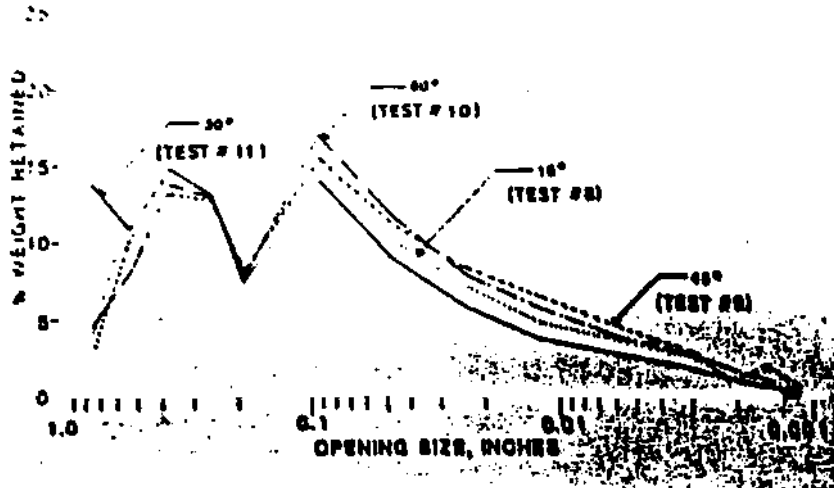


Figure 26. Opening size vs. percent of weight retained as a function of four different bit attack angles when cutting against the face cleat.

THE RESPIRABLE DUST CENTER

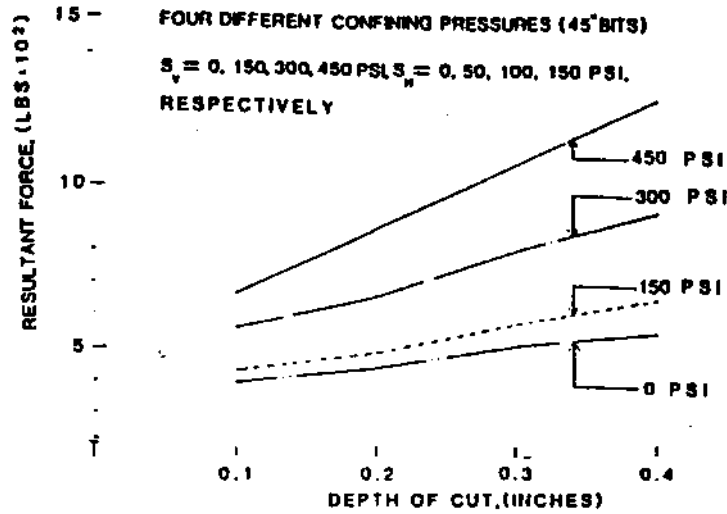


Figure 27. Resultant force vs. depth of cut as a function of equivalent in-situ pressures (face cleat direction). (1 psi = 0.144 KPa)

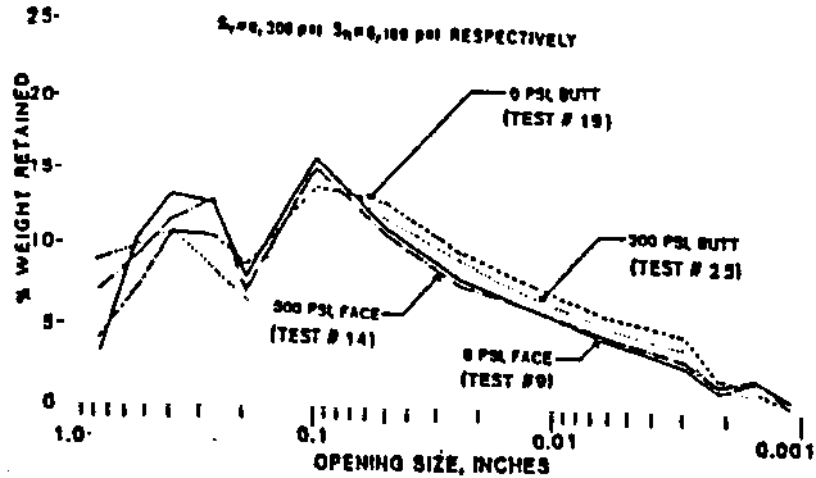


Figure 28. Opening size vs. percent of weight retained as a function of in-situ stresses and cleat directions (30° attack angle).

FRAGMENT SIZE DISTRIBUTION AND FRACTURE SURFACE

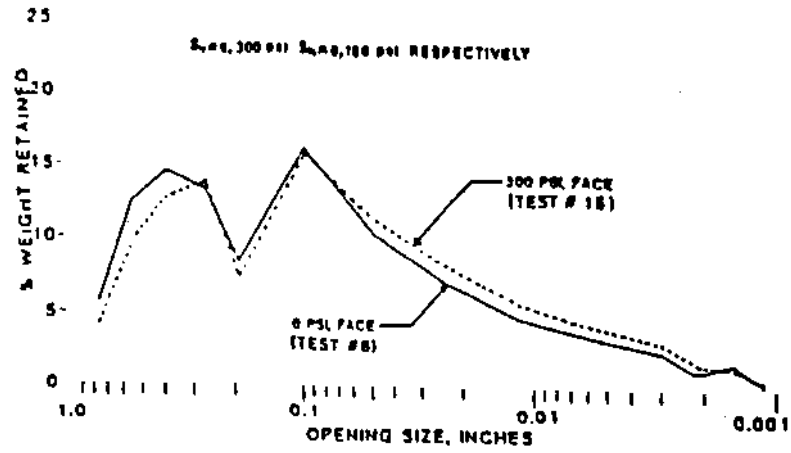


Figure 29. Opening size vs. percent of weight retained as a function of in-situ stresses when cutting along the face cleat for a 15 degree attack angle.



Figure 30. Photograph of the test specimen prepared from Pittsburgh coal seam (IV-7-30-1.5-1/32-25-F).

THE RESPIRABLE DUST CENTER

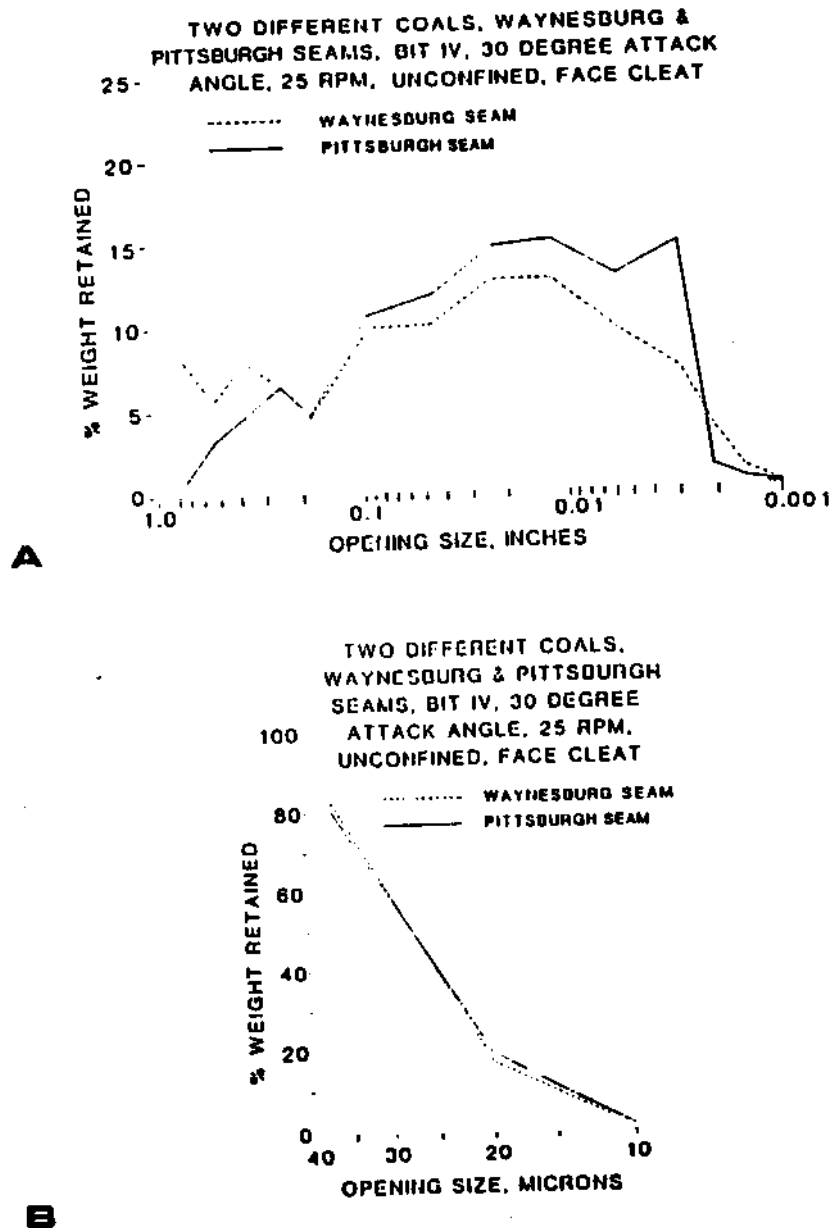


Figure 31. Mesh size versus percent of weight retained as a function of coal type (a) fragment size distribution from 0.742 in. (1.885 cm) to 0.0015 in. (0.0038 cm) or 400 mesh and (b) dust size distribution from 27 microns (400 mesh) to -10 microns.

FRAGMENT SIZE DISTRIBUTION AND FRACTURE SURFACE

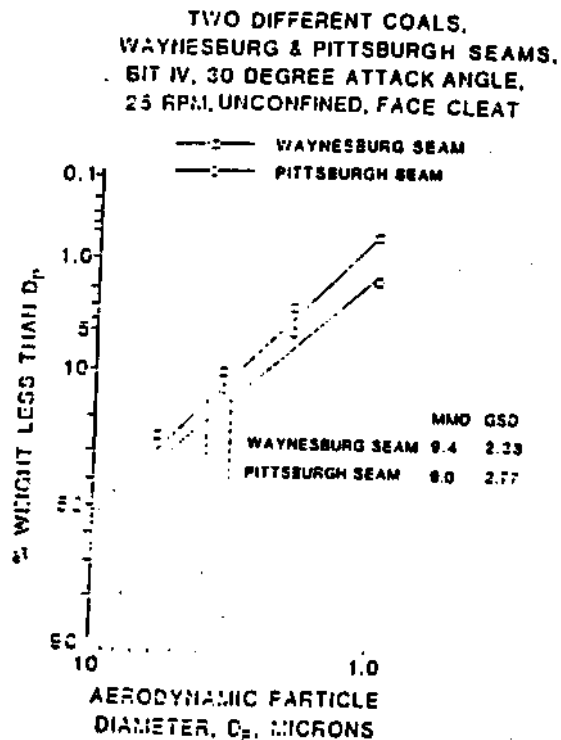


Figure 32. Particle size distribution of respirable dust sampled by cascade impactors while cutting two different coals.

Coal Fracture Analysis Using Two Simultaneous Wedge Indentors and Laser Holographic Interferometry

by

Richard D. Begley* and A. Wahab Khair

Department of Mining Engineering
West Virginia University
Morgantown, West Virginia 26506-6070

Abstract

This paper presents results of destructive tests performed on rectangular coal specimen under the influence of two vertical and simultaneous wedge indentation forces. Several wedge designs and spacings were utilized in compression tests. The objective of these experiments was to qualitatively monitor the effect of different wedge designs and spacings on the stress distribution within the coal specimen.

Coal samples from the Waynesburg coal seam were cut and trimmed to cubical dimensions of approximately 5 x 10 x 20 cm. These specimen were subjected to parallel compressive forces through two vertically applied wedge indentors. Loading was achieved with a hydraulic hand pump in order to facilitate interferogram construction. The load increments were limited due to the sensitivity of the holographic interferometric technique (holometry) in measuring small displacements; therefore, interferograms were taken only during similar increments in order to allow for a qualitative comparison between different wedge design and spacings. In some cases, interferograms were taken immediately before and after failure of the specimen.

Introduction

Failure Modes

Three distinct modes of failure occur when geologic materials are subjected to wedge indentation forces. As shown in Figure 1, a crushed zone is located immediately adjacent to the indenter while chipping can occur if the fractures initiated in the crushed zone extend upwards to the free surface. The third failure mode is a zone of intricate fractures located between the crushed zone and the chipping zone.

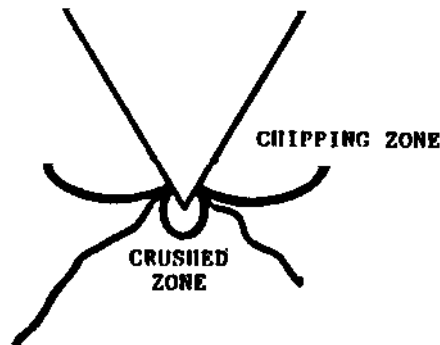


Figure 1. Failure zones that occur when geologic materials are subjected to wedge indentation forces.

*Presently with Fairmont State College, Division of Technology, Fairmont, West Virginia 26554 (304) 367-4156

COAL FRACTURE ANALYSIS

Several experiments have been conducted over the years to better understand crater formation and stress distribution within geologic materials under the influence of an indenter. Generally speaking, crack initiation and propagation observed in these experiments correlate fairly well with wedge indentation theory; however, the nature of the fractures is greatly influenced by different material properties such as grain size and cleavage planes. In other words, a wide range of behavior has been found in different rocks subjected to wedge penetration. For example, it has been observed that some rocks are merely crushed and indented while others are more prone to cracking and chip formation. Therefore, the development or nondevelopment of chips depends mostly on wedge geometry, rock type and depth of penetration. This work is part of the study associated with optimization of cutting parameters, which is best modeled by using brittle materials and subjecting them to rigid wedge penetration tests.

Holographic Interferometry

This technique has been well documented over the last few years and a thorough description can be found elsewhere.² However, holometry has only been applied to the field of rock mechanics only recently and therefore, little documentation is available. For example, over the last five years only two authors in the United States have utilized holometry in experiments reported at the Annual Rock Mechanics Symposia.^{3,4}

Holometry offers remote micromasurements and therefore requires no surface instrumentation. This capability allows one to analyze how materials deform under different levels of stress both immediately before and after failure. Since geologic materials are well known for anisotropic and inhomogeneous behavior, they are a perfect material to analyze with holometry because the effect of local flaws and inhomogeneities are easily seen.

Holometry also enables a three dimension analysis to be performed as shown in Figure 2 which compares three separate photographs of the same hologram. It seems that the surface displacement is progressing; however, since only the angle of reconstruction was varied, the different fringe orientation can be attributed to the third dimension.

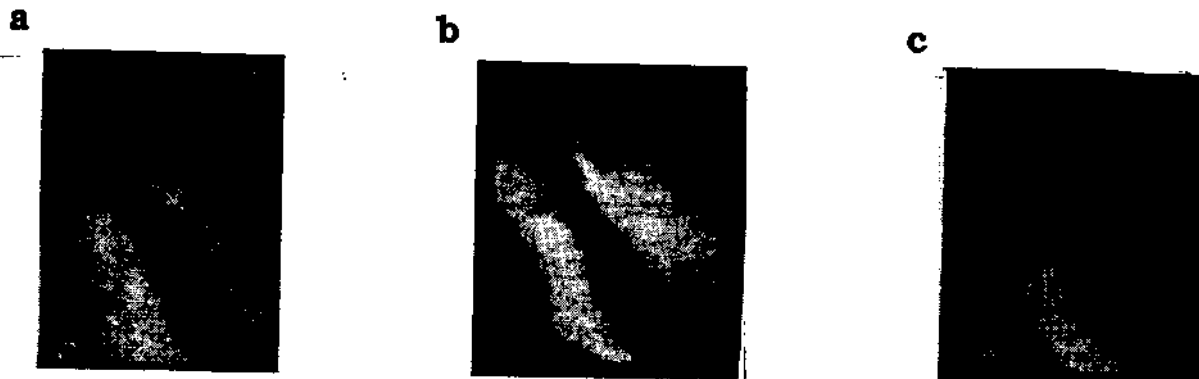


Figure 2. Compares three different photographs of the same interferogram with various angles of reconstruction.

Mechanical Properties of Coal

The mechanical behavior of coal under stress is dependent on its inherent nonhomogeneous and anisotropic condition. These inhomogeneities cause localized stress concentrations within the material. For example, all coal seams are intersected by cleavage planes perpendicular to bedding plane as illustrated in Figure 3. These cleavage planes partially contribute to the anisotropic behavior of coal. The mechanical properties are determined with destructive tests of strain gaged samples subjected to uniaxial compression loads. The results of these tests are shown in Table 1.

THE RESPIRABLE DUST CENTER

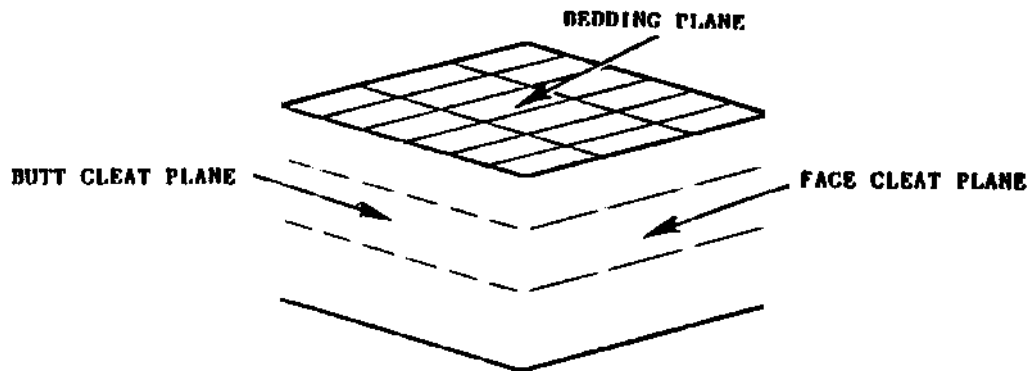


Figure 3. Illustrates cleavage planes present in coal.

Table 1. Mechanical Properties of Waynesburg Coal

Cleat/Bedding Plane Orientation	Compressive Strength psi (KPa)	Young's Modulus psi (KPa)	Poisson's Ratio	Indirect Tensile Strength psi (KPa)	Direct Shear Strength psi (KPa)
Face Cleat	3289 (473.6)	5.1×10^5 (7.3×10^4)	0.25	154 (22.2)	204 (29.4)
Butt Cleat	3459 (498.1)	4.7×10^5 (6.8×10^4)	0.31	205 (29.5)	180 (25.9)
Bedding Plane	4912 (707.4)	4.6×10^5 (6.6×10^4)	0.32	146 (21.0)	80 (11.5)

Experimental Program

Optical Procedures

All experiments were conducted on an optical table which consisted of a granite slab resting on air cells (Figure 4). The light source was a 50 milliwatt helium-neon gas laser. All interferograms were constructed with double exposures on Kodak high speed holographic glass plates and utilized the single beam construction theory as shown in Figure 4.

The angle of construction (angle between the object beam and reference beam) was 20°; therefore, using the following equation, each fringe is equivalent to a surface displacement of 13 micro-inches:

$$d = \frac{\lambda}{2 \cos \theta} \quad (1)$$

where d is the magnitude of displacement represented by each fringe, λ is the angle between the reference beam and the object beam, and θ represents the wavelength of light utilized (623.4 Angstroms).

The plates were developed in D-19 for four minutes at full strength. After a brief stop bath and a two minute fix, the plates were then rinsed thoroughly using running water and then bathed in methanol for five minutes. The plates were then bleached in a mixture of potassium bromide, potassium ferricyanide and water.

The interferograms were then photographed on technical pan film using an automatic camera with a micro lens. In order to achieve good fringe contrast, film speed was set at 250 and the film was developed in D-19 developer for four minutes. Also, a small lens opening was required. However, a considerable amount of print dodging and a very cold print paper (F-6) was required to produce adequate prints.

COAL FRACTURE ANALYSIS

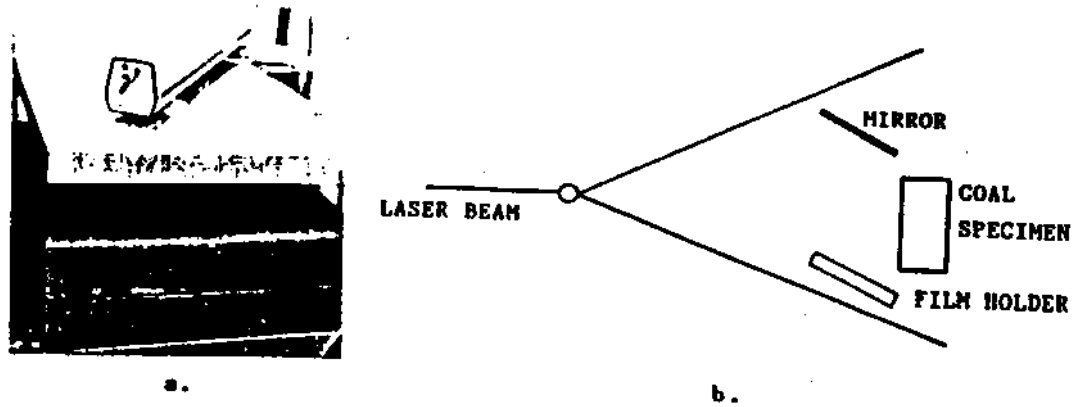


Figure 4. a) Photograph of optical table. b) Illustrates the single beam hologram construction theory.

Wedge Indentation Set Up

In order to uniformly load the specimen in between exposures of the holographic film, a specially designed loading system was required. The loading frame, as shown in Figure 5a, was designed and assembled to allow space for the reference mirror and film holder. A hydraulic cylinder was attached to the top of the frame in order to provide a vertical compressive force. Although great care is taken in specimen preparation, it is virtually impossible to achieve perfect specimen geometry; therefore, the loading system was designed to tolerate small differences in specimen dimensions without creating undesirable stress concentrations. In order to accomplish this, a series of spherical seats was utilized. As shown in Figure 5b, the vertical force was applied to the coal specimen via the wedges and a steel plate. The steel plate, which has holes drilled allowing wedge spacings of two and three inches, utilized spherical seats at the ends of the hydraulic piston and the wedges to provide uniform stress distribution. Figure 6 shows the different wedges and wedge geometries that were utilized.

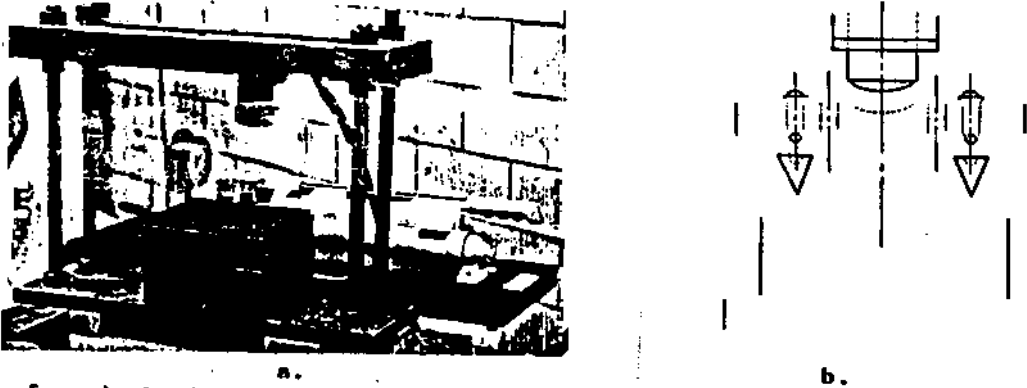


Figure 5. a) Loading frame used in the wedge indentation experiments. b) Schematic diagram of the specimen loading configuration.

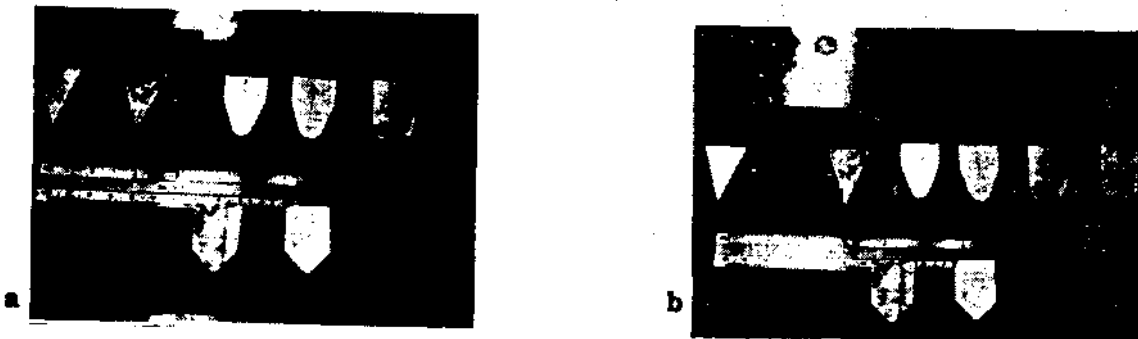


Figure 6. Four different wedge geometries and two different spacings; a) two inch and b) three inch.

Specimen Preparation

Large coal blocks were obtained from a surface mine in Northern West Virginia. These blocks of coal were cut and trimmed to suitable dimensions. The surfaces of the sample were then grinded to a smooth finish and allowed to dry. Since coal is so anisotropic, specimen orientation was considered throughout preparation. The objective was to produce several specimen with a consistent orientation with respect to the major cleavage planes. In other words, the specimen were cut in order to keep the surface of the specimen that was going to be holographed parallel to the cleavage planes. This surface was then painted with white paint to improve fringe contrast.

Typical Experiment

The finished specimen was then placed in the loading frame. Wedge spacing was selected and the specimen was preloaded and a brief relaxation time followed before beginning hologram construction. Laser alignment was then checked and blocked by a mechanical shutter, before placing the film in the film holder. The film was then exposed by the laser light via the shutter, about 1/50 of a second. A small increment of hydraulic pressure was then applied to the specimen and after another brief relaxation allowance, the film was exposed for the final time, another 1/50th of a second. The film was then ready for processing.

Results

Experiments were conducted with four different wedge designs and two different spacings applied perpendicular to the face cleat plane. However, since holometry is so sensitive, load increments during interferogram construction was limited to a few pounds. Therefore, only a few interferograms were made of each specimen as shown in Figure 7. A quantitative analysis can be made by comparing interferograms taken in sequence at different load increments assuming that displacement is perpendicular to the fringe orientation and utilizing equation 1. Total displacement can be calculated using the following equation:

$$D = \#f \times d \tag{2}$$

where D equals total displacement, d equals displacement represented by each fringe (result of equation 1), and #f equals the total number of fringes or fringe count.

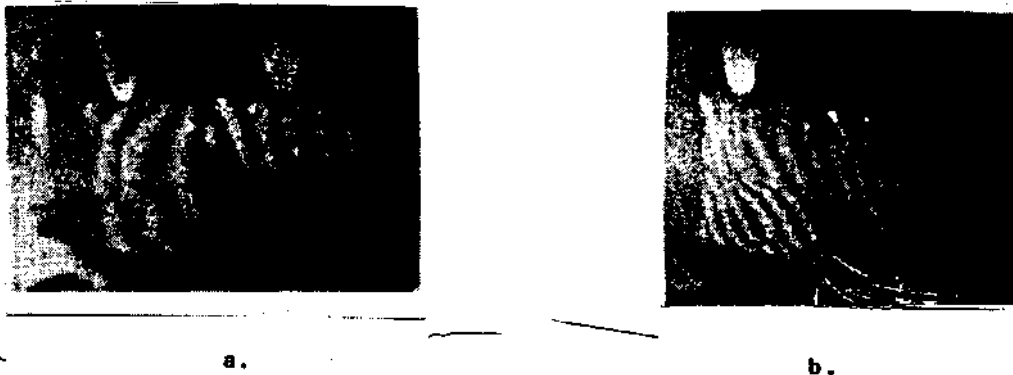


Figure 7. Compares sequential Interferograms taken with 20° wedges grinded dull 1/4 inch from sharp: a) 200-220 pounds b) 220-240 pounds.

Therefore, the total displacement represented is proportional to the number of fringes and since the load increment and fringe count varies by a factor of approximately two, a linear relationship between load and displacement is illustrated. This linear relationship has been observed in every case during initial loading, regardless of loading configuration as shown in Figure 8.

COAL FRACTURE ANALYSIS

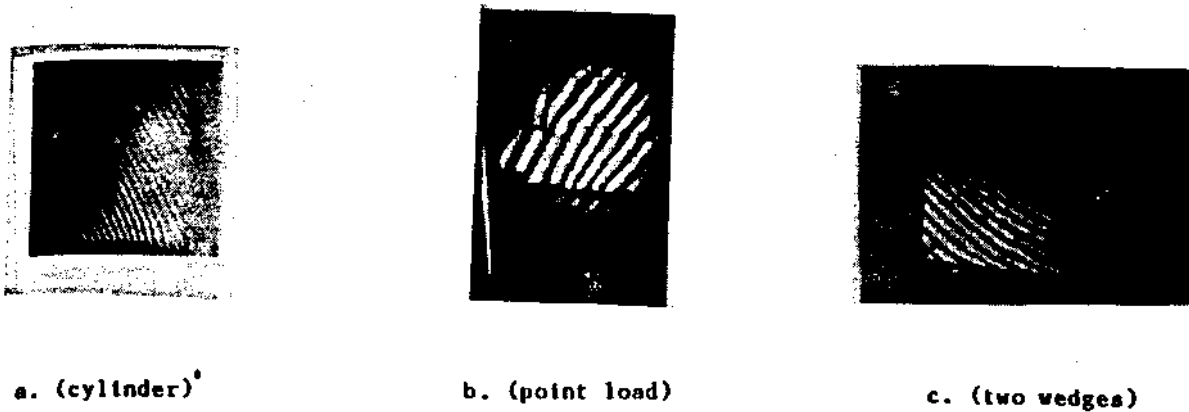


Figure 8. Compares interferograms observed during initial loading for different loading configurations.

The most interesting behavior was recorded immediately before failure as shown in Figure 9. This interferogram was captured during progressive failure under constant load. There was no load increment between film exposure. Observation of the failed specimen (Figure 9b) which occurred seconds after the interferogram in Figure 9a without an increase in load, shows a crack that propagated inwards rather than outwards toward the free surface. A chip developed on one side (far end of the specimen - see Figure 9b) but no chipping occurred on the other side. Therefore, crack propagation and direction has been recorded. Also, as mentioned earlier, the effect of local inhomogeneities is illustrated since the failure crack propagated towards an inhomogeneity.

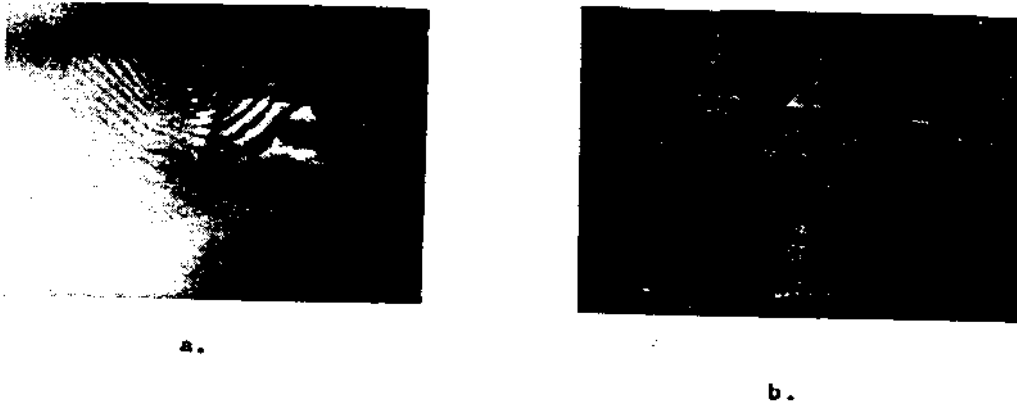


Figure 9. a) Interferogram taken immediately before failure. b) Resultant failed specimen (45° wedge with 2 inch spacings).

When wedge spacing is increased to three inches using 45° indentors, crack development occurred in between the wedges as shown in Figure 10. Failure resulted from bending of the specimen between the two wedges, indicated by the intensity of fringes present, rather than from stress concentrations caused by the wedge load sources.

Figure 11 illustrates a comparison between an interferogram constructed immediately before failure with an interferogram constructed immediately after failure. Wedge spacing was two inches and wedge geometry was 20° grinded dull by 1/4 inch from sharp. The individual zone of influence for each wedge are most apparent in this case; however, no intersection of these influence zones were recorded. In Figure 11a, the influence zone is larger under the left indenter, indicating either a deeper penetration or the effect of local inhomogeneities, which ultimately lead to failure as shown in Figure 11b.



a.



b.

Figure 10. a) Interferogram resulting from a 40 pound increment with 45° indentors and three inch spacing. b) Photograph of failed specimen.

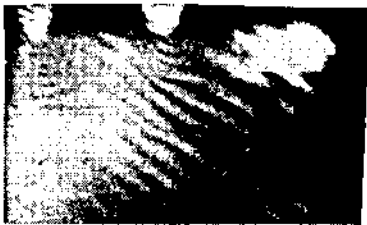


Figure 11. Compares interferograms taken before and immediately after failure. (20° wedge grinded 1/4 inch and 2 inch spacing).
a) 280 - 300 pounds b) 440 - 470 pounds-failure increment.

Localized stress concentrations were also observed using 45° wedges and two inch spacing as shown in Figure 12. Figure 13 compares failed specimens from different loading conditions illustrating that chip development and size varies with wedge geometry. The largest chips resulted from the bluntest 20° wedge as shown in Figure 13b.



Figure 12. Interferogram resulting from a 20 pound increment illustrating localized stress concentration (45° wedges with two inch spacing).

COAL FRACTURE ANALYSIS

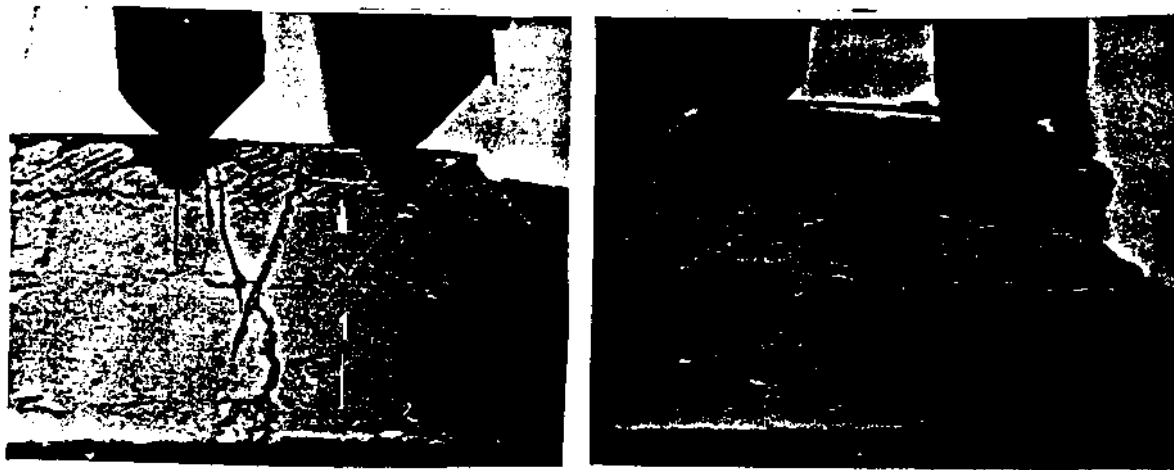


Figure 13. Compares failed specimen from different load sources. a) 45° b) 20° grinded dull by one inch from sharp.

Conclusions

During initial loading, fringe direction was generally parallel with the direction of load application and equally spaced. This indicates that the deformation was approximately uniform at initial load levels. Fringe orientation and direction generally did not reflect different loading configurations or the presence of local inhomogeneities until the load was increased to significant levels (over 300 pounds). The presence of these local inhomogeneities and flaws induce inhomogeneous stress fields resulting in non-uniform displacements in the specimen. For example, an interbedded shale layer would increase the mechanical integrity of the specimen, while clay layers or cleavage planes would decrease the integrity. Therefore, displacement fields and failure mechanisms in the specimen were more reflective of these local inhomogeneities and stress fields rather than the spacing or shape of the indentors.

The sensitivity of this technique limits the amount of displacement that can be accurately identified; therefore, this technique would be more suitable for the study of fracture mechanisms of brittle materials characterized by minimum deformation prior to failure (i.e. granite, sandstone or limestone). Also, the capability of this technique would be enhanced when combined with measurements such as the acoustic emission technique in the study of the fracture mechanisms in geologic materials. Furthermore, in order to study the entire deformation history of the specimen (pre and post failure) under stress, an extended number of sequential interferograms combined with continuous measurements of stress and strain during the testing is recommended.

Acknowledgement

These experiments were funded by the Generic Center for Respirable Dust Research sponsored by the United States Bureau of Mines under grant #G1135142.

References

1. Paul, B. & Sikarskie, D.L., 1965, "A Preliminary Theory of Static Penetration by a Rigid Wedge into a Brittle Material", Transactions, AIME Dec. pp. 372-383.
2. Begley, R. D. & Khair, A. K., 1985, "Application of Holographic Interferometry to Rock Mechanics and Underground Coal Mining Ground Control", Proceedings, 3rd International Congress on the Applications of Lasers and Electro Optics, Volume 45, Boston, MA, pp 39-46.
3. Khair, A. W., 1983, "Analysis of Interaction Between Models of Mine Roof-Pillar-Floor Using Holographic Interferometry and Analytical Techniques", Proceedings of the 24th U.S. Symposium on Rock Mechanics, College Station, TX, pp. 107-117.
4. Brodsky, N. S. & Spetzler, H.A., 1984, "Strain Localization during Deformation of Westerly Granite", Proceedings, 25th U.S. Symposium on Rock Mechanics, Northwestern University, Evanston, Illinois, pp. 87-96.
5. Wilson, A.D. & Lee, C.H., "Holographic and Analytical Study of a Semiclamped Rectangular Plate Supported by Struts", Experimental Mechanics, Vol. II, May 1970.
6. Khair, A.W., 1984, "Study of Fracture Mechanisms in Coal Subjected to Various Types of Surface Traction Using Holographic Interferometry", Proceedings of the 25th U.S. Symposium on Rock Mechanics, Chicago, Illinois.

THE EFFECT OF IN-SITU AND OPERATING PARAMETERS ON FRAGMENTATION OF COAL

A. Wahab Khair
and
Nagendra P. Reddy

Department of Mining Engineering
College of Mineral and Energy Resources
West Virginia University
Morgantown, WV 26506

ABSTRACT

This paper presents an analysis of preliminary tests on the effect of in-situ and operating parameters on fragmentation of coal using a specially designed unique automated rotary coal cutting simulator (ARCCS). In these tests coal blocks with an approximate dimension of 18 in. x 15 in. x 6 in. (45.7 cm x 38.1 cm x 15.2 cm) were first subjected to confining pressures, equivalent to in-situ conditions. Such blocks were then cut by the cutting head of the ARCCS, thus simulating the action of the continuous miner in underground coal mining. During the tests under a particular set of in-situ and operating parameters a number of other parameters such as 1) penetration of bit into coal, 2) penetration resistance (thrust and cutting pressures), 3) rotating velocity of cutting head, and 4) acoustic emission activity in the coal block were monitored. After each cutting cycle the fractured surfaces were photographed and a velocity survey was conducted by using a sonic technique. At the end of each experiment the cutting paths of the bits in coal were photographed using an optical microscope with a camera attached to it. Furthermore, the coal fragments were collected in bags using a vacuum cleaner. These fragments were then sieved for size distribution analysis. The results of the preliminary tests indicated that underground coal cutting can be simulated in the laboratory and the effects of the important parameters, i.e. operating and in-situ parameters, can be studied successfully.

Prepared for presentation at the 26th U. S. Symposium on Rock Mechanics, South Dakota School of Mines and Technology, Rapid City, SD, June 26-28, 1985.

EFFECT OF IN-SITU AND OPERATING PARAMETERS

INTRODUCTION

The continuous-mining machines which were introduced in the 1950's now account for more than half the production of coal from underground mines. Unfortunately, these continuous miners, which were designed for increased productivity, have also increased the concentration of respirable dust in mines. As a result, the Federal Coal Mine Health and Safety Act of 1969 was enacted to enforce on the coal operators that the airborne respirable dust not exceed 2 mg/m^3 , and was intended to reduce the incidence of coal workers pneumoconiosis. This plus the other aspects of the legislation and the subsequent monitoring and enforcement by MSHA made it very imperative that the coal operators provide a relatively healthier and safer working environment for the coal miners. Since 1970, the Federal government has paid over 11.7 billion dollars to more than 470,000 miners with coal workers pneumoconiosis and their survivors (1). These regulations, coupled with the assessment of the continuing burden on miners, the mining industry and taxpayers appear to have provided an impetus for the mining community towards comprehending the different parameters that influence dust generation and entrainment.

Dust control techniques such as conventional water sprays and dust collectors are only partially effective and require additional equipment expenditures. A more authentic approach would be to reduce respirable dust at the source, the continuous mining machine cutting head, where the fragmentation process occurs. Improving the fragmentation process by characterizing the coal breakage will not only reduce respirable dust at the face, but it will also decrease the amount of respirable dust that is liberated during the secondary handling.

Fragmentation of coal can be expressed as a function of three major groups of parameters; namely, 1) coal properties, 2) in-situ conditions and 3) operating parameters. Presently, this paper deals with the characterization of coal breakage as a function of machine operating parameters such as rate of advance, angle of attack, bit configuration, bit lacing (spacing and pattern) and bit speed.

STUDY PROGRAM

Laboratory Equipment and Instrumentation

Review of the literature on coal cutting technology and the basic parameters that effect this technology revealed that most of the existing coal cutting machinery is of the rotary type and that the parameters that effect the fragmentation of coal in such cutting depend on the following (3-15):

$$\text{Coal fragmentation} = f(C_p, I_c, O_p)$$

where C_p is the mechanical properties of coal, I_c is the in-situ conditions (vertical and horizontal stresses), and O_p is the operating parameters. Based on this premise a unique automated rotary coal cutting simulator (ARCCS) (Fig. 1) was designed and fabricated in the Mining Engineering Department at West Virginia University. This design incorporates the capability to study the different machine and in-situ parameters that influence the fragmentation of coal and the resulting dust. It operates under the simulated mining conditions with in-situ stresses (horizontal and vertical stresses) being applied to a coal block of 18 in. x 15 in. x 6 in. (45.7 cm x 38.1 cm x 15.2 cm) located in a suitably designed confining chamber. The cutting drum with a maximum tip to tip diameter (varies with the bit angle) of 19 inches has the capability of rotating from 1 to 50 rpm. The drum can be stopped any time after a predetermined number of revolutions. Tests can be performed with four different bit angles, 15, 30, 45 and 60 degrees. A maximum of seven bits can be mounted on the drum in an echelon pattern. The ARCCS can be operated and controlled manually or automatically, and the operating parameters can be preset with a series of hydraulic valves and could be recorded in analog/digital or in both forms.

Test and monitoring facilities can be seen in Fig. 1, ARCCS (Fig. 1a), programmable control and monitoring unit (Fig. 1b), sonic testing unit (Fig. 1c), acoustic emission (Fig. 1d), microscopic photographic unit (Fig. 1e), cascade impactors (Fig. 1f), hood and air current generating unit (Fig. 1g) and data acquisition and recording unit (Fig. 1h). In addition to this, linear variable transformers, pressure transducers, flow meters, flow controls and drum rpm were some of the other monitoring devices. LVDT's are used to monitor the displacement of the coal block as well as the

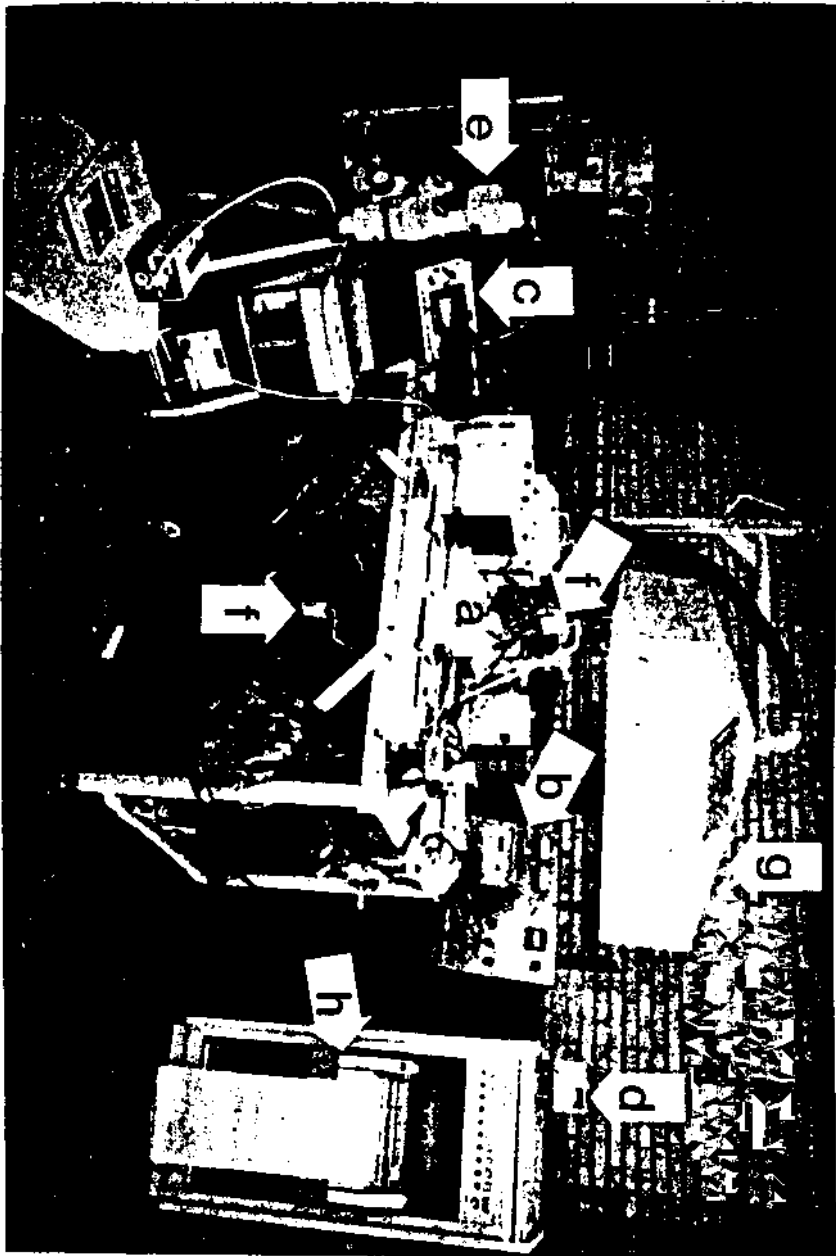


Fig. 1. Test and monitoring equipment facilities (a) automated rotary coal cutting simulator, (b) programmable control and monitoring unit, (c) sonic testing unit, (d) acoustic emission, (e) microscope and the attached camera unit, (f) cascade impactors, (g) hood and air current generating unit and (h) data acquisition and recording unit.

depth of cut. Pressure transducers are used to monitor the changes in pressure, both due to the thrust and due to the intermittent cutting nature of the rotary cutting. Flow controls are used to run the drum at a particular rpm between 1 and 50 and to provide a different rate of advance. All of the above mentioned devices are operated and monitored by a fully automated control system. The fracture size, shape and intensity is characterized, a) with the help of photographs taken at the end of each test by using a camera attached to an optical microscope, b) by monitoring the acoustic emission and c) by monitoring the sonic signal in the coal block located in the confining chamber with the help of sonic transducers, signal generator, and an oscilloscope.

Specimen Preparation

Large blocks of coal were obtained from a surface mine. These blocks were then cut in the laboratory to an approximate dimension of 17 in. x 13 in. x 6 in. (43.2 cm x 33.0 cm x 15.2 cm). A typical specimen with cutting face as face cleat was then placed in a wooden box of 18 in. x 15 in. x 6 in. (45.7 cm x 35.6 cm x 15.2 cm) in dimension. Two blocks of wood 1.25 in. x 1.5 in. x 5 in. (3.2 cm x 3.8 cm x 12.7 cm) are wedged between the coal sample and the wooden box. Plaster of paris is then poured in the box to fill all the remaining space other than that occupied by the coal block. This process gives a perfect dimension of 18 in. x 15 in. x 6 in. (45.7 cm x 35.6 cm x 15.2 cm) which is very essential to avoid stress concentration in the specimen when confining pressure is applied. After a week the moulded coal samples are removed from the box and the wooden blocks that were wedged before pouring the mould are dislodged from the sample carefully, thus creating room to house the sonic transducers. A typical specimen ready to be cut is shown in Figure 2.

Experimental Procedure

During a typical experiment the moulded specimen was placed in the confining chamber, the test conditions were set, and the in-situ and operating parameters were marked on the top mould layer of the sample. Such parameters can be seen in Figures 14 through 18. These parameters, for example in Figure 15, can be explained as follows. I is the type of bit, 1.5 in. is the bit spacing, 5 is the number of bits, 15 degrees is the bit attack angle, 1/8 in. is the depth of cut, 15 is the drum rpm, F is the face cleat, S_v is

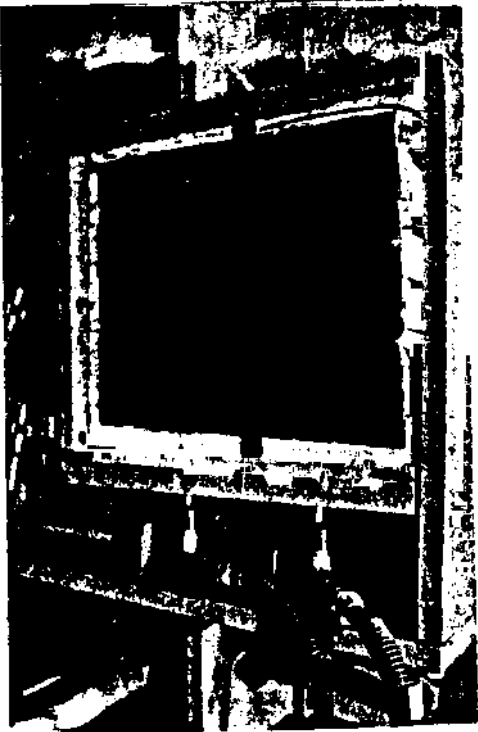


Fig. 2. Typical specimen ready for experiment.

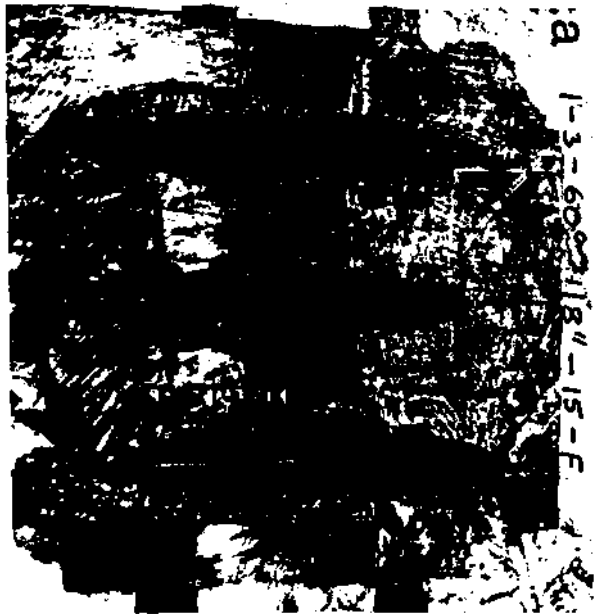


Fig. 3. Coal blocks with different bit spacing (a) 3 in. (7.62 cm) spacing and (b) 1.5 in. (3.81 cm) spacing.

THE RESPIRABLE DUST CENTER

the vertical confining pressure and S_h is the horizontal confining pressure. A sonic test was done by which the stress wave travel time through the coal sample and the amplitude of the signal was measured and recorded. Equivalent in-situ stresses were then applied to the specimen using two sets of hydraulic jacks (two for horizontal and two for vertical). A 1 in. (2.54 cm) thick steel plate was positioned between the sample and hydraulic jacks in order to distribute the pressure uniformly over the whole surface of the specimen. Each set of hydraulic jacks were connected in parallel to a hand pump. After the confining pressure was applied another sonic test was made and the corresponding stress wave travel time and amplitude was measured and recorded. Before the test, the operating parameters such as velocity of the cutting drum and rate of advancement were adjusted to predetermined values. Then bit blocks of specific attack angle (15, 30, 45 and 60 degrees) were mounted on the cutting drum at a particular spacing (Fig. 3a-b), i.e. 1.5 in. to 3.0 in. (3.8 cm to 7.6 cm) and pattern. Bits of specific make and type were inserted into the bit block slots and were kept in position by a screw in such a way so as to allow bit rotation inside the lock which prevents non-symmetric bit wear. The number of rotations by the cutting head was set in the counter unit in the control module and then the machine was started to execute the program in a continuous or counter mode. The counting of the number of rotations starts when the hydraulic pressure is increased, due to the cutting process, or when the cutting head has traveled to a preset distance measured mechanically and by LVDT. After the execution of the predetermined number of rotations the cutting head retreats and stops. After each cutting cycle, the samples were photographed and a sonic test was done. During the test a number of parameters were recorded (Fig. 4). At the end of the experiment the specimens were photographed and using a microscope with an attached camera, the path of the cutting bits were photographed at three locations, at entrance, center, and exit of the bits. Airborne particles were collected by using a cascade impactor while the larger particles were collected in a large bag with the vacuum cleaner.

RESULTS AND DISCUSSION

The coal used in the experimental study is part of the Waynesburg coal seam. Prior to the experiments the physical and mechanical properties of this coal were determined in the laboratory. The physical and mechanical properties can be seen in Table 1.

EFFECT OF IN-SITU AND OPERATING PARAMETERS

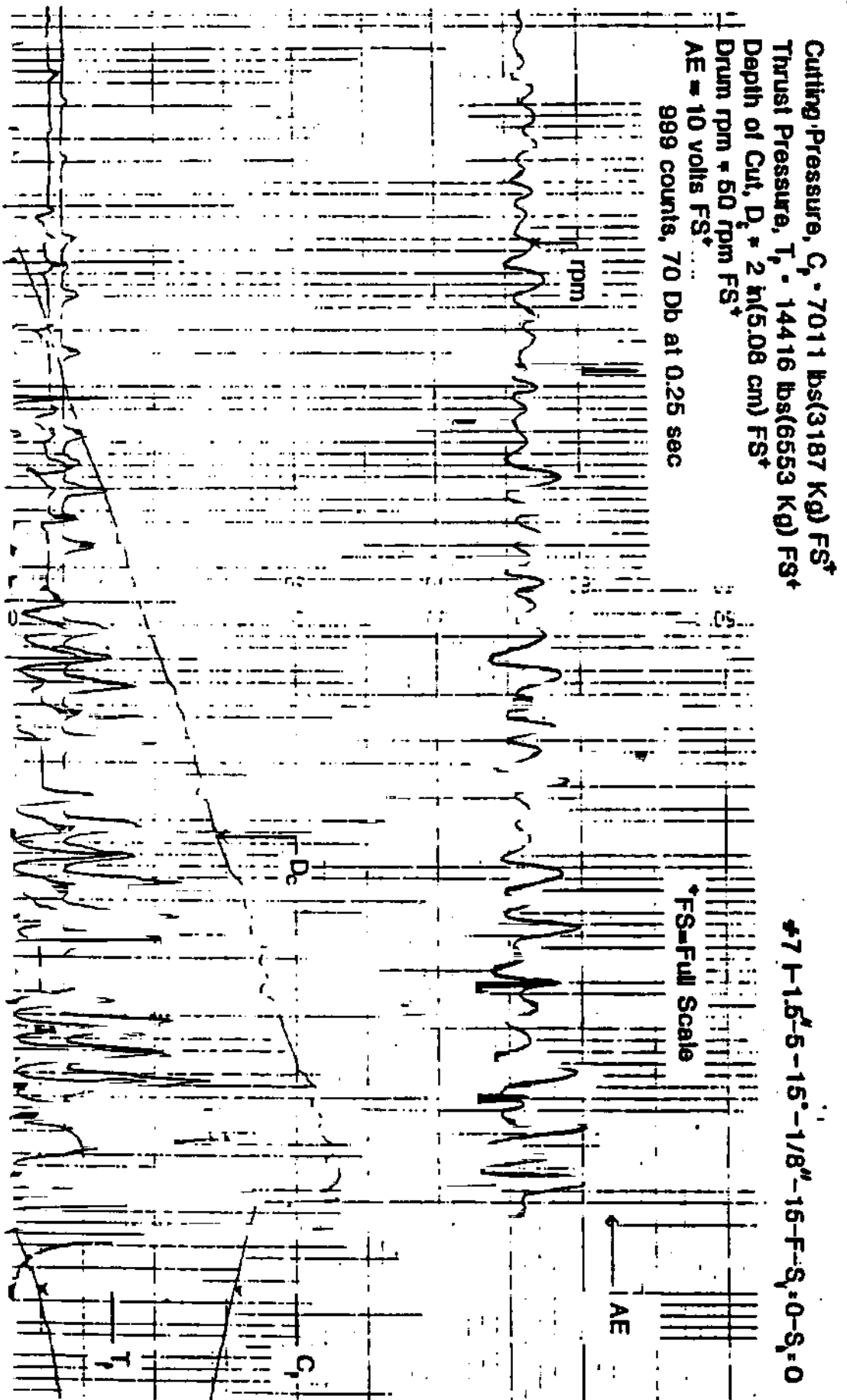


Fig. 4. Typical chart on which the different parameters such as the A.E., cutting pressure, thrust pressure, drum rpm and depth of cut are recorded for a particular set of operating parameters under zero confining pressure.

Table 1. Physical and Mechanical Properties of Waynesburg Coal

Cleat/Bedding Plane Orientation	Compressive Strength psi (KPa)	Young's Modulus psi (KPa)	Poisson's Ratio	Indirect Tensile Strength psi (KPa)	Direct Shear Strength psi (KPa)	Sp. Gr.
Bedding Plane	3289 (473.6)	5.1 x 10 ⁵ (7.3 x 10 ⁴)	0.25	154 (22.2)	204 (29.4)	1.42
Face Cleat	3459 (498.1)	4.7 x 10 ⁵ (6.8 x 10 ⁴)	0.31	205 (29.5)	180 (25.9)	
Butt Cleat	4912 (707.4)	4.6 x 10 ⁵ (6.6 x 10 ⁴)	0.32	146 (21.0)	80 (11.5)	

EFFECT OF IN-SITU AND OPERATING PARAMETERS

A study of twenty experiments have been completed so far and more are being done to study the effects of operating and geologic parameters on the fragmentation of coal in detail. The parameters observed were spacing, effect of velocity, depth of cut, confining pressure and angle of attack. Despite a limited number of tests, enormous data was collected of which only a part will be presented here for discussion.

Using a 3 in. (7.62 cm) and 3 bits mounted in an echelon pattern, a cut of up to 2.5 to 3 in. (6.35 cm to 7.62 cm) depth was made without breaking the boundary walls between the bit paths (Fig. 3). These series of tests with 3 in. (7.62 cm) spacing were done for 15, 30, 45 and 60 degree attack angles.

With 1.5 in. (3.81 cm) spacing and 5 bits mounted in an echelon pattern, the side walls of the bit paths were broken. These series of tests were done for attack angles of 15, 30, 45 and 60 degrees and at 0, 300 and 450 psi (0, 43.2 and 64.8 KPa) confining pressures.

The preliminary findings resulting from these tests are:

Force. Due to the enormous amount of data, a statistical analysis was done to calculate the resultant force. Figures 5 through 8 show the resultant force necessary to cut coal as a function of the various parameters. Figure 5a shows that the resultant force necessary to cut increases as the bit attack angle increases from 30 to 60 degrees. However, the force required with a 15 degree attack angle is much higher. This could be attributed to the fact that with a 15 degree attack angle the bit rubs along the cutting path more than the other angles and hence requires high thrust and cutting pressure. A similar trend was observed with confining pressures of 300 psi (43.2 KPa) and 100 psi (14.4 KPa), vertical and horizontal, respectively, except that the rate of increase of the resultant force is higher as the depth of cut increases (Fig. 5b). Using a 45 degree attack angle, it was observed that as the equivalent in-situ confining pressure increases the required resultant force increases (Fig. 6). Also the rate of increase gets higher as the vertical and horizontal confining pressures increase from 0 to 400 psi (57.6 KPa) and 0 to 133 psi (19.15 KPa), respectively. Figure 7 shows that for a 45 degree attack angle as the rpm increases the resultant force increases. Also the rate of increase is higher. Figure 8 shows the high rate of increase of the force necessary when the spacing is increased. This could be due to the fact that there is no free space available when there is a cut with a 3 in. (7.62

FOUR DIFFERENT ATTACK ANGLES (15, 30, 45, 60 Degree)

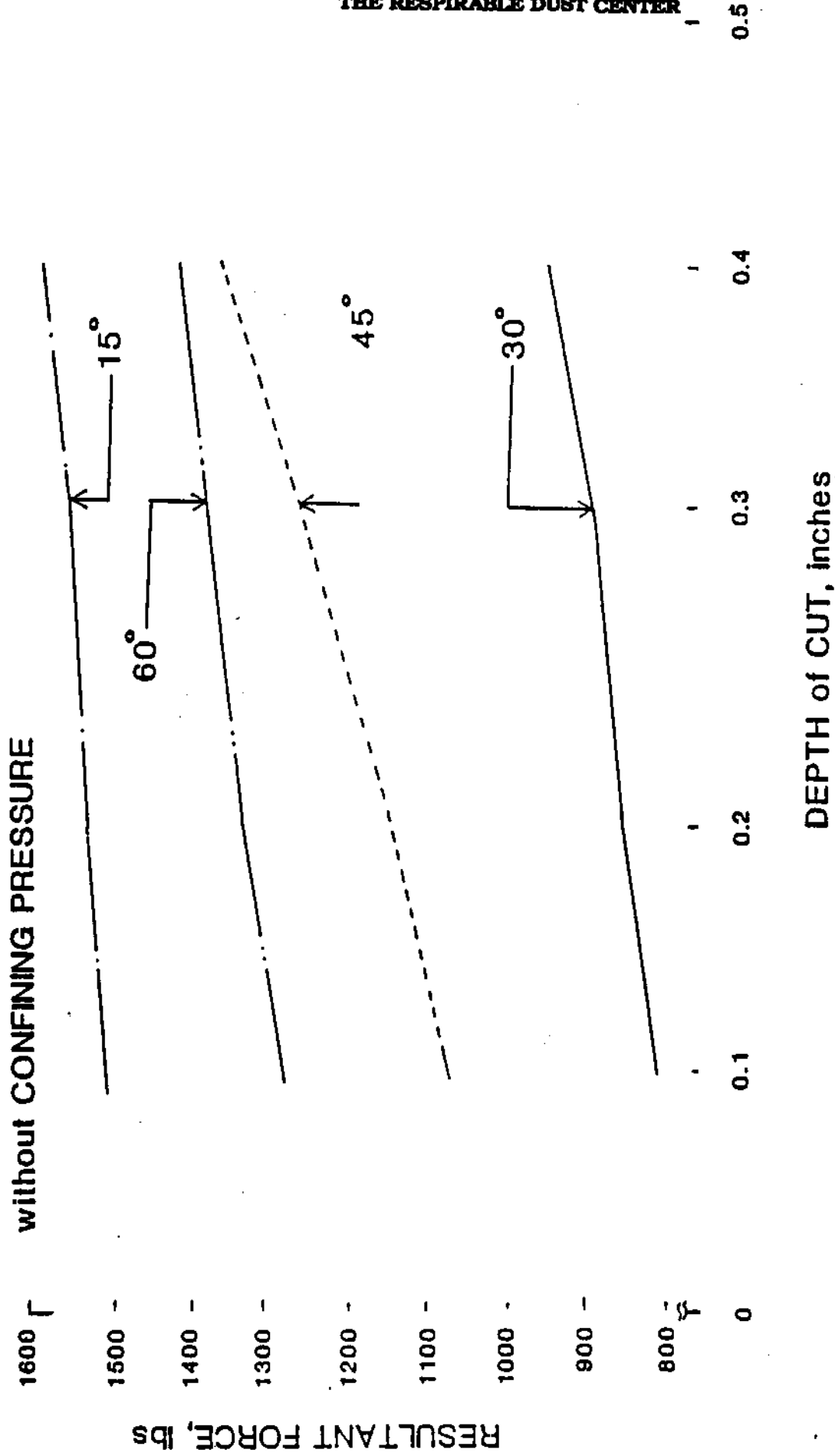


Fig. 5a. Resultant force vs. depth of cut as a function of bit attack angle.

FOUR DIFFERENT ATTACK ANGLES (15, 30, 45, 60 Degree)

$S_v = 300$ psi, $S_h = 100$ psi

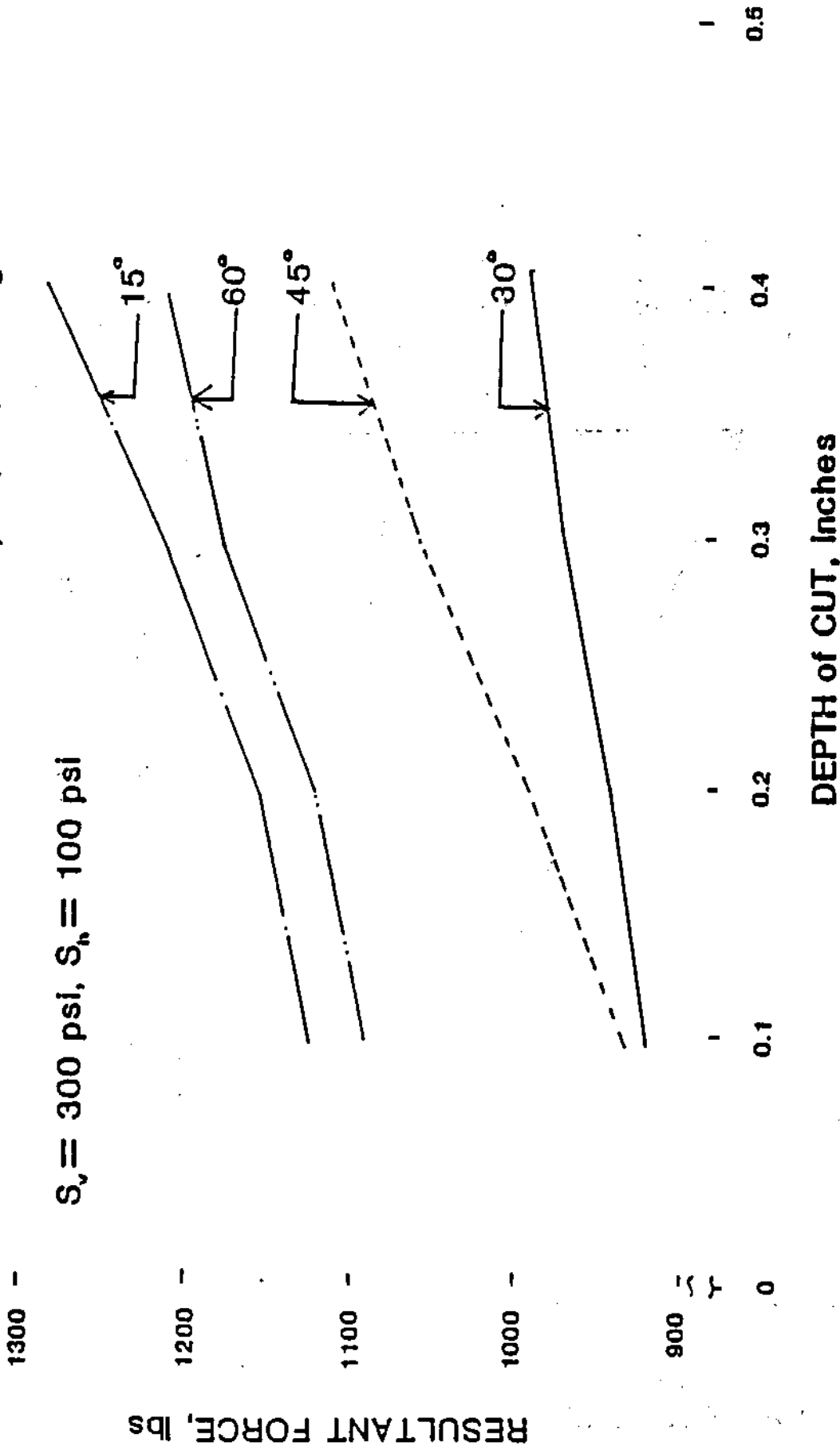


Fig. 5b. Resultant force vs. depth of cut as a function of bit angle attack and confining pressure.

FOUR DIFFERENT CONFINING PRESSURES with 45° BITS

$S_v = 0, 150, 300, 450$ psi $S_h = 0, 50, 100, 150$ psi Respectively

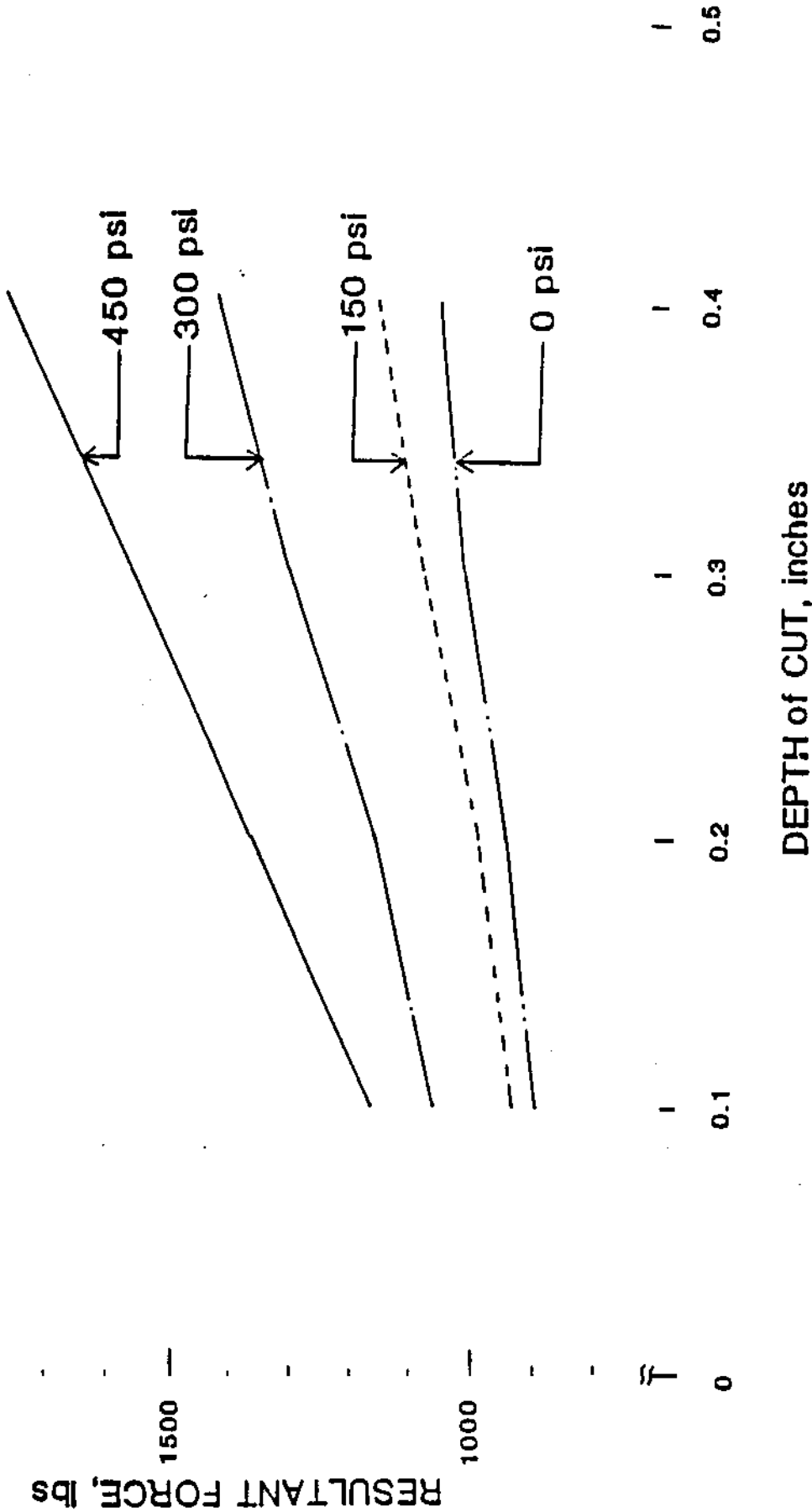


Fig. 6. Resultant force vs. depth of cut as a function of confining pressure.

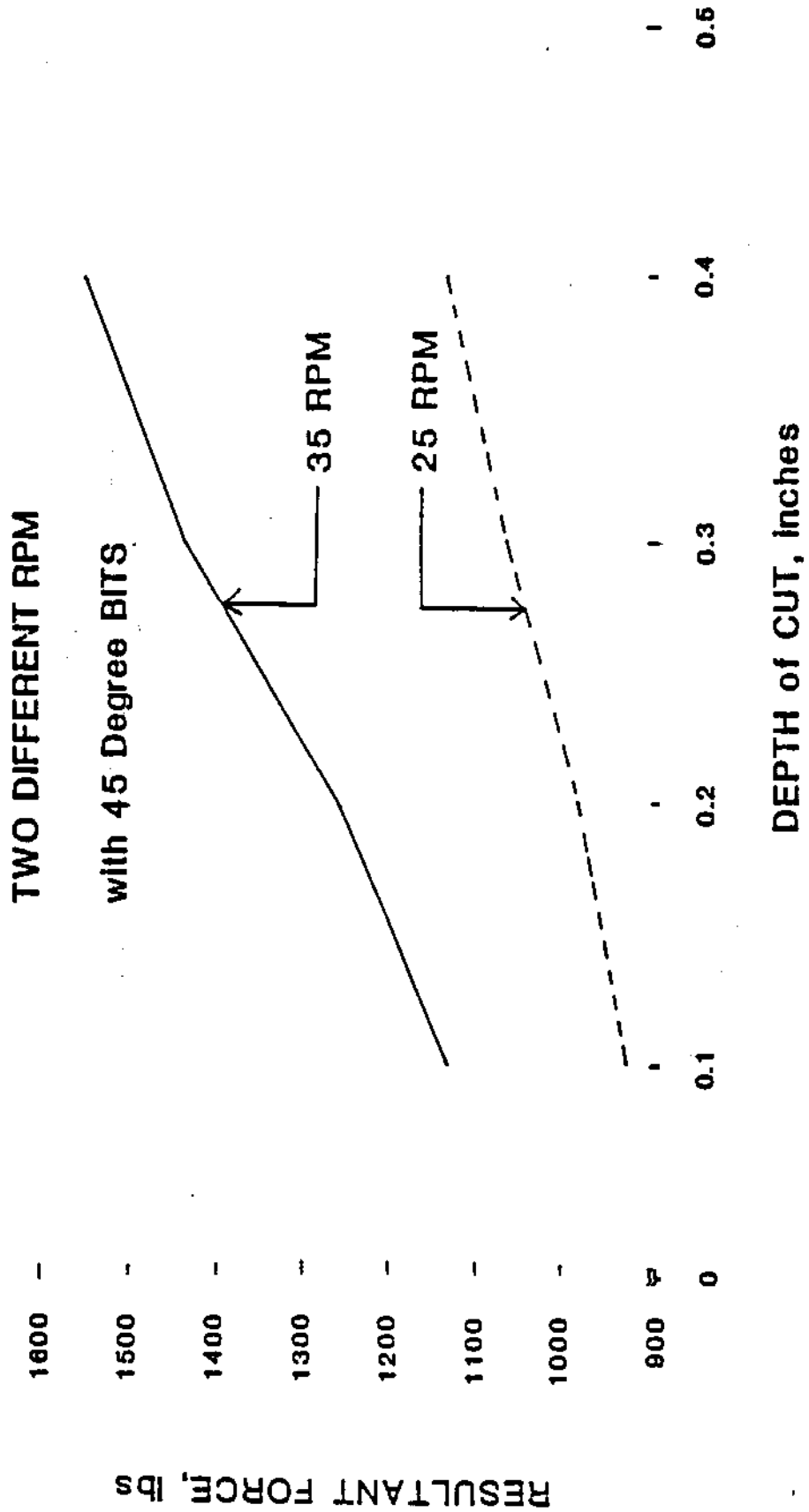


Fig. 7. Resultant force vs. depth of cut as a function of rpm.

TWO DIFFERENT SPACING for 45° BITS (1.5, 3 in.)

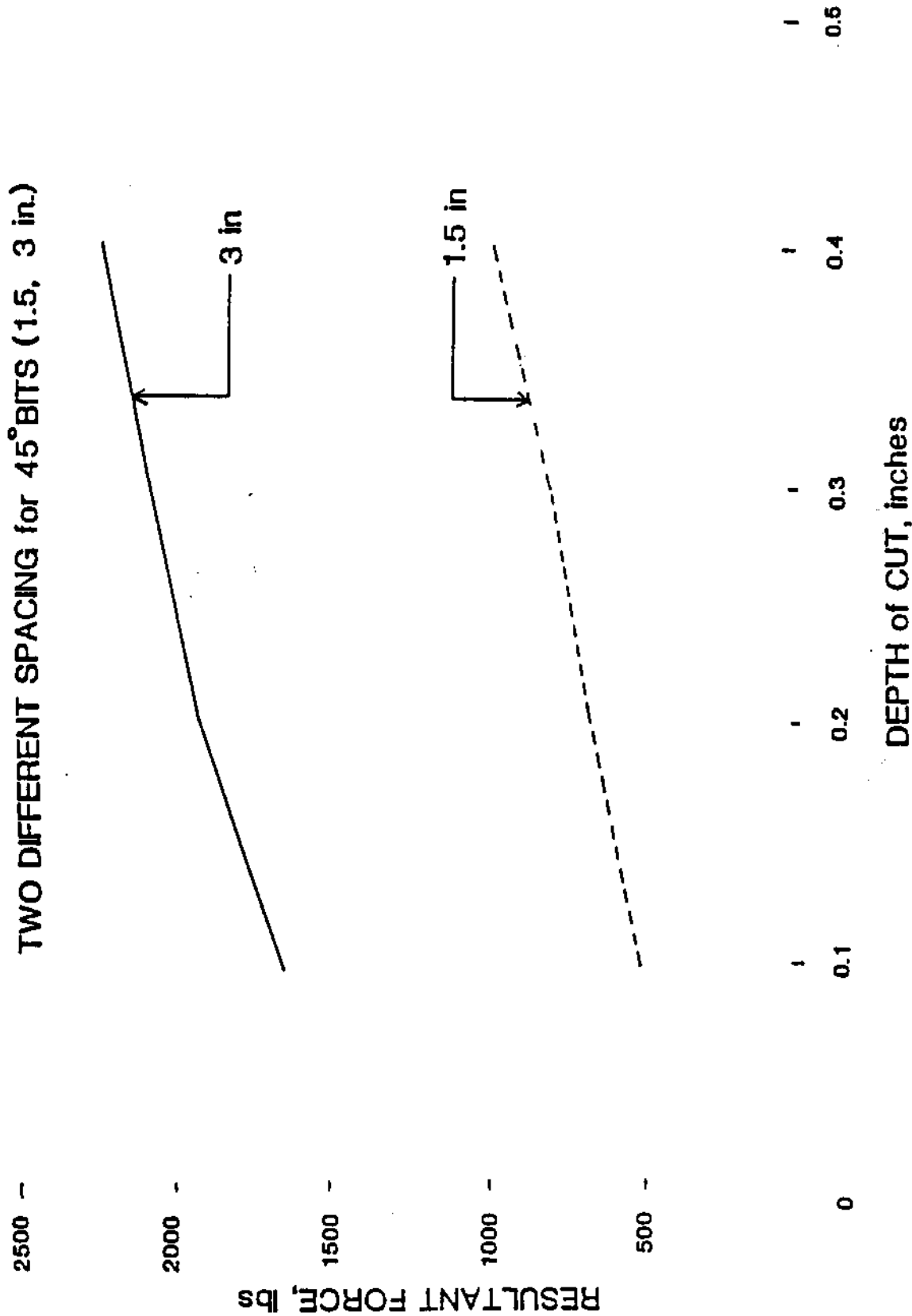


Fig. 8. Resultant force vs. depth of cut as a function of bit spacing.

EFFECT OF IN-SITU AND OPERATING PARAMETERS

cm) spacing, in which the walls between the two bits were cut when using a 1.5 in. (3.81 cm) bit spacing.

Size Distribution. A statistical analysis was done to fit the curves for the size distribution. The curves are plotted on the semi log graph. Figures 9 through 13 show the mesh size versus the percent of weight retained as a function of various parameters. Figure 9 indicates that the percent weight decreases as the opening size decreases for all angles. However, the percent weight is the highest for all angles at 0.1 in. (0.25 cm) opening size. The percent weight for the 30 degree attack angle is larger below 0.1 in. (0.25 cm) than for the other angles. With confining pressures of 300 psi (43.2 KPa) and 100 psi (14.4 KPa), vertical and horizontal, respectively, a similar trend was observed except that the percent weight for the 60 degree attack angle is more under 0.1 in. (0.25 cm) than at the higher size (Fig. 10). Using a 45 degree attack angle, it was observed that as the confining pressure increases the weight percent increases in the finer range and decreases in the larger range (Fig. 11). Figure 12 shows that the percent weight of the fragments larger than 0.1 in. (0.25 cm) are higher with 35 rpm while the percent weight of the fragments smaller than 0.1 in. (0.25 cm) are more with 25 rpm. The weight percent of fragments larger than 0.3 in. (0.76 cm) are more for 1.5 in. (3.8 cm) spacing while the weight percent of fragments less than 0.3 in. (0.76 cm) are higher for 3 in. (7.6 cm) spacing. This could be imputed to the fact that the walls of the bit cut paths do not break for the 3 in. (7.6 cm) spacing while they break with 1.5 in. (3.8 cm) spacing (Fig. 3a-b).

Fracture Extension. Before and after applying the confining pressure, but before the first cut was made, the time that a stress wave takes to pass across the width of the coal sample and the amplitude and attenuation of this wave was measured, and the photograph was taken with a camera attached to an oscilloscope. Using this data, the velocity of this wave and the dynamic Young's modulus of the coal sample were calculated. A similar procedure was followed to calculate the velocity and the dynamic Young's modulus after every cut (Fig. 14). Results indicated that the application of confining pressure increases the dynamic Young's modulus of coal as evidenced in Figure 14. During cutting the fracture extended from the cut surface through the block. The magnitude and the length of extension of these cracks depend on the original condition of the block (pre-existence of cracks), the operating parameters such as velocity of the cutting drum, depth of cut, angle of attack, magnitude of the dynamic shock produced and magnitude of the confining pressure. At lower or zero confining pressures, the shock due to the impact of the bits fractures the coal

FOUR DIFFERENT ATTACK ANGLES (15, 30, 45, 60 Degree)

without CONFINING PRESSURE

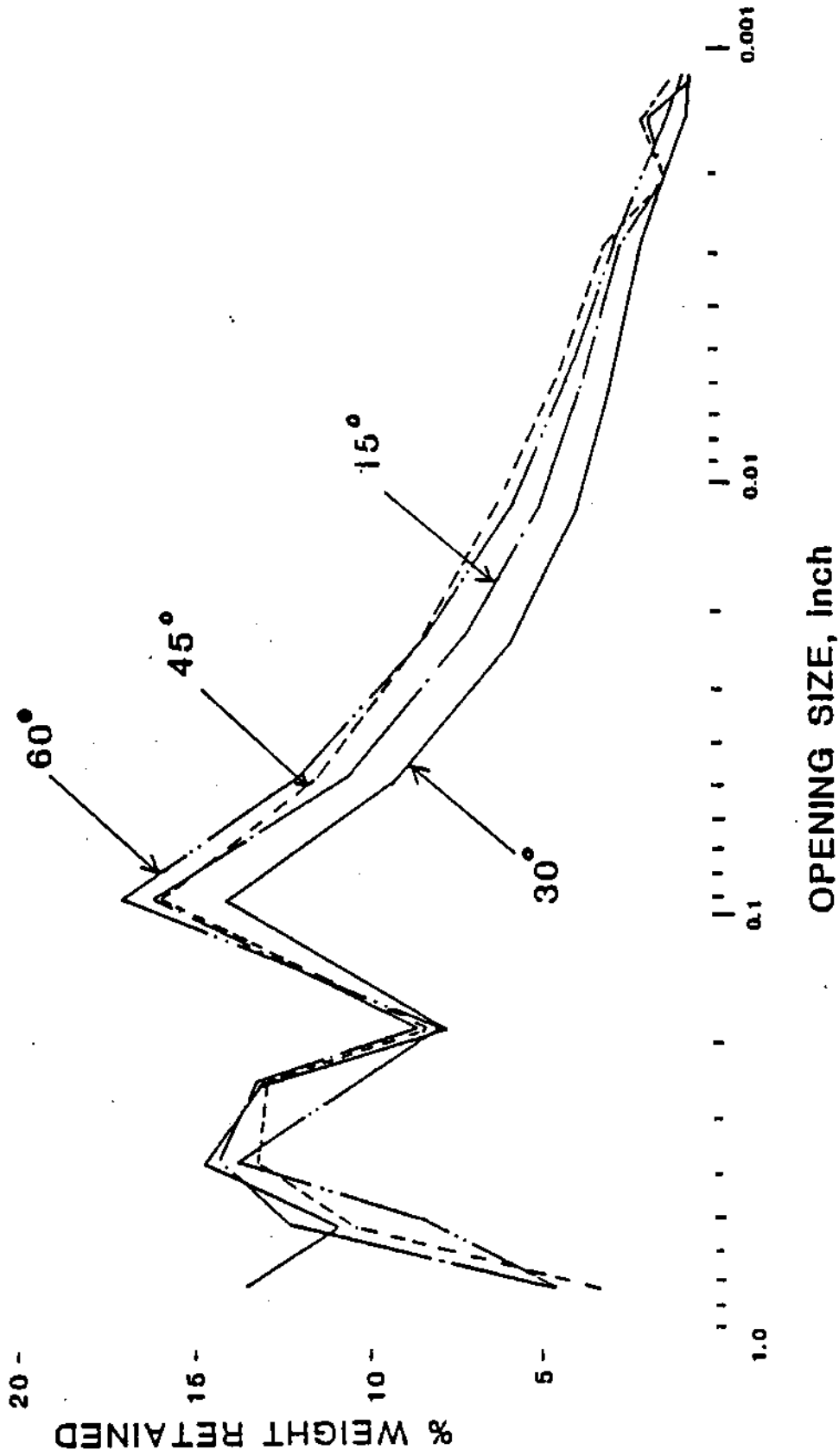


Fig. 9. Mesh size vs. percent of weight retained as a function of bit attack angle.

26-

FOUR DIFFERENT ATTACK ANGLES (15, 30, 45, 60 Degree)

$S_v = 300$ psi, $S_h = 100$ psi

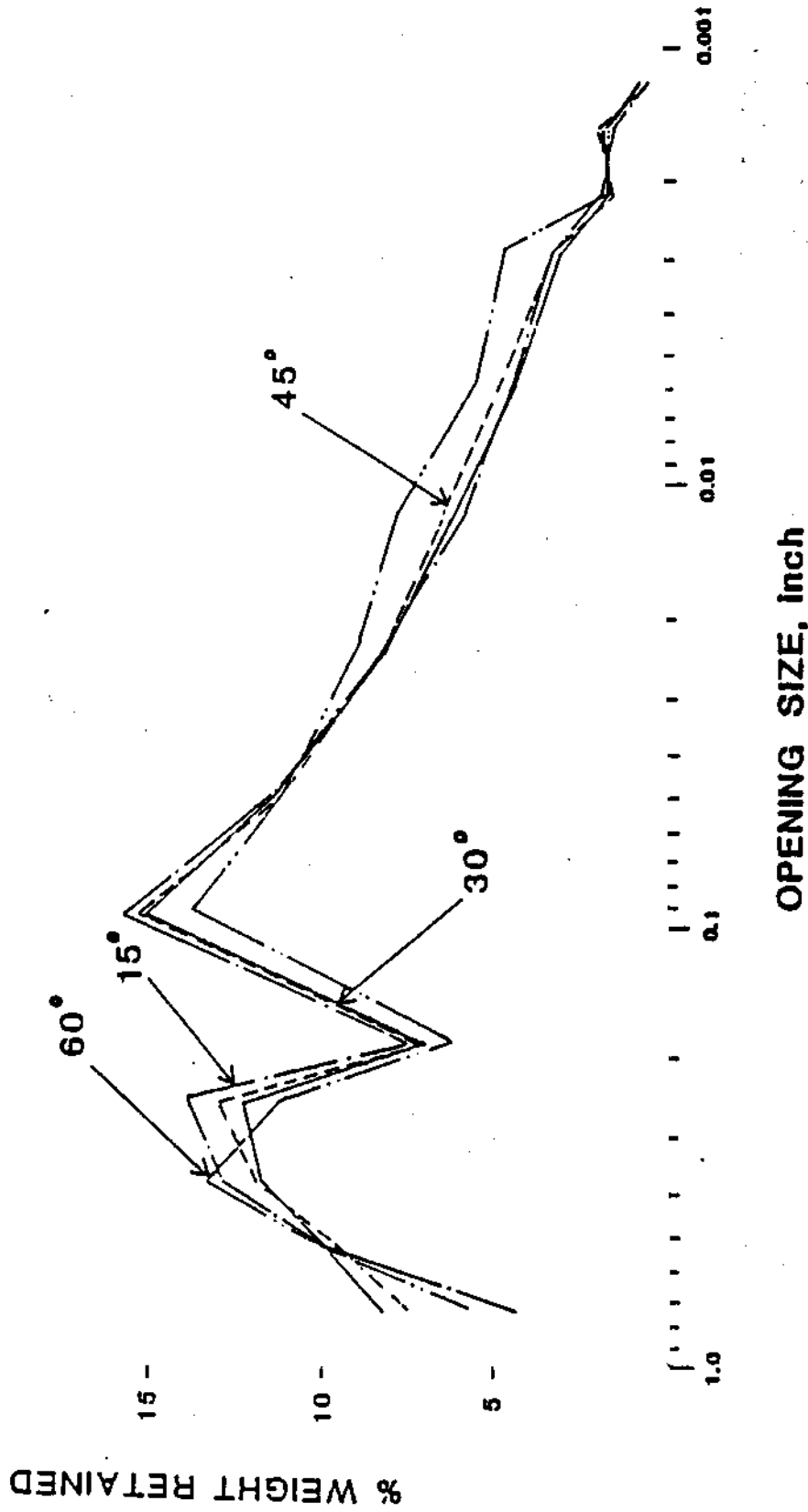


Fig. 10. Mesh size vs. percent of weight retained as a function of bit attack angle and confining pressure.

FOUR DIFFERENT CONFINING PRESSURES WITH 45° BITS

$S_v = 0, 150, 300, 450$ psi $S_h = 0, 50, 100, 150$ psi;
Respectively

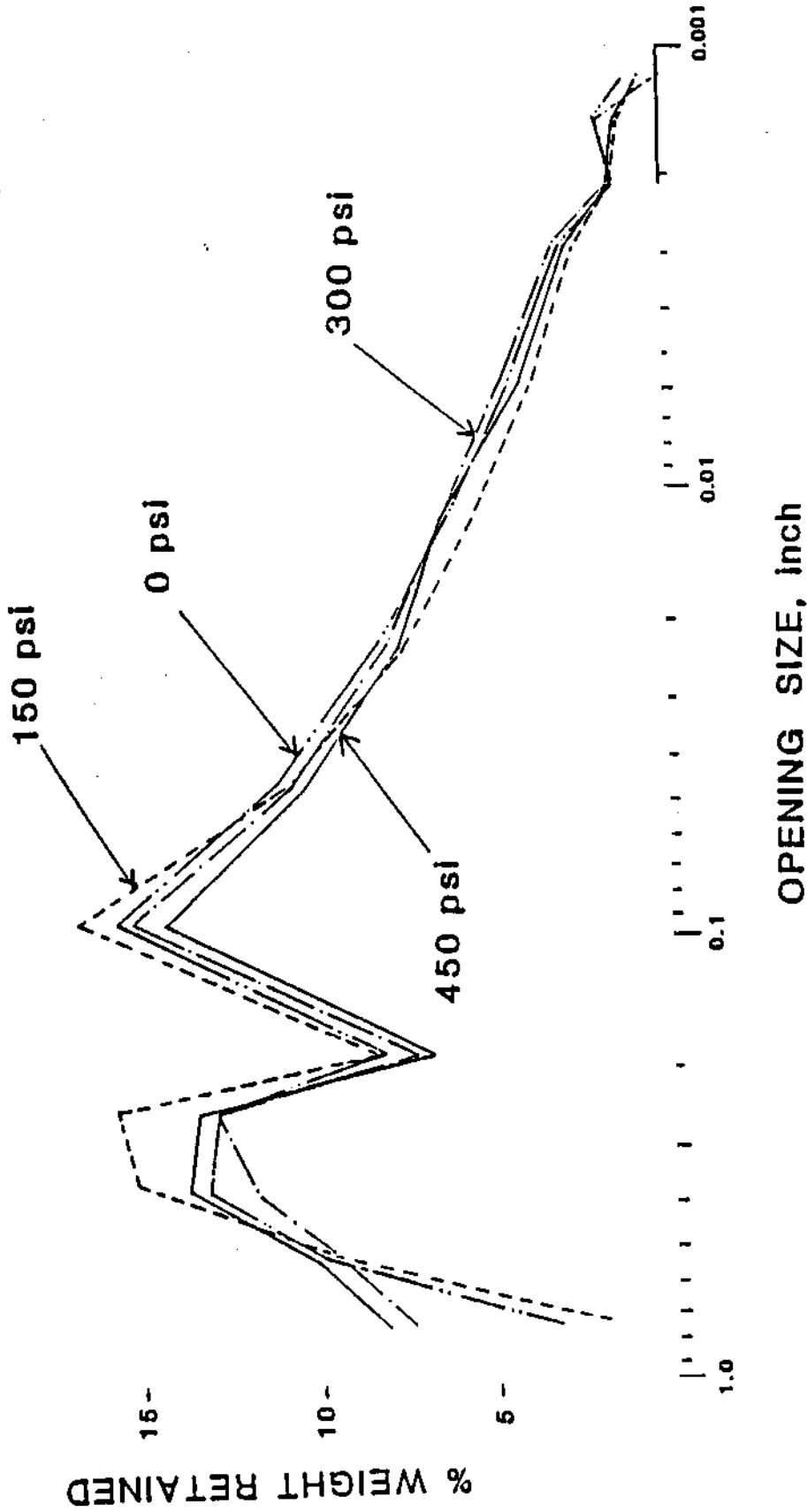


Fig. 11. Mesh size vs. percent of weight retained as a function of confining pressure.

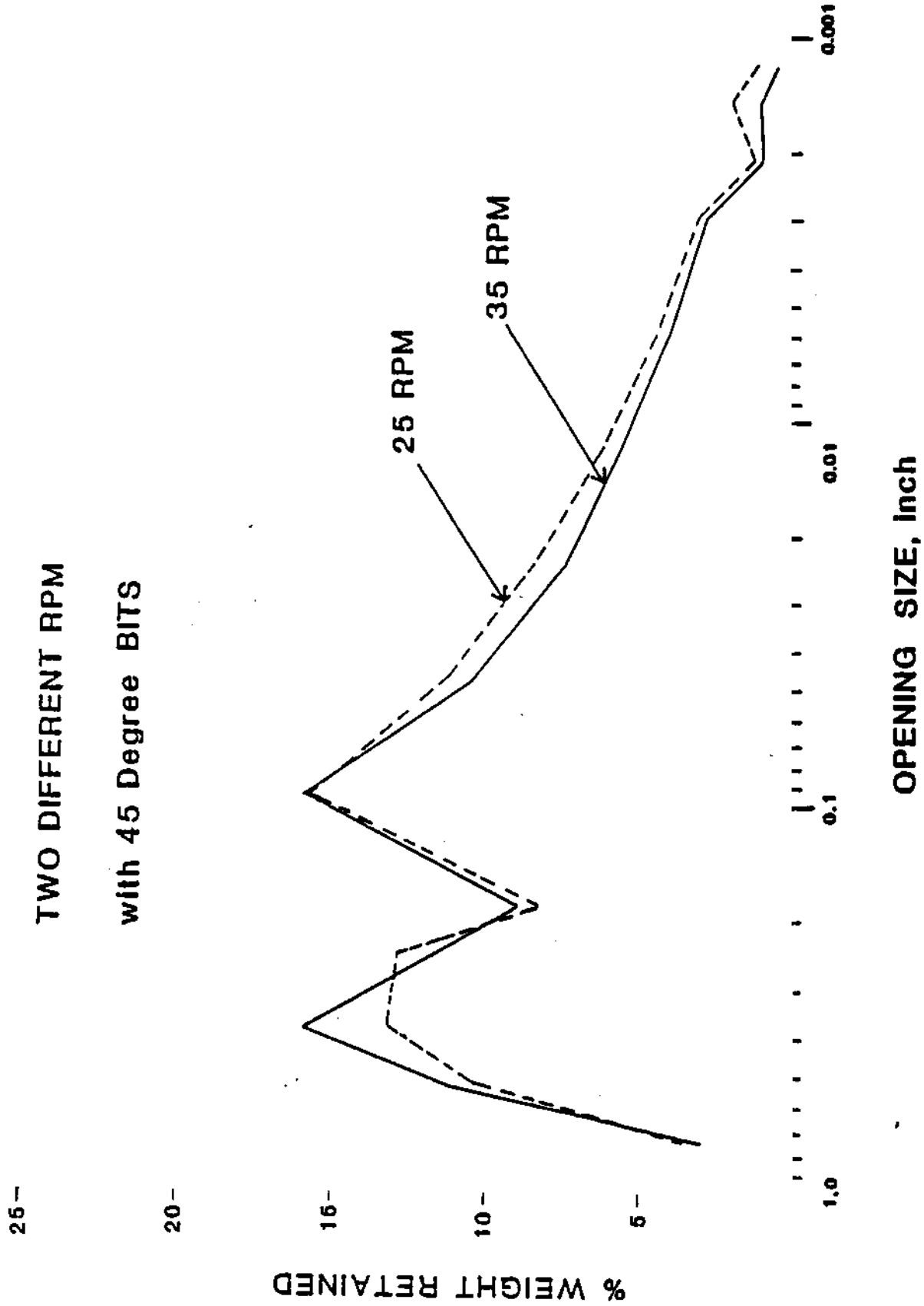


Fig. 12. Mesh size vs. percent of weight retained as a function of rpm.

TWO DIFFERENT SPACING FOR 45° BITS (1.5, 3 in.)

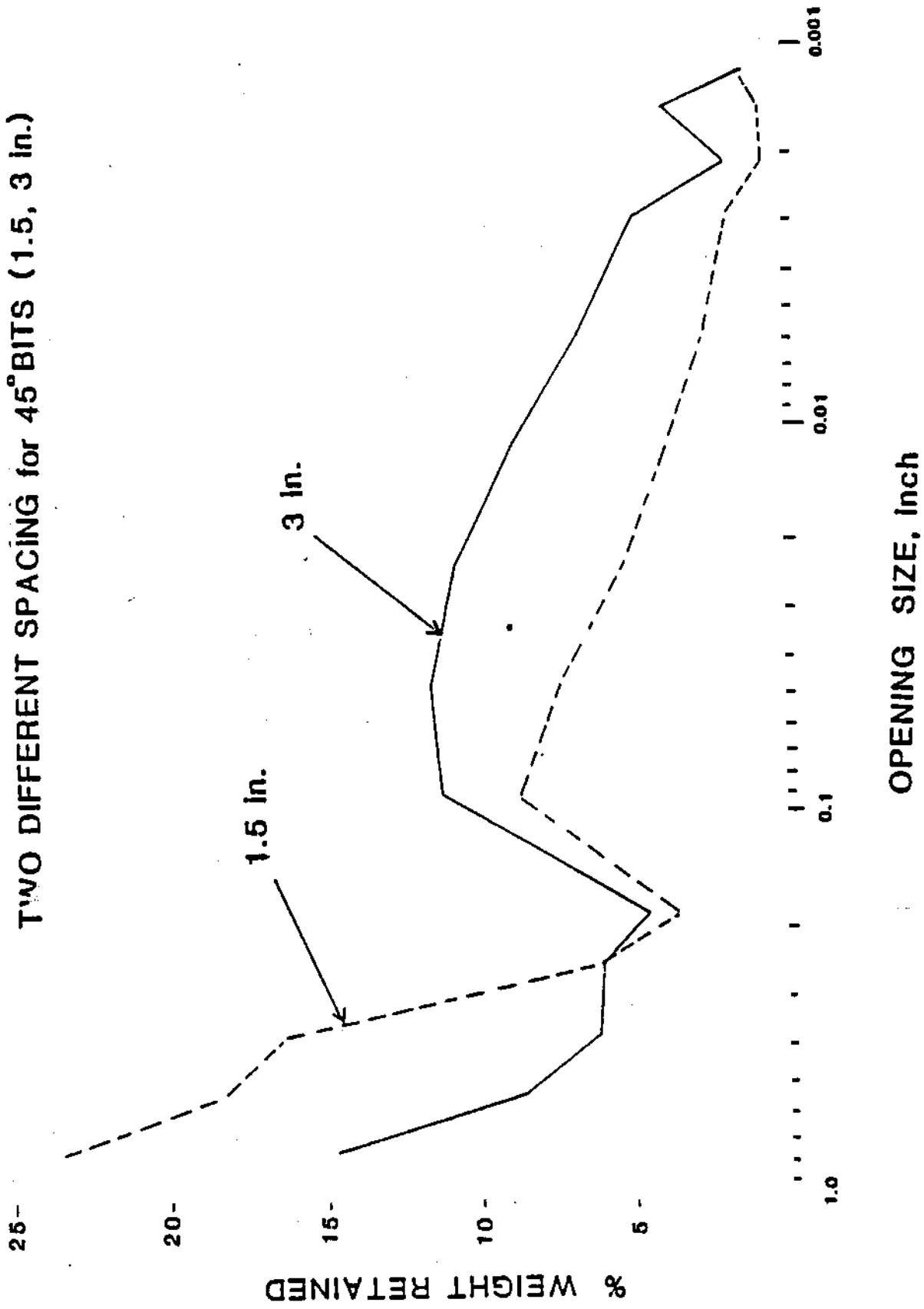


Fig. 13. Mesh size vs. percent of weight retained as a function of bit spacing.

EFFECT OF IN-SITU AND OPERATING PARAMETERS

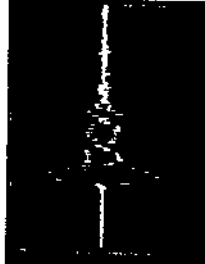
TEST #17 I-1.5"-5-45°-1/4"-25-S_y=150-S_h=50-F

DEPTH OF CUT 0.0"
VEL 8158 1/s
Vmax 0.20 v
Ed 1.08 E08 psi
50mV/DIV
0.1ms/DIV



INITIAL-UNCONFINED

DEPTH OF CUT 0.0"
VEL 8158 1/s
Vmax 0.23 v
Ed 1.08 E08 psi
50mV/DIV
0.1ms/DIV



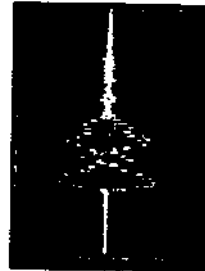
INITIAL-COMFINED

DEPTH OF CUT 0.82"
VEL 8380 1/s
Vmax 0.26 v
Ed 1.12 E08 psi
50mV/DIV
0.1ms/DIV



FIRST

DEPTH OF CUT 1.48"
VEL 8232 1/s
Vmax 0.22 v
Ed 1.08 E08 psi
50mV/DIV
0.1ms/DIV



SECOND

DEPTH OF CUT 1.28"
VEL 4818 1/s
Vmax 0.008 v
Ed 3.70 E05 psi
5.0mV/DIV
0.1ms/DIV



INITIAL

DEPTH OF CUT 2.04"
VEL 2888 1/s
Vmax 0.001 v
Ed 1.33 E05 psi
1.0mV/DIV
0.1ms/DIV



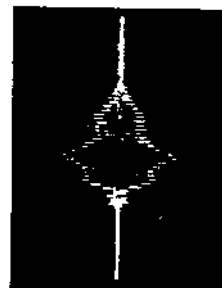
THIRD

DEPTH OF CUT 0.48"
VEL 7818 1/s
Vmax 0.08 v
Ed 8.00 E08 psi
20mV/DIV
0.1ms/DIV



FIRST

DEPTH OF CUT 0.88"
VEL 7448 1/s
Vmax 0.08 v
Ed 8.83 E08 psi
20mV/DIV
0.1ms/DIV



SECOND

DEPTH OF CUT 3.04"
VEL 7087 1/s
Vmax 0.04 v
Ed 8.02 E08 psi
50mV/DIV
0.1ms/DIV



THIRD

DEPTH OF CUT 3.04"
VEL 8829 1/s
Vmax 0.83 v
Ed 8.40 E08 psi
50mV/DIV
0.1ms/DIV



FOURTH

FOURTH-UNCONFINED

b

TEST #7 I-1.5"-5-15°-1/8"-15-S_y=0-S_h=0-F

DEPTH OF CUT 0.0"
VEL 7581 1/s
Vmax 0.16 v
Ed 8.17 E08 psi
20mV/DIV
0.1ms/DIV



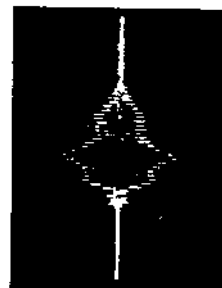
INITIAL

DEPTH OF CUT 0.48"
VEL 7818 1/s
Vmax 0.08 v
Ed 8.00 E08 psi
20mV/DIV
0.1ms/DIV



FIRST

DEPTH OF CUT 0.88"
VEL 7448 1/s
Vmax 0.08 v
Ed 8.83 E08 psi
20mV/DIV
0.1ms/DIV



SECOND

a

Fig. 14. Sonic stress wave patterns at different stages of the experiment under a particular set of parameters (a) without any confining pressure (b) with confining pressure.

block after one or two cycles of cutting and the fractures thus formed remain open as depicted by the diminishing rate of acoustic emission (A.E. hereafter) (Fig. 15). However, under higher confining pressures, the magnitude and extension of the fractures is less, and furthermore, the fractures developed during the cutting tend to close due to the confining pressure. Figure 16 illustrates the continued A.E. activity even after cutting is over. This is an indication of the fracture closure. The high rate of A.E. during the application of confining pressure can also be seen in this figure at location a. Apart from this, the other recorded data such as cutting pressure, thrust pressure, rpm of the drum and depth of cut can also be seen in Figures 15 and 16. The fluctuation in the depth of cut and rpm curves in Figure 16 in contrast to Figures 4 and 15 is due to the higher depth of cut than the anticipated 1/4 in. (0.64 cm). This was due to the higher temperature of the hydraulic oil. Figure 17 shows the photographs of the two coal blocks a and b after test #8 and #11, respectively. It also shows the microscopic photographs taken at a zoom setting of 1.5 at three areas. These photographs indicate that the bit chips at the entrance (area 1), grades at the center (area 2), and shears at the exit (area 3).

CONCLUSIONS

The analysis of these experiments is very preliminary. More experiments need to be done in order to make assertive conclusions. However, some of the conclusions based on the general trends are:

(1) The resultant force necessary is the least for the 30 degree attack angle while it increases for lesser than or greater than the 30 degree attack angle.

(2) The 30 degree attack angle produces more larger fragments than any other attack angle.

(3) The higher the equivalent in-situ pressure the finer are the coal fragments.

(4) The higher the drum rpm the greater is the force required to cut.

(5) The optimum spacing was found to be 1.5 in. (3.81 cm) to break the boundary walls between the bit paths.

EFFECT OF IN-SITU AND OPERATING PARAMETERS

#10 I-1.5"-5-60°-1/4"-25-F-S₁=0-S₂=0

Cutting Pressure, C_p = 6273 lbs(2851 Kg) FS*

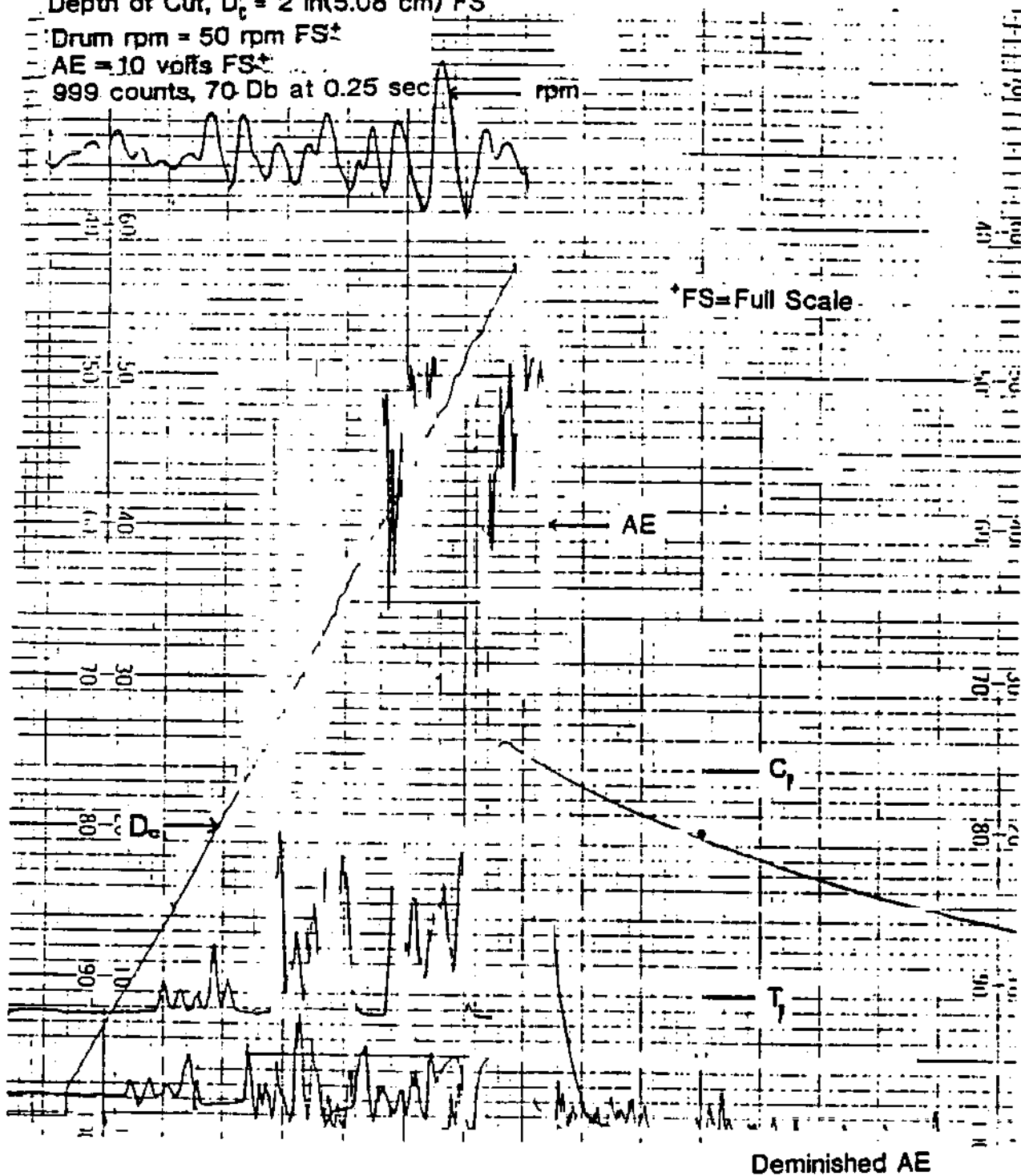
Thrust Pressure, T_p = 12898 lbs(5863 Kg) FS*

Depth of Cut, D_c = 2 in(5.08 cm) FS*

Drum rpm = 50 rpm FS*

AE = 10 volts FS*

999 counts, 70 Db at 0.25 sec



Deminished AE

Fig. 15. Typical chart on which the different parameters such as A.E., cutting pressure, thrust pressure, drum rpm and depth of cut are recorded for a particular set of parameters. Angle, depth of cut and rpm are different from that of Figures 16 and 4.

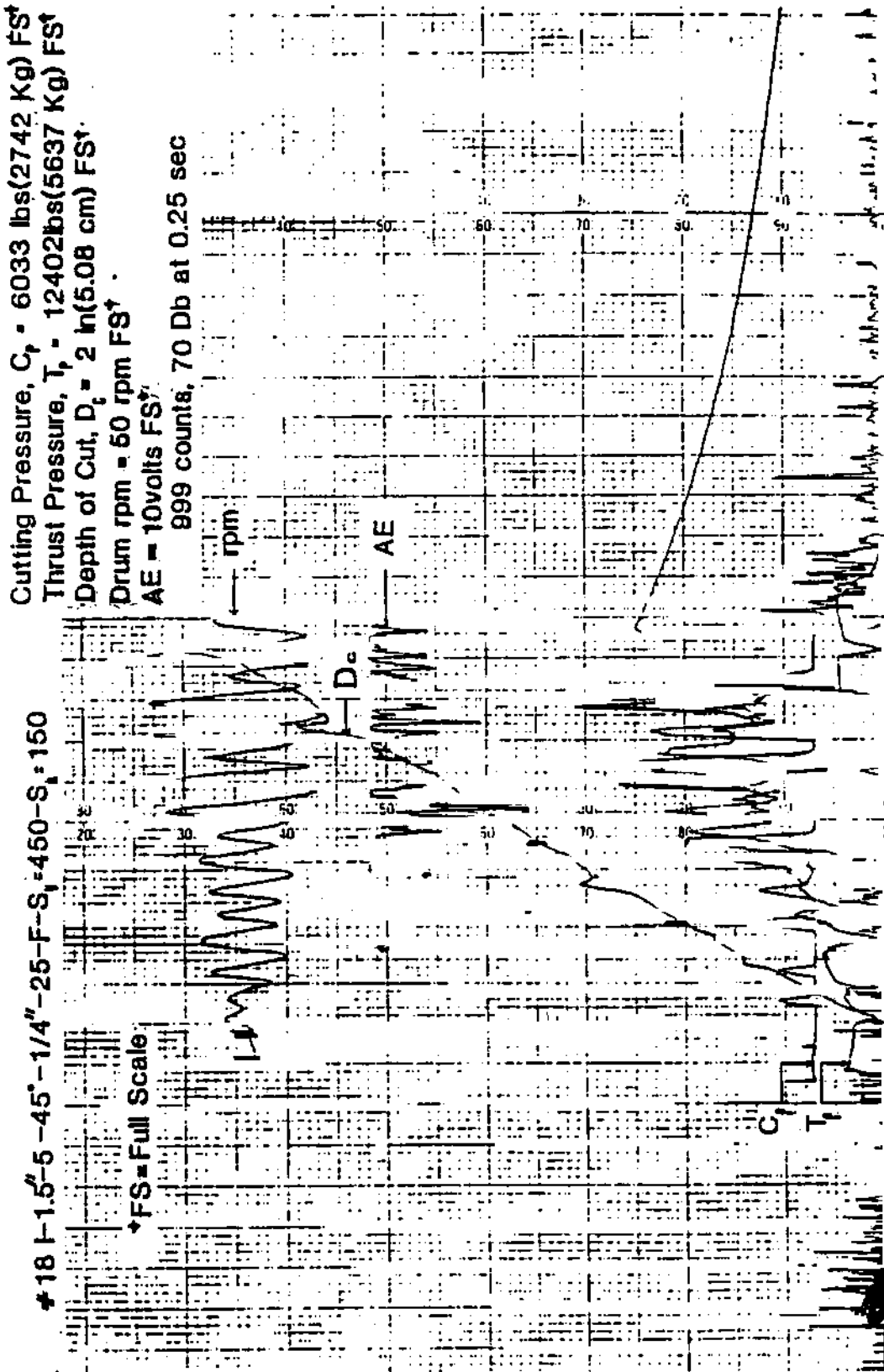


Fig. 16. Typical chart on which the different parameters such as the A.E., cutting pressure, thrust pressure, drum rpm and depth of cut are recorded for a particular set of parameters under vertical and horizontal confining pressures of 450 and 150 psi (64.8 and 21.6 KPa), respectively.

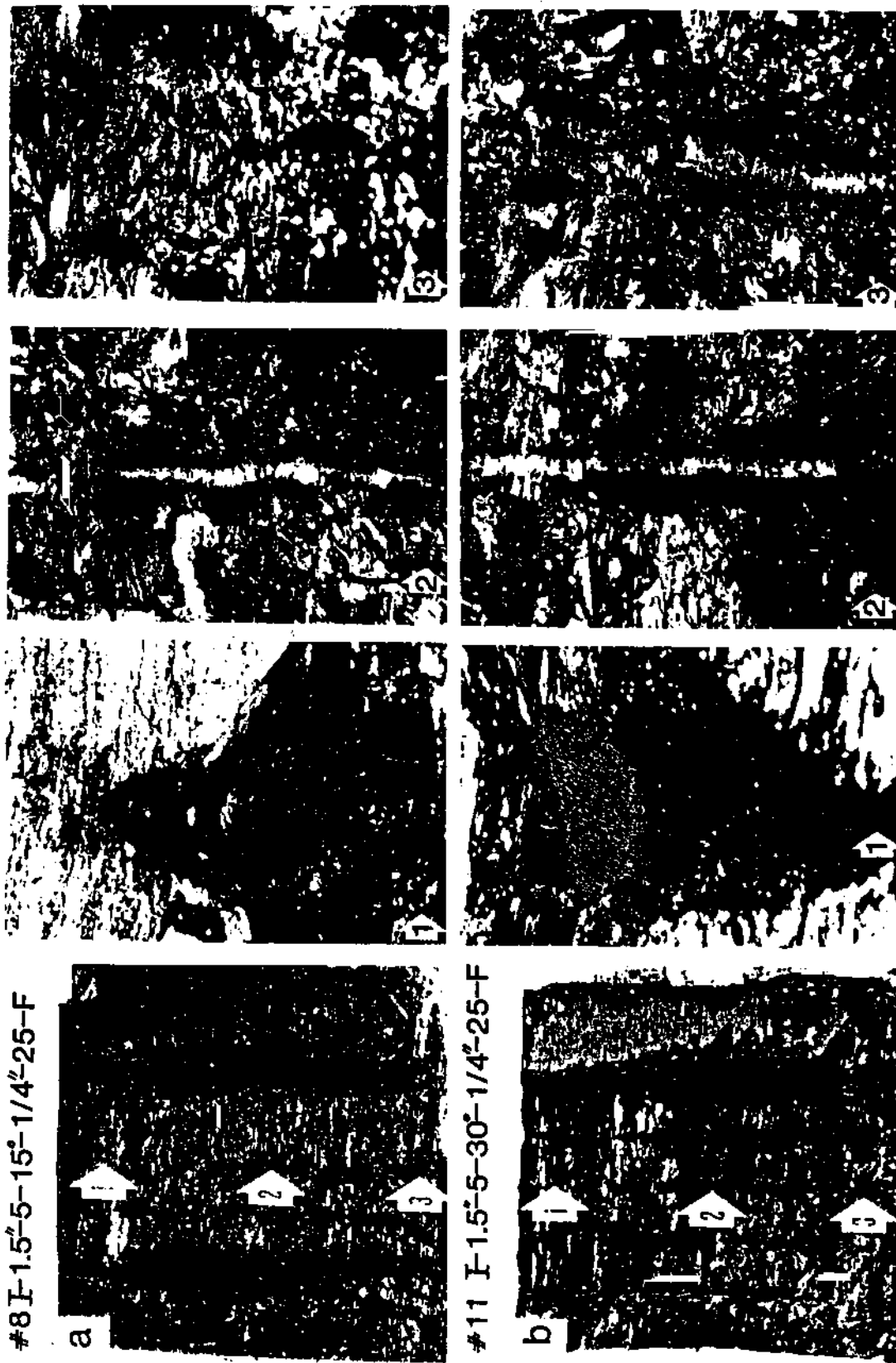


Fig. 17. Photographs of the coal block after cutting and microscopic pictures at three locations. (a) Photograph of the coal block of test #8; (b) photograph of the coal block of test #11. 1, 2, and 3 are the microscopic photographs of three areas all taken with a zoom setting of 1.5. Area 1, 1 in. (2.54 cm) after the bit enters the coal block; Area 2, center of the coal block and area 3, 1 in. (2.54 cm) before the bit exits the coal.

THE RESPIRABLE DUST CENTER

ACKNOWLEDGMENTS

The authors acknowledge the assistance of M. Quinn, R. Begley, G. Begley and S. Jung, graduate students in the Mining Engineering Department, in preparing this paper. This project was funded by the Generic Center for Respirable Dust Research sponsored by the United States Bureau of Mines under Grant Number G1135142.

EFFECT OF IN-SITU AND OPERATING PARAMETERS

REFERENCES

1. Newmeyer, G. E., 1981, "Cost of the Black Lung Program," Mining Congress Journal, Vol. 67, No. 11, November, pp. 74-75.
2. Khair, A. W., 1984, "Design and Fabrication of a Rotary Coal Cutting Simulator," Proceedings of the Coal Mine Dust Conference, October, pp. 190-197.
3. Pomeroy, C. D. and Foote, P., 1960, "A Laboratory Investigation of the Relation Between Ploughability and the Mechanical Properties of Coal," Colliery Engineering, April, pp. 146-154.
4. Terry, N. B., 1959, "The Dependence of the Elastic Behavior of Coal on the Microcrack Structure," Fuel, London, 38, pp. 125-146.
5. Evans, I. and Pomeroy, C. D., 1966, "Strength, Fracture, and Workability of Coal," Pergamon Press.
6. Pomeroy, C. D., 1963, "The Breakage of Coal by Wedge Action, Factors Influencing Breakage by Any Given Shape of Tool-1," Colliery Guardian, November, pp. 642-677.
7. Pomeroy, C. D., 1964, "Breakage of Coal by Wedge Action, Factors Affecting Tool Design-2," Colliery Guardian, July, pp. 115-121.
8. Bower, Jr., A. B., 1970, "Bit Design: Key to Coal Cutting," Coal Age, July, pp. 70-75.
9. Hurt, K. G., 1980, "Rock Cutting Experiments with Point Attack Tools," Colliery Guardian Coal International, April, pp. 47-50.
10. Ford, L. M. and Friedman, M., 1983, "Optimization of Rock-Cutting Tools Used in Coal Mining," Proc. 24th U. S. Symposium on Rock Mechanics, June, pp. 725-732.
11. Fuh, G. F., 1983, "On the Determination of Cutter Bit Spacing for Optimum Coal Mining," Proc. 24th U. S. Symposium on Rock Mechanics, June, pp. 703-711.
12. Friedman, M. and Ford, L. M., 1983, "Analysis of Rock Deformation and Fractures Induced by Rock Cutting Tools Used in Coal Mining," Proc., 24th U. S. Symposium on Rock Mechanics, June, pp. 713-723.
13. Warner, E. M., 1970, "Machine and Cutting Element Design," Mining Congress Journal, August, pp. 35-43.
14. Pomeroy, C. D., 1968, "Mining Applications of the Deep Cut Principle," Mining Engineer, June, pp. 506-517.
15. Evans, I., 1984, "A Theory of the Cutting Force for Point-Attack Picks," Technical Note, International Journal of Mining Engineering, pp. 63-71.

SOCIETY OF MINING ENGINEERS OF AIME

CALLER NO. D, LITTLETON, COLORADO 80127

PREPRINT
NUMBER

85-413



MECHANISMS OF RESPIRABLE DUST GENERATION BY CONTINUOUS MINER

A. W. Khair

M. K. Quinn

West Virginia University
Morgantown, West Virginia

For presentation at the SME-AIME Fall Meeting
Albuquerque, New Mexico - October 16-18, 1985

Permission is hereby given to publish with appropriate acknowledgments, excerpts or summaries not to exceed one-fourth of the entire text of the paper. Permission to print in more extended form subsequent to publication by the Institute must be obtained from the Executive Director of the Society of Mining Engineers of AIME.

If and when this paper is published by the Society of Mining Engineers of AIME, it may embody certain changes made by agreement between the Technical Publications Committee and the author, so that the form in which it appears here is not necessarily that in which it may be published later.

These preprints are available for sale. Mail orders to PREPRINTS, Society of Mining Engineers, Caller No. D, Littleton, Colorado 80127.

PREPRINT AVAILABILITY LIST IS PUBLISHED PERIODICALLY IN
MINING ENGINEERING

MECHANISMS OF RESPIRABLE DUST GENERATION

Abstract. This paper presents an analysis of respirable dust generation due to the action of a continuous miner. Underground coal cutting by a drum-type continuous miner was simulated in the laboratory using a specially designed unique automated rotary coal cutting simulator (ARCCS). An analysis of -400 mesh particles was done on gravity collected material. Samples of entrained dust were collected through the use of cascade impactors. Both samples were analyzed for size distribution and particle shape. Using the simulated coal cutter permitted variation of operating and in-situ parameters to provide information on the effects on generation of -400 mesh particles. In these tests coal blocks with an approximate dimension of 18 in. x 15 in. x 6 in. (43.7 cm x 38.1 cm x 15.2 cm) were first subjected to confining pressures, equivalent to in-situ conditions. Such blocks were then cut by the cutting head of the ARCCS, thus simulating the action of the continuous miner in underground coal mining. During the tests under a particular set of in-situ and operating parameters a number of other parameters such as 1) penetration of bit into coal, 2) penetration resistance (thrust and cutting pressures), 3) rotating velocity of cutting head, and 4) acoustic emission activity in the coal block were monitored. After each cutting cycle the fractured surfaces were photographed and a velocity survey was conducted by using a sonic technique. At the end of each experiment the cutting paths of the bits in coal were photographed using an optical microscope with an attached camera.

Introduction

The continuous-mining machines introduced in the 1950's now account for more than half the production of coal from underground mines. Unfortunately, these continuous miners, designed for increased productivity, have also increased the concentration of respirable dust in mines. As a result, the Federal Coal Mine Health and Safety Act of 1969 was enacted to enforce on the coal operators that the airborne respirable dust not exceed 2 mg/m³, and was intended to reduce the incidence of coal workers pneumoconiosis. This plus the other aspects of the legislation and the subsequent monitoring and enforcement by MSHA made it very imperative that the coal operators provide a relatively healthier and safer working environment for the coal miners. Since 1970, the Federal government has paid over 11.7 billion dollars to more than 470,000 miners with coal workers pneumoconiosis and their survivors (Newmeyer, 1981). These regulations, coupled with the assessment of the continuing burden on miners, the mining industry and taxpayers appear to have provided an impetus for the mining community towards comprehending the different parameters that influence dust generation and entrainment.

Dust control techniques such as conventional water sprays and dust collectors are only partially effective and require additional equipment expenditures. A more authentic approach would be to reduce respirable dust at the source, the continuous mining machine head, where the fragmentation process occurs. Improving the fragmentation process by understanding the mechanisms of coal breakage will not only reduce

respirable dust at the face, but it will also decrease the amount of respirable dust that is liberated during the secondary handling.

Fragmentation of coal can be expressed as a function of three major groups of parameters; namely, 1) coal properties, 2) in-situ conditions and 3) operating parameters. This paper deals first with the analysis of mechanisms that take place in the breakage of the coal along the cutting path, and second with the study of the generation of -400 mesh coal particles as a function of machine operating parameters such as rate of advance, angle of attack, bit configuration, bit lacing (spacing and pattern) and bit speed.

Study Program

Laboratory Equipment and Instrumentation

Review of the literature on coal cutting technology and the basic parameters that effect this technology revealed that most of the existing coal cutting machinery is of the rotary type and that the parameters that effect the fragmentation of coal in such cutting depend on the following (Terry, 1959; Pomeroy and Foote, 1960; Pomeroy, 1963, 1964; Evans and Pomeroy, 1966; Pomeroy, 1968; Bower, 1970; Warner, 1970; Hurt, 1980; Ford and Friedman, 1983; Friedman and Ford, 1983; Fuh, 1983; Evans, 1984):

$$\text{Coal fragmentation} = f(C_p, I_c, O_p)$$

where C_p is the mechanical properties of coal, I_c is the in-situ conditions (vertical and horizontal stresses), and O_p is operating parameters. Based on this premise a unique automated rotary coal cutting simulator (ARCCS) (Fig. 1) was designed and fabricated in the Mining Engineering Department at West Virginia University (Khair, 1984). This design incorporates the capability to study the different machine and in-situ parameters that influence the fragmentation of coal and the resulting dust. It operates under the simulated mining conditions with in-situ stresses (horizontal and vertical stresses) being applied to a coal block of 18 in. x 15 in. x 6 in. (43.7 cm x 38.1 cm x 15.2 cm) located in a suitably designed confining chamber. The cutting drum with a maximum bit tip to tip diameter (varies with the bit angle) of 19 inches has the capability of rotating from 1 to 30 rpm. The drum can be stopped any time after a predetermined number of revolutions. Tests can be performed with four different bit angles, 15, 30, 45 and 60 degrees. A maximum of seven bits can be mounted on the drum in an echelon pattern. The ARCCS can be operated and controlled manually or automatically, and the operating parameters can be preset with a series of hydraulic valves and could be recorded in analog/digital or in both forms.

Test and monitoring facilities can be seen in Fig. 1. ARCCS (Fig. 1a), programmable control and monitoring unit (Fig. 1b), sonic testing unit (Fig. 1c), acoustic emission monitoring unit (Fig. 1d), microscopic photographic unit (Fig. 1e), cascade impactors (Fig. 1f), hood and air current generating unit (Fig. 1g) and data acquisition and recording unit (Fig. 1h). In addition to

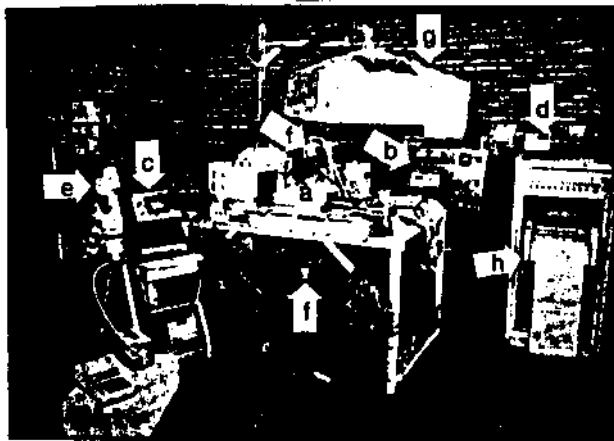


Fig. 1. Test and monitoring equipment facilities (a) automated rotary coal cutting simulator, (b) programmable control and monitoring unit, (c) sonic testing unit, (d) acoustic emission, (e) microscope and the attached camera unit, (f) cascade impactors, (g) hood and air current generating unit and (h) data acquisition and recording unit.

to this, linear variable transformers, pressure transducers, flow meters, flow controls and drum rpm were some of the other monitoring devices. LVDT's are used to monitor the displacement of the coal block as well as the depth of cut. Pressure transducers are used to monitor the changes in pressure, both due to the thrust and due to the intermittent cutting nature of the rotary cutting. Flow controls are used to run the drum at a particular rpm between 1 and 50 and to provide a different rate of advance. All of the above mentioned devices are operated and monitored by a fully automated control system. The fracture surface (i.e., size, shape and intensity) is characterized, a) with the help of photographs taken at the end of each test by using a camera attached to an optical microscope, b) by monitoring the acoustic emission and c) by monitoring the sonic signal in the coal block located in the confining chamber with the help of sonic transducers, signal generator, and an oscilloscope.

Specimen Preparation

Large blocks of coal were obtained from a surface mine. These blocks were then cut in the laboratory to an approximate dimension of 17 in. x 13 in. x 6 in. (43.2 cm x 33.0 cm x 15.2 cm). A typical specimen with cutting face (face/butt cleat) was then placed in a wooden box of 18 in. x 15 in. x 6 in. (45.7 cm x 35.6 cm x 15.2 cm) in dimension. Two blocks of wood 1.25 in. x 1.5 in. x 5 in. (3.2 cm x 3.8 cm x 12.7 cm) were wedged between the coal sample and the wooden box. Plaster of paris was then poured in the box to fill all the remaining space other than that occupied by the coal block. This process

gave a perfect dimension of 18 in. x 15 in. x 6 in. (45.7 cm x 35.6 cm x 15.2 cm) which was very essential to avoid stress concentration in the specimen when confining pressure was applied. After a week the moulded coal samples were removed from the box and the wooden blocks that were wedged before pouring the mould were dislodged from the sample carefully, thus creating room to house the sonic transducers. A typical specimen ready to be cut is shown in Figure 2.

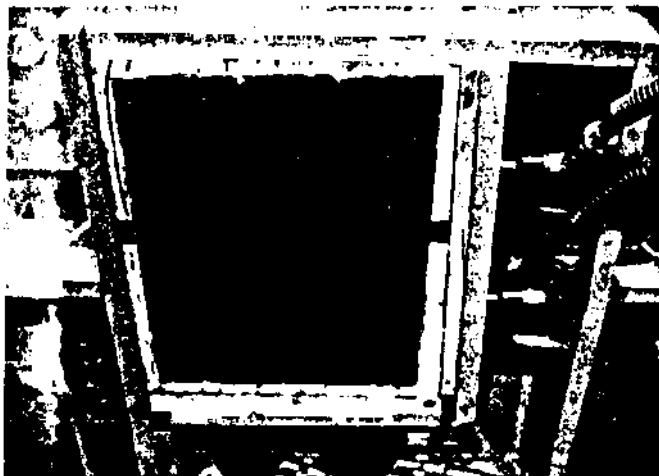


Fig. 2. Typical specimen ready for experiment.

Experimental Procedure

During a typical experiment the moulded specimen was placed in the confining chamber, the test conditions were set, and the in-situ and

MECHANISMS OF RESPIRABLE DUST GENERATION

operating parameters were marked on the top mould layer of the sample. A sonic test was done by which the stress wave travel time through the coal sample and the amplitudes of the signal were measured and recorded. Equivalent in-situ stresses were then applied to the specimen using two sets of hydraulic jacks (two for horizontal and two for vertical). A 1 in. (2.54 cm) thick steel plate was positioned between the sample and hydraulic jacks in order to distribute the pressure uniformly over the whole surface of the specimen. Each set of hydraulic jacks was connected in parallel to a hand pump. After the confining pressure was applied another sonic test was made and the corresponding stress wave travel time and amplitude were measured and recorded. Before the test, the operating parameters such as velocity of the cutting drum and rate of advancement were adjusted to predetermined values. Then bit blocks of specific attack angle (15, 30, 45 and 60 degrees) were mounted on the cutting drum at a particular spacing (Fig. 3), i.e. 1.5 in. to 3.0 in (3.8 cm to 7.6 cm). Bits of specific make and type were inserted into the bit block slots and were kept in position by a screw in such a way so as to allow bit rotation inside the lock which prevents non-symmetric bit wear. The number of rotations by the cutting head was set in the counter unit in the control module and then the machine was started to execute the program in a continuous or counter mode. The counting of the number of rotations starts when the hydraulic pressure is increased, due to the cutting process, or when the cutting head has traveled to a preset distance measured mechanically and by LVDT. After the execution of the predetermined number of rotations the cutting head retreated and stopped. After each cutting cycle, the samples were photographed and a sonic test was done. During the test a number of parameters were recorded (Fig. 4). Test conditions were marked on each specimen as well as on the recorded data (i.e., 1-bit type; 1.5"-bit spacing; 5-number of bits; 15°-bit attack angles; 1/8"-depth of cut; 15-drum rpm; F-face cleat; S_v , S_h -vertical and horizontal confining pressures, respectively). At the end of the experiment the specimens were photographed and using a microscope with an attached camera, the path of the cutting face was photographed at three locations, entrance, center, and exit of the bit paths. Airborne particles were collected by using a cascade impactor while the larger particles were collected in a large bag with the vacuum cleaner.

Results and Discussion

The coal used in the experimental study is part of the Waynesburg coal seam. Prior to the experiments the physical and mechanical properties of this coal were determined in the laboratory. The physical and mechanical properties can be seen in Tables 1 and 2.

A study of thirty-four experiments has been completed analyzing both the mechanisms of respirable dust generation and also the effects of operating, in-situ and geologic parameters on the fragmentation of coal. The parameters observed were bit spacing, drum velocity, depth of cut, confining pressure, coal cleat direction, angle of attack and types of bit. Despite a

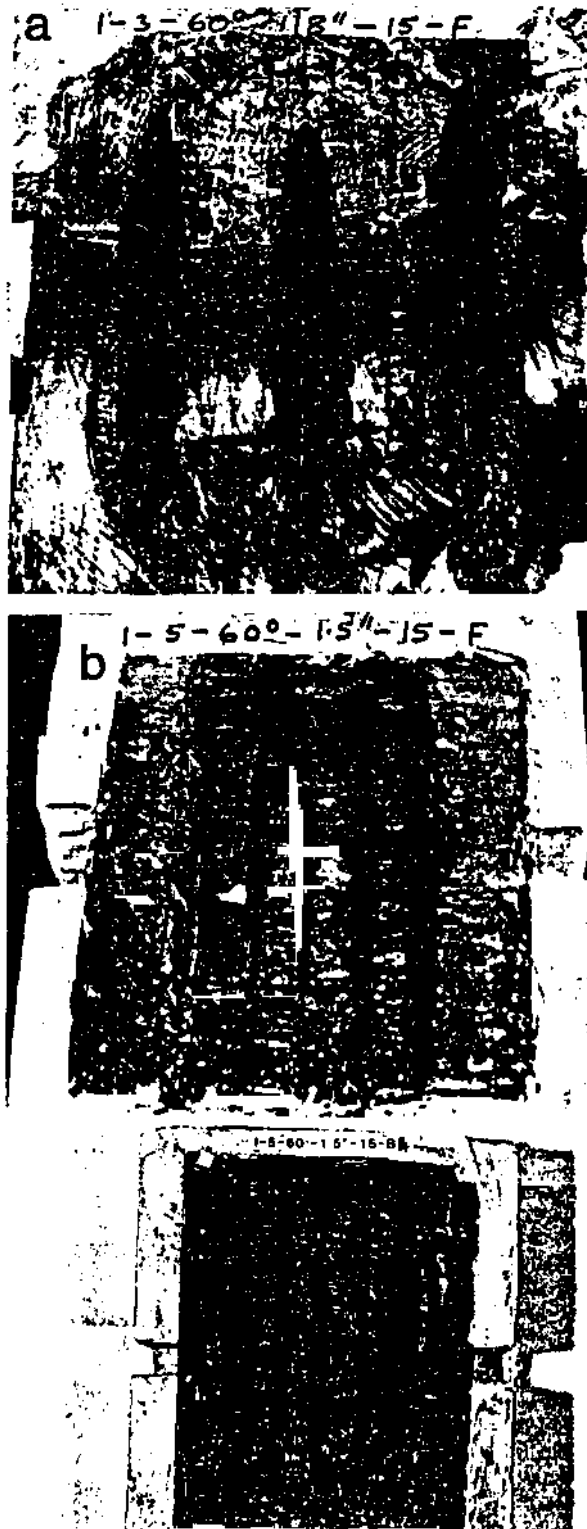


Fig. 3. Coal blocks with different bit spacing (a) 3 in. (7.62 cm) spacing-face cleat, (b) 1.5 in. (3.81 cm) spacing-face cleat and (c) 1.5 in. (3.81 cm) spacing-but cleat.

THE RESPIRABLE DUST CENTER

Table 1. Physical Properties of Waynesburg Coal

Moisture %	Ash %	Sulfur %	Rank	HGI*	Sp.Gr.
0.0-1.5	13.5-13.7	2.03-2.06	hv8b**	50.43	1.42

*Hardgrove Grindability
**High Volatile B Bituminous

Table 2. Mechanical Properties of Waynesburg Coal

Cleave/B bedding Plane Orientation	Compressive Strength psi (KPa)	Young's Modulus psi (KPa)	Poisson's Ratio	Indirect Tensile Strength psi (KPa)	Direct Shear Strength psi (KPa)
Face Cleave	3289 (473.6)	5.1×10^5 (7.3×10^4)	0.25	154 (22.2)	204 (29.4)
Butt Cleave	3459 (498.1)	4.7×10^5 (6.8×10^4)	0.31	205 (29.5)	180 (25.9)
Bedding Plane	4912 (707.4)	4.6×10^5 (6.6×10^4)	0.32	146 (21.0)	80 (11.5)

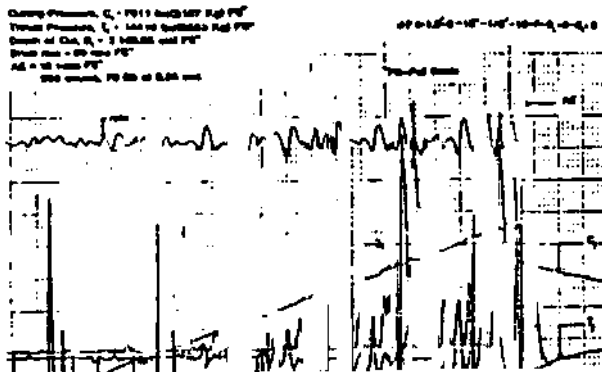


Fig. 4. Typical chart on which the different parameters such as acoustic emission rate (A.E.), cutting pressure (C_p), thrust pressure (T_p), drum speed (rpm) and depth of cut (D_c) are recorded for a particular set of operating parameters under zero confining pressure.

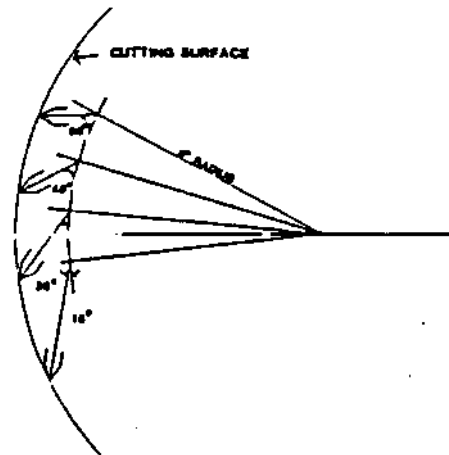


Fig. 5. Illustrates the cutting surface (cutting path) and the area of contact between the cut surface and bits mounted at various attack angles on the cutting head.

Limited number of tests, a large volume of data was collected of which only a part will be presented for discussion.

Mechanisms of respirable dust generation due to the action of a continuous miner is complex. It is a function of the fragmentation process and machine-bit-coal interaction. To understand the fragmentation process it is necessary to analyze the fracture surface. The cut face or path can be partially smooth and partially rough

(Fig. 3) and has an arched shape with a radius equal to the cutting head (Fig. 5). The fracturing process is governed by dynamic and quasi-static forces. The dynamic forces cause fracture formation and fracture extension (rough surface) where the quasi-static forces are responsible for the grading of fracture surface (smooth surface).

Thus fragmentation of coal under the action of the cutting head is not a continuous process relatively speaking. To elaborate this further,

MECHANISMS OF RESPIRABLE DUST GENERATION

observations during the tests indicated that after the cutting head induces certain fractures (different intensities, magnitudes and lengths) its rotational velocity slows down and even drops to a momentary stop stage depending on the amount of energy placed on the coal. This fluctuation of the velocity of the cutting head can be seen in Fig. 4 (rpm). The higher the rotational velocity of the cutting head the higher the magnitude of these fluctuations can be observed (Fig. 6). Furthermore the magnitude of fluctuation depends on the required dynamic forces for cutting coal (Fig. 7).

In Fig. 7, due to the application of confining pressures and increasing depth of cut, the magnitude of required dynamic forces to cut the coal increased, therefore the magnitude of fluctuation in the drum velocity also increased. After each impact, the cutting head graded the fractured surface in quasi-static motion and accelerated to a rotational velocity above the preset level. The time duration between the peaks acceleration and deceleration between the period energy used by the cutting head to fracture and grade the coal respectively.

Observations during the tests as well as data analysis indicated that the largest magnitude of the rotational velocity of the cutting head occurred when the bit first hit the coal (entered the coal body) and the least when the bit was at the center of the cutting path. The magnitude of the tangential force (cutting force) was the highest during dynamic loading, while the magnitude of the normal force (thrust force) was the highest during the grading loading stage. Therefore one can expect much higher fracture intensity, magnitude and length close to the entrance portion of the cutting path than at its center.

Macroscopically the condition of the fracture surface is a function of bit-spacing, cleat direction, pre-existence of cracks and discontinuities, compressive strength, and brittle-ductile characteristics of coal. For example when spacing between the bits is large enough the influence of one bit on the path of the adjacent bit is not sufficient, therefore the wall between the paths of the bits remain intact and the paths of the bits (cutting face) will look smooth (Fig. 3a), otherwise the cutting face will look rough but regular (Fig. 3b). In comparing Fig. 3b and 3c, it is obvious that the fracture surface in Fig. 3c is rougher and more irregular than the fracture surface of the coal block shown in Fig. 3b. This difference is mostly due to the higher compressive strength of coal along the butt cleat, higher cutting resistance offered by the coal in the butt cleat direction, and failure characteristics of coal along the face/butt cleat directions.

Microscopically the condition of the fracture surface is affected by the tip of the bit and the area of contact between the bit and the coal block. Figure 8 illustrates a microscopic view of the fractured surfaces at three positions; namely, entrance, center, and exit using an attack angle of 15° (Fig. 8a) and 30° (Fig. 8b). In general the fracture surface at the area under the top of the bit at the entrance position had features like microscopic ridges where the fragments had been dislodged. These microscopic ridges were characterized by a thin shiny line

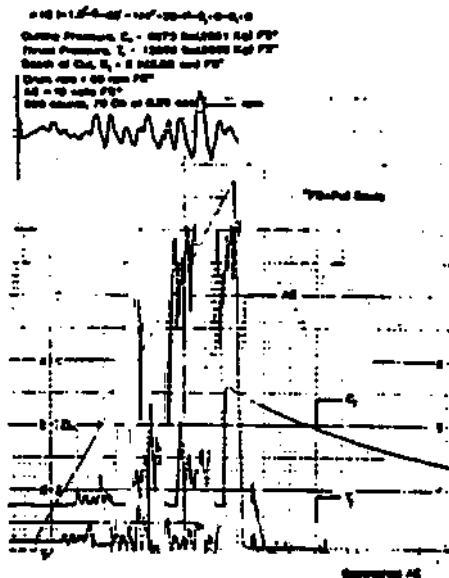


Fig. 6. Illustrates typical data obtained during the experiment. Emphasis here is on the higher fluctuation of the cutting head speed at higher rpm and the diminishing A.E. soon after the cut under zero confining test condition.

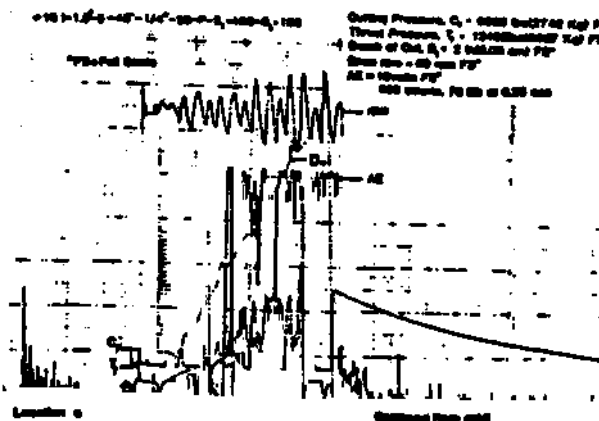
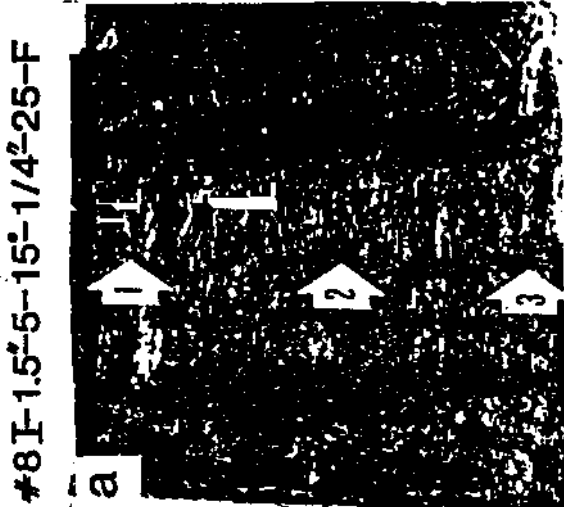


Fig. 7. Typical data obtained in confined test condition. Emphasis here is on the high fluctuation of cutting head speed (rpm) and continued rate of A.E. after completion of the test. Also shows high rate of A.E. during application of confining pressure (location a).

at their edges, indicative of crushing of the fracture surface during the dislodging of the fragment. At the center and most of the cutting path of the bit (at the bottom of the grooves) the fracture surface was smooth and was characterized by a wide shiny line (Fig. 8a-b, area 2). At the end of the cutting path, the bit often sheared off part of the coal (when the

#8 I-1.5'-5-15'-1/4'-25-F



#11 I-1.5'-5-30'-1/4'-25-F

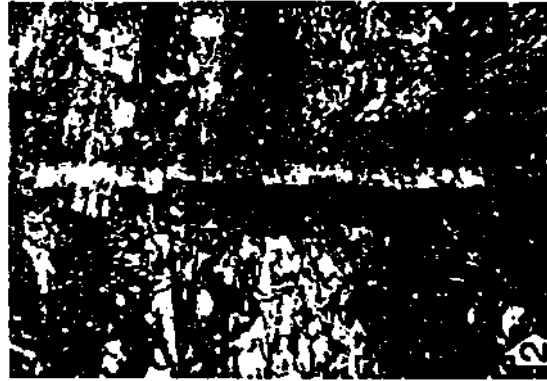
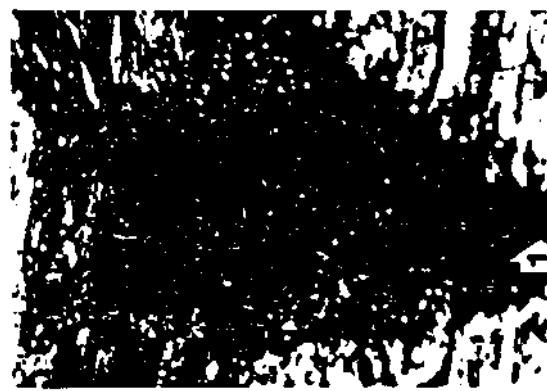
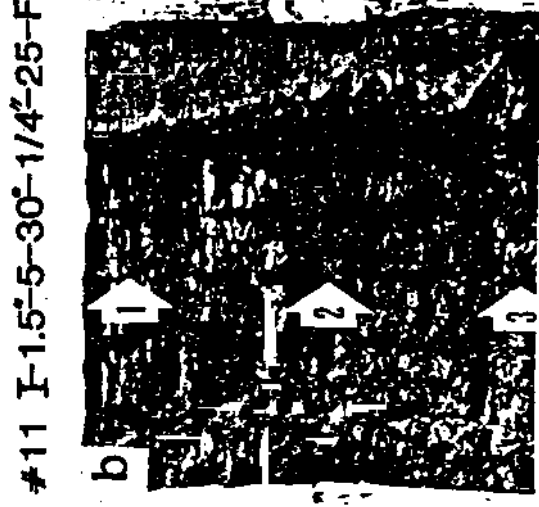


Fig. 8. Photographs of the coal block after cutting and microscopic pictures at three locations. (a) Photograph of the coal block of test #8; (b) photograph of the coal block of test #11. 1, 2, and 3 are the microscopic photographs of three areas all taken with a zoom setting of 1.5. Area 1, 1 in. (2.54 cm) after the bit enters the coal block; Area 2, center of the coal block and area 3, 1 in. (2.54 cm) before the bit exits the coal.

MECHANISMS OF RESPIRABLE DUST GENERATION

cutting path reached close to the edge of the coal block) creating a rough surface similar to the condition described in the case of the entrance position (Fig. 8a, area 3). If the coal did not break at the ends of the path, the area under the bit remained smooth and shiny (Fig. 8b, area 3).

Before discussing tool coal interaction, it is necessary to define particle size limits used in this paper. Large materials are defined as (+) 0.0937 in. (0.2368 cm), fine particles between 0.0937 to 0.0015 in. (400 mesh) and dust is -0.0015 in. (-400 mesh). These size distributions are the product of the analysis of the settled fragment using standard screening methods. It should be noted that although cascade impactors were used for collection of the floating dust, however due to short duration of the experiments the quantity of the floating dust collected was insufficient for analysis.

The interaction of the bit with coal has two elements which have an impact on the generation of respirable dust, namely 1) bit configuration and 2) attack angle. Figure 9 illustrates the interaction of the bit with coal where the bit configuration influences the fractured surface along the cutting path. During cutting (grading) the body of the bit exerts compressive and shear stresses on the wall between the bit path and consequently induces fractures and dust.

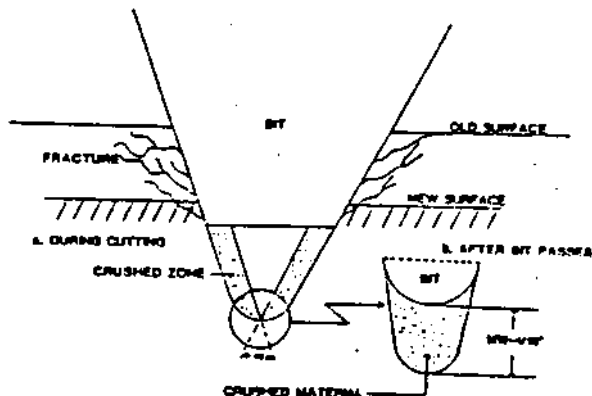


Fig. 9. Shows interaction of a bit with coal at the cutting path (a - during cutting, b - after cutting, bit passes).

A carbide tip is located at the end of the bit body. Although these carbide tips are of different sizes and shapes (angle α) they are not in alignment with the bit body. Therefore there is a gap between the carbide tip and the cut surface thus trapping crushed material (Fig. 9a). As the bit passed through the path (groove), frictional heat, generated by the rubbing of the bit (body/base of the carbide tip) against the coal, liquify part of these crushed material (Fig. 9b) leaving a shiny surfaced film (Figs. 8a-b, area 2). Microscopic analysis of the shiny surfaces, show that a larger volume

of the crushed material was trapped. The crushed material was like an agglomerate but could be picked apart easily. This trapped (crushed) material becomes a source of dust after subsequent cutting cycles.

The size and shape of the carbide tip also has a significant impact on producing dust during dynamic loading. Even though dynamic loading causes fracture formation and fracture extension it also produces a local crushing zone where the bit tip is in contact with the coal. The size of this crushing zone is proportional to the size and width (angle α) of the carbide tip.

To evaluate the effects of bit configuration and carbide tip shape, a series of experiments were performed and test procedures were modified to eliminate the influence of other factors in fragmentation. Four test specimens were cut from a large block of coal and were tested against the face cleat. The vertical and horizontal stresses on the specimens were kept constant at 512 psi (73.73 KPa) and 300 psi (43.2 KPa) respectively. Using a 30° attack angle and a cutting head revolution of 15 rpm, the cutting depths were kept constant to 0.20 in/rev (0.51 cm/rev) to a total of 1.9 in. (3.55 cm).

The coal cutting machine was completely covered with plastic sheets to avoid loss of floating dust. After each test all the material was removed with a brush without the aid of a vacuum cleaner. The four tested specimens and the associated cutting bits are shown in Fig. 10. The cutting bits used were: pencil bit, Type II (Fig. 10a), plumbob bit with a large carbide tip, Type III (Fig. 10b), slender/sharp bit with fins, Type IV (Fig. 10c), and regular plumbob, Type V (Fig. 10d). Fragment size distribution for the above four tests are shown in Fig. 11.

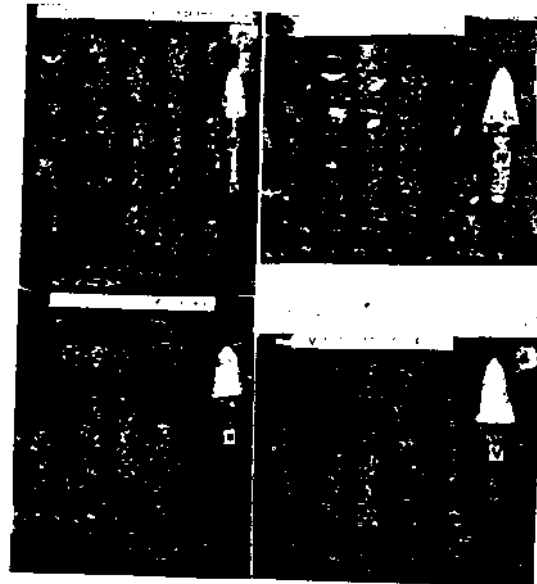


Fig. 10. Shows four tested specimens and the associated cutting bits.

THE RESPIRABLE DUST CENTER

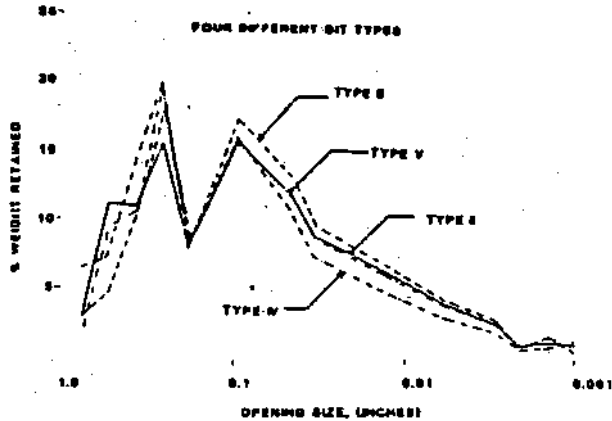


Fig. 11. Illustrates fragment size distribution characteristics for four different types of bits.

Results indicated that the blunt bit (type III) produced less large material and more fine material than the slender/sharp (type IV) bit. However the curves in Fig. 10 crossing at 400 mesh size suggest that the blunt bit produces more uniform sizes and the slender/sharp bit produces more non-uniform sizes (more large and dust and less fine sizes).

The two dips that appear in the size distribution curve (Fig. 11) are due to the type of screens used in the analysis. A standard $\sqrt{2}$ series was used from 0.742 in. to 0.187 in. (1.883 cm to 0.4746 cm), then the screens were used alternatively, meaning that the previous screen size was divided $\sqrt{2}$ to get the net size. From 0.187 in. to 0.0019 in. (0.475 cm to 0.00736 cm) the screens were used alternatively, or a 2 series where the previous screen size was divided by 2. The 0.0059 in. (0.01497 cm) sizes are screened with the $\sqrt{2}$ series again. This method was used to reduce the number of screens thus reducing dust loss, and also distributing irregularities at both ends of the size range. The dips occurred because the screens that start the change in the series receives twice the amount of material it would have in a straight series. The bump occurring at the 0.0015 in. (400 mesh) size was natural and is characteristic of this material not related to the screening. This was substantiated by using a 0.0021 in. (0.00533 cm) screen tested against another screen with similar results.

Four different attack angles, namely 15°, 30°, 45°, and 60° were used in this study (Fig. 12). Figure 5 demonstrates that the area of contact between the cut surface (in the cutting path) of the coal and the cutting bit for different attack angles are not the same. The most ideal condition for force transmission by the bit to the coal will be a 30° attack angle, where the area of contact between the bit and coal is the least and causes a high stress concentration in the coal block. As a result less force is required to break the coal. The smaller attack angle, i.e. 15° will not only have a larger area of contact (Fig. 5), it will also require a larger normal force (thrust) to penetrate the coal,

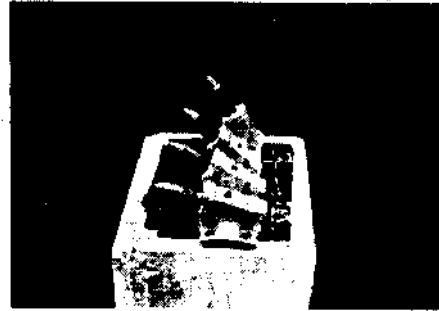


Fig. 12. Shows bit block with four different attack angles (60°, 45°, 30° and 15° from top to bottom).

consequently producing more friction caused heat especially during the quasi-static loading condition (grading).

The second ideal condition concerning force required to cut the coal would be the 45° angle of attack. The 60° angle of attack is similar to the 15°, however in this case the front portion of the bit will have a larger surface area of contact with the coal. Its influence on fragmentation will be during the dynamic loading cycle and the larger area of contact will make the bit act blunt.

Figure 13 shows the resultant forces needed to cut the coal at various depths for all four different bit attack angles. As it can be seen from Fig. 13 the least resultant force required to cut the coal is 30° bit attack angle and the highest of all is the 15° attack angle. Figure 13 also indicates that the resultant force to cut the coal is increasing with depth of cut for all bit attack angles.

Particle size distribution for four types of bit attack angles are shown in Fig. 14. From Fig. 14 it is clear that a 30° attack angle produces more large particles and less fine and dust size particles than the three other types when tested against both face cleat and butt cleat. However the tests using all four bit attack angles against the butt cleat produced less large particles and more fine and dust size particles comparing against face cleat. In Fig. 14 tests against the face cleat indicated the least fine particles for a 30° attack angle, next for 15°, third 60°, and fourth 45° attack angles. In tests against the face cleat the least dust produced order was 30°, 60°, 45°, and 15° attack angles, while in tests against the butt cleat the order was 15°, 30°, 45°, and 60°. Figure 14 also shows a smooth transition from fine range to dust range for a 60° attack angle tested against the butt cleat. This means that more material (particles) is produced at 0.0015 in. (400 mesh) size.

Increasing rotational velocity (rpm) of the cutting head increased the required resultant force to cut the coal (Fig. 15). Under high speed cutting most of the energy imposed on the

MECHANISMS OF RESPIRABLE DUST GENERATION

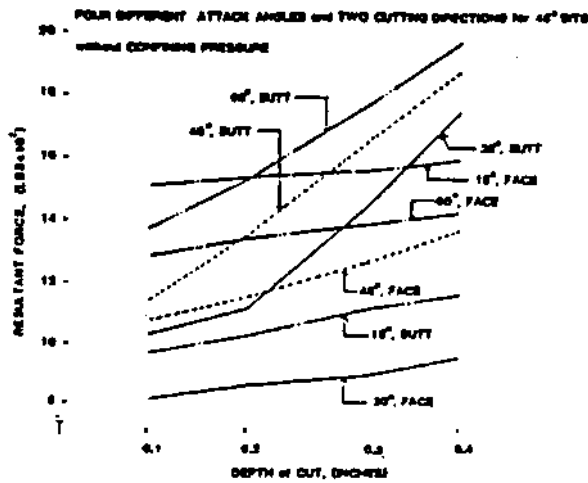


Fig. 13. Shows relationship between the resultant force vs. depth of cut as a function of bit attack angle and coal cleat directions.

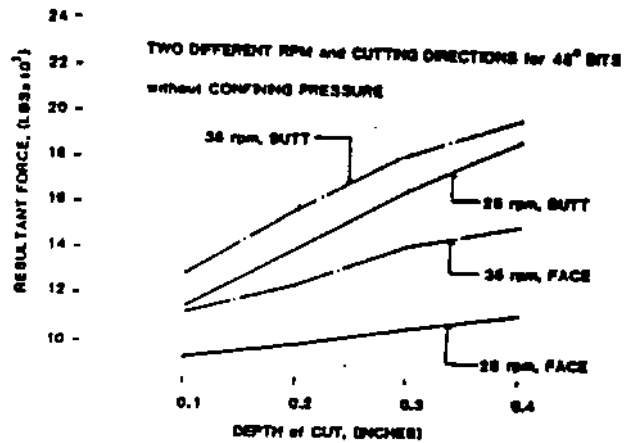


Fig. 15. Shows relationship between the resultant force vs. depth of cut as a function of cutting head speed (rpm) for both face and butt cleat directions.

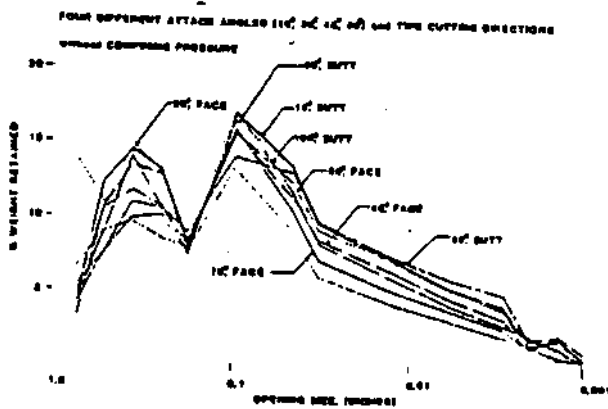


Fig. 14. Shows mesh size vs. percent of weight retained as function of bit attack angle and coal cleat directions.

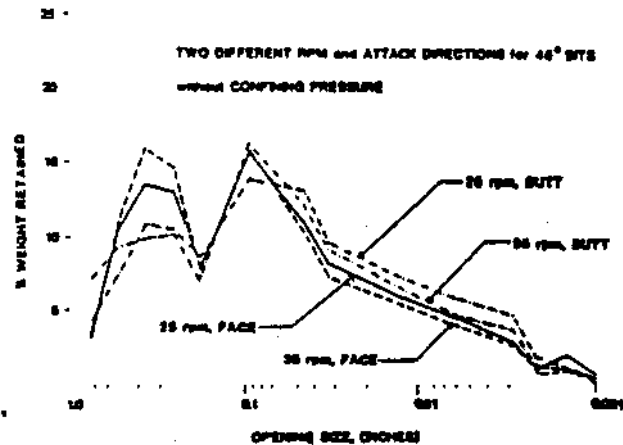


Fig. 16. Mesh size vs. percent of weight retained as a function of cutting head speed (rpm) and cleat directions.

coal was utilized during dynamic loading and less energy was utilized during the quasi-static loading (grinding). Therefore, more large and deep fractures into the coal surface were produced. Consequently there were more large particles than fine. Also the higher velocity of the cutting head increased the kinetic energy of the particles which then increases entrainment. Observations of the experiments verified this. Higher entrainment does not necessarily imply higher airborne particles but in this case it did increase the magnitude of airborne particles at the expense of settled material.

Figure 16 illustrates size distribution characteristics for 25 rpm and 35 rpm using a 45° bit angle against the face cleat and butt cleat in an unconfined situation. Figure 15 clearly demonstrates that the 35 rpm cutting head speed produced more large particles and less fine and dust size particles in comparison with the 25 rpm speed both in the face and butt cleat directions. However, in general the

cutting head at any speed produced more large and less fine size particles in the face cleat direction than in the butt cleat direction (Fig. 16).

Characteristics of size distribution indicated that whenever the cutting head produced more large and less fine particles the magnitude of the dust size particles was also higher (Fig. 17). Figure 17 illustrates size distribution of coal particles, using a 45° attack angle, 25 rpm cutting head speed under equivalent in-situ condition of 300 ft (90.91 m) against both the butt and face cleat. The equivalent in-situ stresses are assumed to be 1 psi/ft of depth (0.475 KPa/m) vertically (S_v) and horizontally (S_h) is $(\nu/1-\nu)S_v$, where ν is Poisson's ratio (Peng, 1978).

It is evident that in tests against the butt cleat more fine and less large and dust size particles are produced in comparison to tests against the face cleat direction. When large particles dislodged or broke away during the

THE RESPIRABLE DUST CENTER

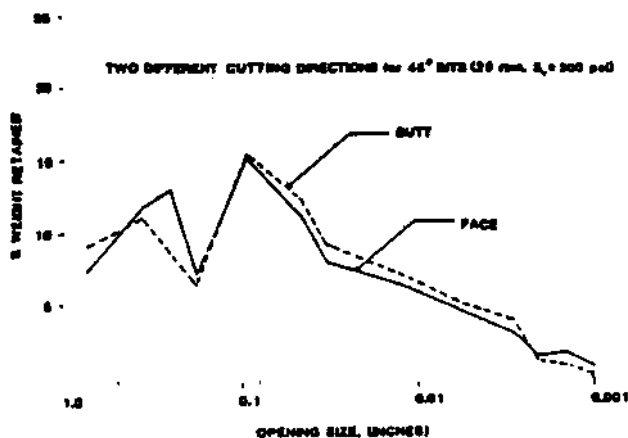


Fig. 17. Mesh size vs. percent of weight retained as a function of cleat directions. Emphasis here is the correlation between large and dust size particles.

dynamic loading cycle there always appeared a microscopic crushed zone at the edge of the fracture line (ridges). These crushed zones seem to be one of the major contributors of the dust size particles.

A series of experiments were run to study the effect of bit spacing on the force required to cut the coal and its impact on particle size distribution. Using a 3 in. (7.62 cm) spacing and 3 bits mounted in an echelon pattern a 2.5 to 3 in. (6.35 cm to 7.62 cm) cut was made without breaking the boundary walls between the bit paths (Fig. 3a). These series of tests with 3 in. (7.62 cm) spacing were done for 15°, 30°, 45°, and 60° attack angles. With a 1.5 in. (3.81 cm) spacing and 5 bits mounted in an echelon pattern the side walls of the bit path were broken when the coal blocks were cut in both face and butt cleat directions (Fig. 3b-c). These series of tests were done for attack angles of 15°, 30°, 45°, and 60° at various equivalent in-situ stresses. The fracture surface was more regular when tested against the face cleat (Fig. 3b), however in the case of the butt cleat the walls between the cutting path broke only partially and irregularly (Fig. 3c). Total breakage of the wall created a free surface thus reducing the required resultant forces to cut the coal.

Figure 18 shows the resultant forces required to cut coal at various depths using different bit spacings. Figure 18 clarifies that the force required to cut the coal is much higher when using 3 in. (7.62 cm) bit spacing than when using the 1.5 in. (3.81 cm) spacing. Also a larger resultant force is required to cut the coal along the butt cleat than along the face cleat. This is due to two factors, one that the compressive strength of the tested coal is 5.2% higher in the butt cleat direction than in the face cleat, and second that the butt cleat offers more resistance to cutting than the face cleats.

A typical particle size distribution associated with these tests is shown in Fig. 19.

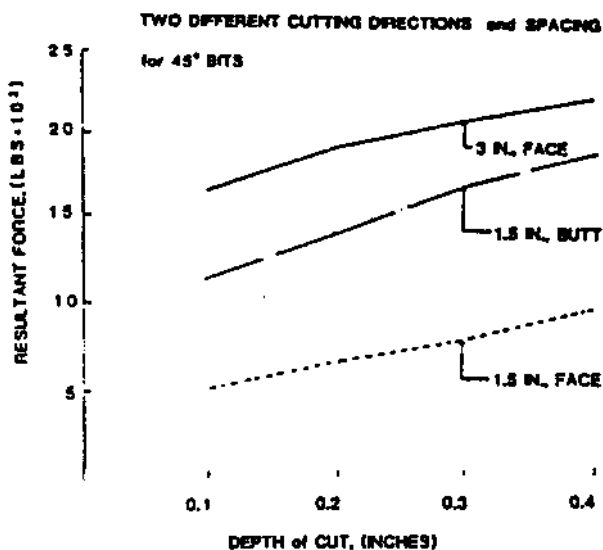


Fig. 18. Resultant forces vs. depth of cut as a function of bit spacing and cleat direction.

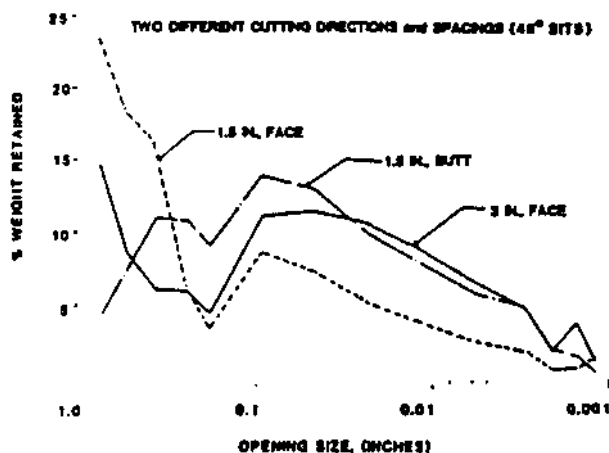


Fig. 19. Mesh size vs. percent of weight retained as a function of bit spacing and cleat direction.

In Figure 19 the use of 3 in. (7.62 cm) bit spacing produced less large size and more fine and dust size particles than in the use of a 1.5 in. (3.81 cm) spacing. Once again, tests against the butt cleat exhibited more fine and less large size particles than the tests carried out against the face cleat.

A number of experiments were conducted to investigate the effects of equivalent in-situ stresses on the resultant forces required to cut the coal as well as on the fragmentation characteristics of coal. Typical resultant force characteristic curves for these experiments are given in Fig. 20. The cutting resistance increased with the increasing confining pressure (Fig. 20). A typical particle size distribution characteristic curve is shown in Fig. 21.

MECHANISMS OF RESPIRABLE DUST GENERATION

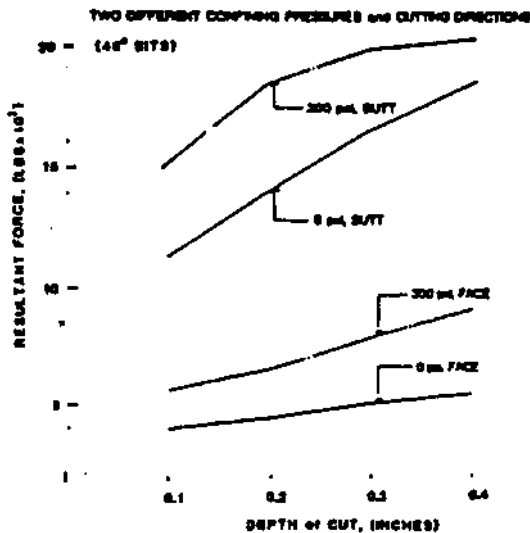


Fig. 20. Resultant force vs. depth of cut as a function of equivalent in-situ stresses (confining pressures) and cleat directions.

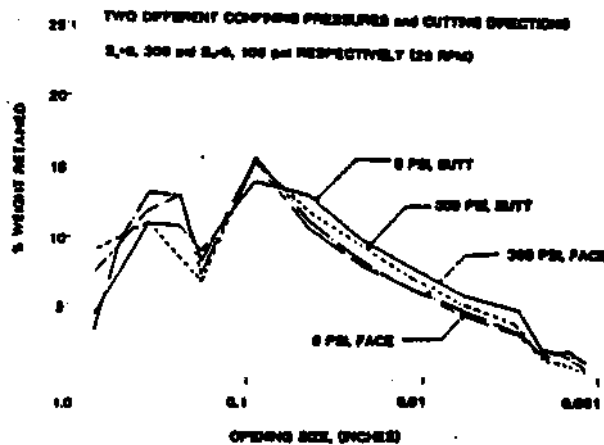


Fig. 21. Mesh size vs. percent of weight retained as a function of equivalent in-situ stresses (confining pressures) and cleat directions.

Figure 21 indicates a slight decrease in fine and dust size particle production with higher equivalent in-situ stresses in the butt cleat direction, however the effects of equivalent in-situ stresses along the face cleat is not quite clear. Confining pressures increase compressive strength (C) and Young's modulus of geologic material (Peng, 1978). The test results verified that confining pressure increased the cutting resistance (Fig. 20) and dynamic Young's modulus (Fig. 22).

The cutting head induces fractures into the coal during cutting thus reducing both the compressive strength and Young's modulus of coal. The degree of reduction in these properties depends on the intensity and size of the induced cracks. In an unconfined situation these cracks extend through the rock after a short penetration of the bit into the coal, and the coal block loses its integrity. Sonic tests indicated a decrease in the dynamic Young's modulus of coal block (Fig. 22a). However, under the confining condition the crack growth is slow and due to the action of confining pressure crack closure is possible (Fig. 22b). This was further substantiated by monitoring acoustic emission activity (A.E.) during the tests (Figs. 6-7). Figure 6 indicated a diminishing rate of A.E. after cutting the coal, while Figure 7 exhibited a continued rate of A.E. after the cutting closure in the coal block. In Figure 7 the high rate of A.E. at location "a" is due to application of confining pressures on the coal block prior to the test.

Figure 22b indicates that even after large penetration of the bit into the coal, the block remained intact. This could be one of the reasons that the cutting resistance increases with higher confining pressures. The energy imparted to the coal under the uniaxial compressive test is a function of normal stress in the

coal and Young's modulus of the coal (i.e., Energy = $1/2 \sigma^2/E$, where σ is the uniaxial compressive stress and E is Young's modulus). At time of failure stress equals the uniaxial compressive strength of coal C_0 and Energy = $1/2(C_0^2/E)$. Therefore more energy can be stored in the material prior to failure if the material has a higher compressive strength (C_0) and a lower Young's modulus (E). The butt cleat exhibits both of these characteristics more than the face cleat (Table 2). Table 2 shows that the butt cleat has a higher compressive strength and a lower Young's modulus than the face cleat. Applying confined pressure increases both the compressive strength and the Young's modulus.

The squared term of the compressive strength outweighed the increased elastic constant by 2 places, or 100 times. This seems to go along with the fact that confining pressure increased entrainment due to the higher energy released at the time of failure. One would expect that a higher confining pressure would increase the production of fine particles because of the higher compressive strength demonstrated by the butt cleat. However Fig. 21a indicates that the higher the dynamic Young's modulus the less fine particles are produced. Figure 21a shows that a higher confining pressure decreases the production of fine particles. More tests should be run to determine the actual position of confining pressures vs. production of fine particles without regard to the dynamic Young's modulus.

Conclusions

Although the results presented in this paper must be considered of a preliminary nature since they are based on a limited number of tests on a specific coal, nevertheless a number of significant points appear evident. These can be summarized as follows.

TEST #17 I-1.5"-5-45°-1/4"-25-S_v=150-S_h=50-F



TEST #7 I-1.5"-5-15°-1/8"-15-S_v=0-S_h=0-F

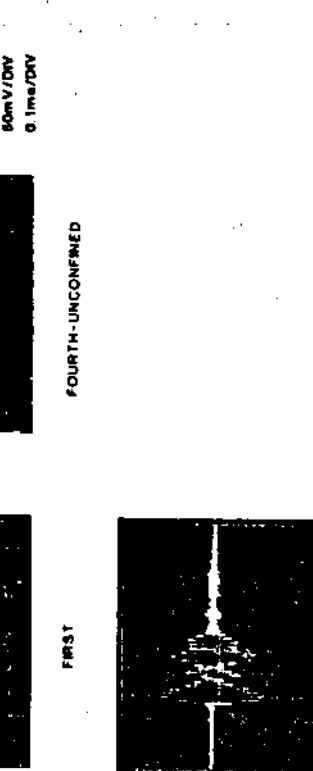
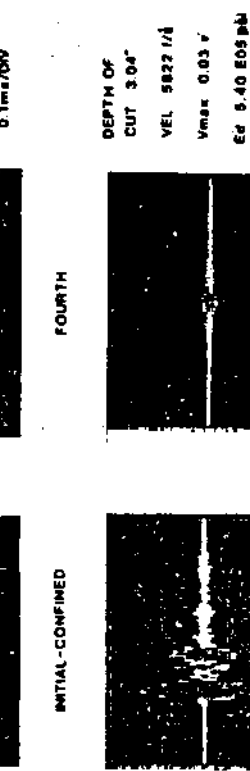
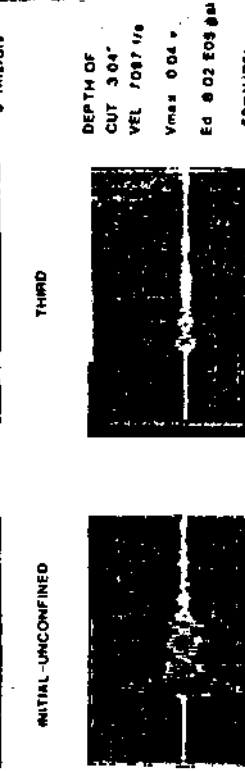


Fig. 22 Sonic stress wave patterns at different stages of the experiment under a particular set of parameters (a) without any confining pressure (b) with confining pressure.

b

a

MECHANISMS OF RESPIRABLE DUST GENERATION

Dust generation is a function of fragmentation process and machine-bit-coal interaction. These two elements have been affected by a number of parameters, namely:

1. Operation parameters
2. Physical and mechanical properties of coal
3. In-situ stresses.

Results of the experiments indicated that among the above major groups, the parameters that affect fragment size distribution characteristics in order of least to most is as follows:

1. Bit attack angle
2. Type of bit, shape and size of carbide tips
3. Compressive strength cleat direction and
in-situ stresses
4. Young's modulus
5. Speed of the cutting head (rpm)
6. Spacing of the bits
7. Depth of cut (advancing rate)

The effect of the above parameters are illustrated in Figs. 23-24. Figure 23 represents a possible ideal size distribution characteristics, where under the condition of low cutting head speed (low rpm), or blunt bit condition or material have a low Young's modulus (low E) one can expect less large and dust size and more fine size particles where high speed (rpm), sharp bit and high E will produce more large and dust size and less of fine size particles. Figure 24 shows a comparison of the results of the experiment conducted under different sets of operating parameters (i.e., rpm, 15 and 25); depth of cut (1/8 and 1/4 in.), bit spacing (1.5 and 3 in.), and bit attack angle (15° and 60°). The results show how depth of cut stands alone in less production of large, fine and dust size particles. That is to say increasing depth of cut more products will be in chunky size and less in the range of smaller sizes which is the subject of concern.

Acknowledgments

The authors acknowledge the assistance of N. P. Reddy, R. Begley, S. Jung and G. Begley, graduate students in the Mining Engineering Department, in preparing this paper. This project was funded by the Generic Center for Respirable Dust Research sponsored by the United States Bureau of Mines under Grant Number G1135142.

References

Bover, Jr., A. B., 1970, "Bit Design: Key to Coal Cutting," *Coal Age*, July, pp. 70-75.

Evans, I., 1984, "A Theory of the Cutting Force for Point-Attack Picks," Technical Note, *International Journal of Mining Engineering*, pp. 63-71.

Evans, I. and Pomeroy, C. D., 1966, *Strength, Fracture, and Workability of Coal*, Pergamon Press.

Ford, L. M. and Friedman, M., 1983, "Optimization of Rock-Cutting Tools Used in Coal Mining,"

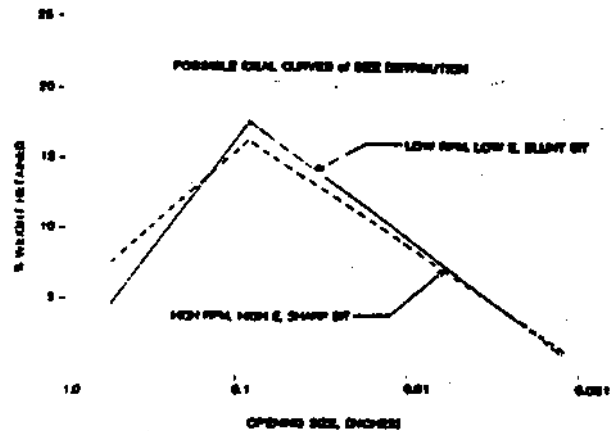


Fig. 23. Ideal curves for mesh size vs. percent of weight retained as function of cutting head speed (rpm), dynamic Young's modulus (E) and bit configuration.

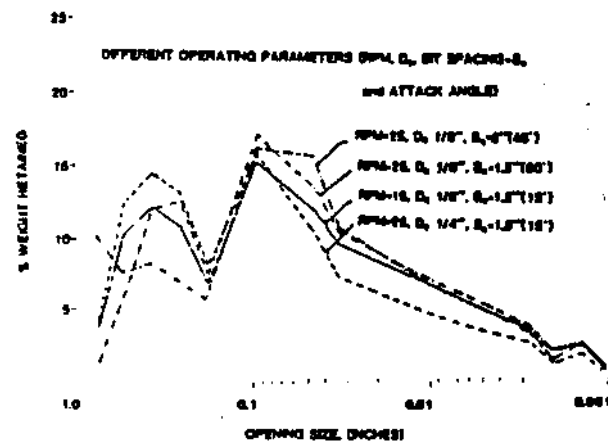


Fig. 24. Mesh size vs. percent of weight retained as a function of various operating parameters.

Proc. 24th U. S. Symposium on Rock Mechanics, June, pp. 725-732.

Friedman, M. and Ford, L. M., 1983, "Analysis of Rock Deformation and Fractures Induced by Rock Cutting Tools Used in Coal Mining," *Proc. 24th U. S. Symposium on Rock Mechanics*, June, pp. 713-723.

Fuh, G. F., 1983, "On the Determination of Cutter Bit Spacing for Optimum Coal Mining," *Proc. 24th U.S. Symposium on Rock Mechanics*, June, pp. 703-711.

Murt, K. G., 1980, "Rock Cutting Experiments with Point Attack Tools," *Colliery Guardian Coal International*, April, pp. 47-50.

THE RESPIRABLE DUST CENTER

- Khair, A. W., 1984, "Design and Fabrication of a Rotary Coal Cutting Simulator," Proc. of the Coal Mine Dust Conference, October, pp. 190-197.
- Newmeyer, G. E., 1981, "Cost of the Black Lung Program," Mining Congress Journal, Vol. 67, No. 11, November, pp. 74-75.
- Feng, S. S., 1978, "Rock Properties and In-Situ Stresses," Chapter 3, Coal Mine Ground Control, John Wiley and Sons, New York, pp. 41-70.
- Pomeroy, C. D., 1963, "The Breakage of Coal by Wedge Action, Factors Influencing Breakage by Any Given Shape of Tool-1," Colliery Guardian, November, pp. 642-677.
- Pomeroy, C. D., 1964, "Breakage of Coal by Wedge Action, Factors Affecting Tool Design-2," Colliery Guardian, July, pp. 115-121.
- Pomeroy, C. D., 1968, "Mining Applications of the Deep Cut Principle," Mining Engineer, June, pp. 506-517.
- Pomeroy, C. D. and Foote, P., 1960, "A Laboratory Investigation of the Relation Between Ploughability and the Mechanical Properties of Coal," Colliery Engineering, April, pp. 146-154.
- Terry, N. B., 1959, "The Dependence of the Elastic Behavior of Coal on the Microcrack Structure," Fuel, London, 38, pp. 125-146.
- Warner, E. M., 1970, "Machine and Cutting Element Design," Mining Congress Journal, August, pp. 35-43.

II

**Dilution, Dispersion, and
Collection of Dust**



SOCIETY OF MINING ENGINEERS OF AIME

CALLER NO. D, LITTLETON, COLORADO 80127

**PREPRINT
NUMBER**

85-154



BEHAVIOR OF DUST CLOUDS IN MINE AIRWAYS

R. Bhaskar

R. V. Ramani

**The Pennsylvania State University
University Park, Pennsylvania**

**For presentation at the SNE-AIME Annual Meeting
New York, New York - February 24-28, 1985**

Permission is hereby given to publish with appropriate acknowledgments, excerpts or summaries not to exceed one-fourth of the entire text of the paper. Permission to print in more extended form subsequent to publication by the Institute must be obtained from the Executive Director of the Society of Mining Engineers of AIME.

If and when this paper is published by the Society of Mining Engineers of AIME, it may embody certain changes made by agreement between the Technical Publications Committee and the author, so that the form in which it appears here is not necessarily that in which it may be published later.

These preprints are available for sale. Mail orders to PREPRINTS, Society of Mining Engineers, Caller No. D, Littleton, Colorado 80127.

**PREPRINT AVAILABILITY LIST IS PUBLISHED PERIODICALLY IN
MINING ENGINEERING**

THE RESPIRABLE DUST CENTER

Abstract. The control of respirable dust in mines has been given paramount importance due to the health and safety implications associated with fine dust. The understanding of the temporal and spatial behavior of dust has been recognized as essential for increasing the efficiencies of the existing control techniques and for developing new control strategies. Mining-related studies in this area are, in general, limited. They are also mostly experimental. Some mathematical and computer analyses have been attempted. In this paper, first a review of the mathematical studies performed in the last three decades in this area is presented. Second, a mathematical model for analyzing dust flow in mines is proposed. The model takes into account a number of factors affecting dust transport. It incorporates varying dust generation source strengths and dispersion, deposition, and coagulation of dust in mine airways. Finally, application areas for the model are discussed. A computer program based on the mathematical model has been developed. The program will output the dust concentration in the mine atmosphere as a function of time and distance from the source. The amount of dust deposited on the sides, roof, and floor of the airway is also determined.

List of Symbols

A' = cross sectional area of particle
 c = concentration at the center of duct
 C = slip correction factor
 C_D = drag coefficient
 C_{fx} = local stress coefficient
 d = particle diameter
 D = diameter or hydraulic diameter of duct/airway
 D_p = Brownian diffusivity
 E_x = dispersion coefficient in x direction
 f = fanning friction factor
 f^* = coefficient of friction
 F = resistance to the motion of settling particles
 F' = flow deposition rate
 F_r = frictional force resisting movement of deposited particle
 g = acceleration due to gravity
 k = surface roughness height
 K_{ij} = collision frequency function
 i = i^{th} class of size distribution
 l' = mean free path of gas
 L = length of airway under consideration
 n_k = number of particles in size class k
 N = deposition rate
 Q = dust production related term
 r_i = radius of particle in i^{th} class
 R = radius of duct
 R' = roof deposition rate
 Re = Reynolds number
 S' = side deposition rate
 Sc_l = molecular Schmidt number
 Sc_t = turbulent Schmidt number
 u_s = friction velocity
 U = airstream velocity
 v_c = terminal velocity
 V = deposition velocity of particles
 V^+ = non-dimensional deposition velocity
 x' = distance from leading edge of a finite surface where $x' = 0$ is the point where the flow starts
 y = distance from surface of deposition
 y^+ = non-dimensional $y = y_u/\nu$

B = coefficient determined from experiment
 δ = rebound factor of gas from a particle's surface
 ϵ = eddy diffusivity
 ϵ_d = energy dissipated by turbulence
 λ = coefficient of friction for smooth pipes
 λ_r = coefficient of friction for rough pipes
 μ = dynamic viscosity
 ν = kinematic viscosity
 ρ = resistance coefficient of the pipe
 ρ_g = density of gas
 ρ_p = density of particles
 σ = dimensionless particle relaxation time
 τ = particle relaxation time

Introduction

An airborne dust cloud is a complex system containing particles of varied size, density, shape and state of aggregation. The behavior of the particles is dependent on a number of complex physical mechanisms, often opposing in nature. The net interaction results in the ambient concentration. This size dependent behavior of particles contrasts with that of gases, an area quite widely studied.

The term aerosol is used to describe clouds of microscopic and submicroscopic particles in air, such as chemical smoke or particulate matter released from smoke stacks. An aerosol system can be regarded as an arbitrary element of volume filled with gas and suspended particles of possible highly variable physiochemical nature. The parameters that are used to describe an aerosol system include concentration, mass average velocity and particle mass and radius. In characterizing such systems, several assumptions are made. Among these is the assumption that particles are smooth, inert and rigid spheres. Again, for example, when the particles are in transport, the possibility of collision exists. As a result of the collision, the particles may coalesce to form larger particles. The probability of sticking is considered a known quantity (Hidy, 1970). In this paper, the application of the principles used in aerosol systems is explored for the study of the transport and deposition of fine coal dust in underground mines.

Recognizing the threat to health and safety of workers underground by fine coal dust, the respirable dust standards in underground coal mines were completely revamped in the 1969 Coal Mine Health and Safety Act. Also, funds were made available to the U.S. Bureau of Mines to research and develop methods for the control of respirable dust problems in mines. Due to the concerted efforts of industry, government and other institutions, considerable progress was achieved in ensuring that underground coal mines were, in fact, in compliance with the mandated dust standards. However, the literature on the transportation and deposition of dust in mines is scant. Theoretical and fundamental studies are few. Experimental results have large variabilities. In a NIOSH study quoted by the committee of the National Academy of Sciences on measurement and control of dust, measurements obtained from each of 22 mine sections for 40 shifts were analyzed. The coefficient of variation between shifts was 91.6%. In addition, there is an estimated 30% variation between measurements when a personal sampler unit is operated by trained personnel (National Bureau of Standards) (Anon., 1975).

BEHAVIOR OF DUST CLOUDS

These statistics only stress the need for more fundamental and theoretical studies on the behavior of dust. In fact, a committee of the National Academy of Sciences on measurement and control of dust (Anon., 1980) made, amongst others, the following recommendations:

Research is needed on the fundamental mechanisms by which fragments are produced in coal mining; how some of these fragments in the respirable range become airborne; and the spatial and temporal characteristics of respirable coal mine dust atmospheres. The mechanisms of fragmentation needs to be understood so that machines can be designed to produce the least amount of coal mine dust in the respirable size range. Entrainment needs to be understood so as to minimize the proportion of the dust that is entrained. The spatial and temporal characteristics need to be understood so that the exposure of workers to the dust can be controlled.

The Committee further stated that this lack of understanding of the formation and behavior of clouds of respirable dust constrains the introduction of more productive methods.

The objective of this paper is to contribute to the understanding of the behavior of dust particles in mine airways. The major thrust of the paper is directed to the development of a mathematical model that would incorporate the various mechanisms that act on dust particles to predict the ambient concentration of dust.

The paper, firstly, reviews the mathematical studies performed in the last three decades in this area. Secondly, a mathematical model for analyzing dust flow in mines is proposed. Finally, application areas of the model are discussed.

A computer program based on the math model has been developed for IBM 370 computers. The program outputs the dust concentration in the mine atmosphere as a function of time and distance from the source. The amount of dust deposited on the sides, roof and floor of the airway is also determined.

Review of the Mathematical Modeling of Dust Flow

Few mathematical models are presently available to study the transportation and deposition of dust in mine airways. Most of them are restricted to experimental data collection (Bradshaw, 1954; Hamilton, et al., 1961; Courtney, et al., 1982; Perceles, 1958) and statistical analyses. Daves and Slack (1954) developed an elementary model based on the understanding of particle behavior. Since their work, increased understanding of particle flows has provided aerosol scientists with a basis to develop better and more representative models.

Perceles (1958) developed the first of depositional models that took into account diffusion and gravitational settlement, and validated the model with the data collected by Daves and Slack (1954). He proposed the following relationships.

$$\frac{F'}{c} = \frac{S'}{c} e^{-a^2} + \frac{v_c}{2} (1 + \operatorname{erf} a) \quad (1)$$

where

$$a = \frac{v_c}{25 \sqrt{v}}$$

and

$$\frac{R'}{c} = \frac{S'}{c} e^{-a^2} - \frac{v_c}{2} (1 - \operatorname{erf} a). \quad (2)$$

This theory gives deposition rates on the roof and floor in terms of side deposition. For side deposition the author proposed the following relationship.

$$S = B/2 \rho U c. \quad (3)$$

The value of B depends on the properties of the flowing fluid as well as on physical properties of the dust. Correlation with the Daves and Slack data gave a best fit value of 0.026 with a scatter of 0.019 to 0.038. The value of B depended on the particle diameter too. The theoretical values for the ratio of floor deposition/airborne concentration for particles less than 4 microns were greater than those from experimental data.

A model was developed by Hwang et al (1972) for the calculation of dust concentration in underground mines. For dust sources in the airway the concentration equation is given as:

$$c_2 = c_1 e^{-BL} + \frac{Q}{B} (1 - e^{-BL}) \quad (4)$$

where B is a factor that incorporates flow velocity, terminal velocity and dimensions of the airway. At $x = 0$, the boundary condition is $c = c_1$, the values of ambient concentration at that point. The deposition calculations are based on the stopping distance concept which has been found to have certain discrepancies (Owen, 1969). In the consideration of the mass balance equation, a suitable dispersion coefficient is not incorporated. When correlated with the Daves and Slack data, for deposition over a cross section, the model predicted values which were within a factor of 15. Also, according to the model the effect of air velocity on deposition is negligible. The model does not incorporate coagulation.

Courtney et al (1982) have proposed the following deposition model for the concentration at time t :

$$c = c_0 \exp(-K_1 t) \quad (5)$$

where,

c_0 = initial concentration of dust at $t = 0$
 K_1 = an experimentally determined proportionality constant

c = mass concentration of airborne dust.

This model is similar to an equation provided by Davies (1966) for settlement of dust from turbulent air in enclosures. This is an approximate representation of the physical phenomena without regard to the nature of deposition or the mechanisms causing deposition. Davies' theory has been shown to vary widely when correlated with acceptable experimental data (Wood, 1981b).

THE RESPIRABLE DUST CENTER

Owen (1969) developed a deposition model based on a continuity equation that is representative of the physical nature of dust deposition. Good correspondence is shown with the Dawson and Slack data for roof/floor and side/floor deposition ratios.

Of the models referred to, the Hwang model is a more complete model which permits studies to be made of the effect of source strength on deposition rates and ambient dust concentrations. The authors also examined thermal and electrophoretic effects though these were not included in the model. Wood (1981b) has shown that thermophoresis, the phenomenon of particle transfer due to thermal gradient, is not significant for rough walls.

Numerical modeling of contaminants has been prolific in the atmospheric sciences. Models have been developed for plumes, motor car fumes in highways and nuclear fallout (Friedlander, 1977; Anspaugh, et al., 1975; Runca, 1977; Chock, 1982). Atmospheric mathematical models can be divided into three categories as:

1. models based on Taylor's statistical theory of dispersion
2. conservative volume models
3. real time computation and predictions.

Models Based on Taylor's Statistical Theory of Dispersion

These are generally used for computation of concentration fields resulting from a large number of distributed urban and industrial sources. The mathematical treatment is a generalization of the equation for molecular diffusion and heat conduction. The general equation used is:

$$\frac{\partial c}{\partial t} = \frac{\partial}{\partial x} (K_x \frac{\partial c}{\partial x}) + \frac{\partial}{\partial y} (K_y \frac{\partial c}{\partial y}) + \frac{\partial}{\partial z} (K_z \frac{\partial c}{\partial z}) \quad (6)$$

where c is pollutant concentration and K_x , K_y and K_z are diffusion coefficients.

Conservative Volume Models

The conservative volume element methods utilize the convective diffusion model of the form

$$\begin{aligned} \frac{\partial c}{\partial t} &= \frac{\partial}{\partial x} (K_x \frac{\partial c}{\partial x}) + \frac{\partial}{\partial y} (K_y \frac{\partial c}{\partial y}) + \frac{\partial}{\partial z} (K_z \frac{\partial c}{\partial z}) \\ &- \frac{\partial}{\partial x} (U(x)c) - \frac{\partial}{\partial y} (U(y)c) - \frac{\partial}{\partial z} (U(z)c) \\ &- \text{sinks} + \text{sources.} \end{aligned} \quad (7)$$

Real Time Computation and Predictions

Such models are used for prediction of pollution distribution using real time data and mathematical models. The prediction may be the distribution of pollutants a few hours after a certain event. Real time computations have been used in such areas as the Los Angeles basin where rapid changes in wind directions are common.

The U.S. Environmental Protection Agency has a users' network for applied models of air pollution (HUMANAP) which contains a library for computer programs.

Particle Deposition

Particle deposition may take place due to the effect of gravitational, electrostatic, thermal, Brownian and eddy diffusion, sedimentation and inertial impaction. Of these, the three major mechanisms of deposition in turbulent flow are Brownian diffusion, eddy diffusion, sedimentation and inertial impaction. Inertial impaction is important only at bends, but at bends the change in direction in flow with resultant powerful eddies may cause increased reentrainment of the deposited particles, thus having a somewhat compensating effect. Among the three major deposition mechanisms, unanimity does not exist amongst researchers as to the delineation of the regimes of the different mechanisms with respect to particle size. The Friedlander classification which considers convective diffusion to be dominant in the 0-1 micron range and inertial deposition for particles greater than 1 micron is adopted in model development. The equations are developed such that all three mechanisms of deposition are adequately accounted for.

Deposition by Convective Diffusion

Turbulent diffusion of particles can be described by a one-dimensional deposition flux equation. In a model proposed by Friedlander and Johnstone (1957), the assumption was that particle deposition on the walls of a pipe can be described by the diffusion of particles to the boundary layer followed by a final free flight.

The equation for the diffusion flux as proposed by Friedlander (1977) is:

$$N = (D_p + \epsilon) \frac{dc}{dy} \quad (8)$$

This is essentially a wall deposition equation since gravity is not accounted for. Inclusion of gravity results in (Schmel, 1973)

$$N = (D_p + \epsilon) \frac{dc}{dy} + v_c c \quad (9)$$

The turbulent eddy diffusivity ϵ varies within the boundary layer. A few equations have been proposed relating ϵ with distance from the boundary layer (Davies, 1966; Lin, et al., 1953; Owen, 1969; Schmel, 1971; Schmel, 1973). Of these, the expressions developed by Owen cover a more representative range and is given as:

$$c/v = 0.001y^{*3} \quad 0 < y^* < 5 \quad (10)$$

$$c/v = 0.012(y^* - 1.6)^2 \quad 5 < y^* < 20 \quad (11)$$

$$c/v = 0.4(y^* - 10.0) \quad y^* > 20 \quad (12)$$

BEHAVIOR OF DUST CLOUDS

In the model development, equation (9) is used to describe deposition for particles with τ^+ in the range 0-17 as it agrees well with experimental data (Davies, 1945). Equation (9) can be non-dimensionalized with respect to core concentration and friction velocity to give:

$$v^+ = \frac{N}{cu_a} + \left(\frac{D}{v} + \frac{\epsilon}{v}\right) \frac{dc^+}{dy^+} + v_c^+ c^+ \quad (13)$$

Rearranging the terms,

$$\frac{dc^+}{v^+ - v_c^+ c^+} = \frac{dy^+}{\left(\frac{D}{v} + \frac{\epsilon}{v}\right)}$$

Integrating through the turbulent core given

$$\int_0^1 \frac{dc^+}{v^+ - v_c^+ c^+} = \int_{(y^+)^0}^{R^+} \frac{dy^+}{\left(\frac{D}{v} + \frac{\epsilon}{v}\right)} \quad (14)$$

The limits of integration are as follows. The upper limit of integration is a value of y^+ which is large enough for c^+ to be equal to unity, i.e., it must be representative of the concentration in the core of the flow. This can be taken to occur at the center of the duct, i.e., at a distance R from the walls, where R is the radius of the duct.

For the lower limit, it will be assumed that particles will be captured when they reach the level of effective roughness height. At this height, concentration can be assumed to be zero (Wood, 1981b; Browne, 1974). This occurs at a distance b above the origin of the velocity profile. Mathematically, this capture can be taken to occur whenever the particles enter within the stop distance. A stop distance is the distance over which a particle with an initial velocity u comes to rest under the action of drag at the boundary layer. This is because any particle with velocity u towards the wall with corresponding stop distance s will eventually be captured. Therefore, particles with the velocity towards the wall at a level y above the origin will be captured and, hence, the lower limit can be taken as

$$(y^+)^0 = b^+ + s^+ \quad (15)$$

where,

b^+ = dimensionless $b = bu_a/v$, and

s^+ = dimensionless stopping distance = su_a/v .

Integration has to be carried out in three parts because of the varying eddy diffusivity across the three layers. The limits of the three layers are:

1. sublayer $y^+ < 5$
2. buffer layer $5 < y^+ < 20$
3. turbulent core $20 < y^+ < R^+$

Assuming $b^+ + s^+ > 5$, that is, $(y^+)^0$ is in the order of the buffer layer height, the integral for the sublayer (i.e., $0 < y^+ < 5$) will be negligible. Therefore, the integration will span

the region $5 < y^+ < R^+$ where R^+ is the dimensionless radius of the duct and is given by $R^+ = Ru_a/v$.

For wall deposition, the original equation (Eq. 8) of Friedlander is adopted.

Turbulent Diffusional Deposition in the Inertial Range

This is the dominant mechanism for particles larger than 1 micron. The suspended particles in this range may not be able to totally follow the motion of the fluid.

Wood (1981a) correlated Liu and Agarwal data (1974) and suggested the following relationships.

$$v^+ = \frac{N}{cu_a} = 0.13. \quad (16)$$

For $\sigma \geq 265$, the modified Reeks and Skyrme relation is

$$v_{\text{Skyrme}}^+ = \frac{2.6}{\sqrt{\sigma}} \left(1 - \frac{30}{\sigma}\right) \quad (17)$$

Real life systems of aerosols are polydisperse and can be specified by a function of the type

$$\int_0^{\infty} n(r) dr = N_0 \quad (18)$$

where N_0 is the bulk concentration.

In such cases the total number of particles N deposited per unit area per unit time is

$$\frac{N}{u_a} = \int_0^{r_1} n(r) dr v_{\text{diffusion}}^+ + \int_{r_1}^{r_2} 0.13 n(r) dr + \int_{r_2}^{r_3} v_{\text{Skyrme}}^+ n(r) dr \quad (19)$$

which takes into account the turbulent diffusional deposition in the continuous size range.

In the case of distributed particle sizes where the distribution is given in the form of a graph of proportion by weight of particles below each value of diameter, discretization of the size distribution is needed.

The size spectrum is divided into small classes with a representative particle diameter (d) and weight (w_d) fraction for each class. Then the total deposition velocity is given by

$$v = u_a v^+ = u_a \int_{d_1}^{d_{\text{max}}} w_d v_d^+ \quad (20)$$

where v_d^+ is the dimensionless deposition velocity for diameter d .

$$N = N_0 u_a \int_{d_1}^{d_{\text{max}}} w_d v_d^+ \quad (21)$$

THE RESPIRABLE DUST CENTER

Inertial Deposition on the Floor Due to Gravity Effects

For deposition on the floor, the effect of gravity is also considered. The rate of deposition due to gravity will depend upon the terminal velocity, v_t . The deposition velocity due to gravity will then be

$$V_{\text{gravity}} = v_t \quad (22)$$

Deposition due to the effect of gravity is taken into account in the computer program by considering the terminal velocity that is appropriate to the particle size class.

Coagulation

Coagulation of airborne particles was also considered in the model. Coagulation occurs when two particles collide to form a larger particle. For liquid drops, the collision results in a larger drop, whose volume is the sum of the volumes of the colliding drops. For coal particles, however, collision results in a larger sized particle of a shape determined by the shapes of the colliding particles and their orientation at the time of collision.

Smoluchowski (Chung, 1981) proposed a model for the rate of change of the number of particles in any size range. His model is

$$\frac{dn_k(t)}{dt} = \frac{1}{2} \sum_{i+j=k}^{k-1} K_{ij} n_i n_j - n_k \sum_{i=1}^{\infty} K_{ik} n_i \quad (23)$$

where $n_k(t)$ is the number of particles of size k at time t and K_{ij} is the collision frequency function between particles of sizes i and j . The first term on the right side represents the gain to size k from collisions between particles i and j and the second represents loss from the k^{th} class by collisions of particles of size k with all other particles. The factor of $1/2$ is introduced because each collision is counted twice in the summation.

The discrete model assumes that when two particles collide the probability of sticking together is 1.0, and also they coalesce to form a third particle whose volume is equal to the sum of the two.

The efficiency of sticking is probably dependent on shape, nature of the surface of the colliding particles, size, as well as electrostatic and Van der Waals forces. In the absence of definitive literature, the efficiency of sticking is usually assumed to be 1.0. In this model an initial sensitivity analysis was done with the simpler model having an efficiency of sticking as 1.0. Since coagulation did not play an important role in determining airborne particle size distribution, the stability of the coagulated particles after collision was not examined.

The modified form of the Smoluchowski equation is used in the model. Porosity of the coagulation particles were ignored as the model with porosity consideration will involve considerable computer run time, mainly due to the necessity of mass balancing. This, together with the fact that coagulation does not play a dominant role

prompted the use of the simpler modified Smoluchowski model.

To account for inconsistencies in the original model due to discretization, the equation is modified as follows (Chung, 1981).

The particles falling in the k^{th} interval will be those whose combinations are such that

$$B_k < x_i + x_j < B_{k+1} \quad (x_i, x_j < x_k)$$

where B_k is the size corresponding to the lower boundary of class k and B_{k+1} is the upper limit of size of class k .

If $x_i + x_j > x_k$, the particle ceases to be counted in that interval. There also exists a class l of particles specified by

$$l-1 < (B_{k+1} - x_k) < l$$

where the association of particles, from class k with those from classes less than l , causes the addition of the resultant volume to the k^{th} interval itself. The rate at which such additions occur is

$$R_{\text{app}}' = n_k \sum_{i=1}^l K_{ik} n_i$$

By the same token, when $l > 1$, disappearance from class k occurs, given by

$$R_{\text{disap}}' = n_k \sum_{i=l+1}^{\infty} K_{ik} n_i$$

The overall disappearance term can therefore be written as

$$R_{\text{disap}} = n_k \sum_{i=1}^l K_{ik} n_i - n_k \sum_{i=l+1}^{\infty} K_{ik} n_i \quad (24)$$

Thus the overall modified rate equation used in this paper is

$$\frac{dn_k(t)}{dt} = \frac{1}{2} \sum_{i+j=k}^{k-1} K_{ij} n_i n_j + n_k \sum_{i=1}^l K_{ik} n_i - n_k \sum_{i=l+1}^{\infty} K_{ik} n_i \quad (25)$$

The determination of the values for K_{ij} requires an understanding of the collision mechanisms.

The collision frequency function is an indicator of the rate at which two particles collide. Thus, the collision frequency function is dependent on the mechanisms causing the collision. The major mechanisms are Brownian motion, turbulent motion of the fluid, differential shear of the fluid due to velocity gradients in the flow and differential settling of particles. It is assumed that the particles are non-interacting, i.e., the forces of attraction between them are negligible except on contact when they are large enough to hold the particles together.

Brownian coagulation is the dominant mechanism for particles in the 0 to 1.0 micron range, where Brownian diffusion plays an important role as a mechanism causing collision of particles. The frequency of probable collision can be statistically determined (Chung, 1981).

Collisions can occur due to turbulent motion of air. Collisions can occur due to two mechanisms:

(1) Spatial inhomogeneities of particles in turbulent motion, a medium whose characteristic length scale of small eddies is larger than the characteristic particle size r_i . Saffman and Turner (1956) term such collisions as "collisions due to the motion of the droplets (in their study, raindrops) with the air."

(2) The second mechanism is due to the fact that particles of different sizes are subject to motion not only with the air but also relative to one another. Collision can thus occur only between unequal particle sizes. This mechanism does not explain collisions of equal size particles.

Saffman and Turner (1956) developed a comprehensive model that took into account (i) the motion of the drops with the air, (ii) relative motion due to the air, and (iii) sedimentation. The formula proposed is

$$K_{ij} = 2(2\pi)^{1/2} (r_i + r_j)^2 \left[\left(1 - \frac{\rho}{\rho_p}\right)^2 \left(\frac{du}{dt}\right)^2 (r_i - r_j)^2 + \frac{1}{3} \left(1 - \frac{\rho}{\rho_p}\right)^2 (r_i - r_j)^2 g^2 + \frac{1}{9} (r_i + r_j)^2 \frac{c_d}{v} \right]^{1/2} \quad (26)$$

where $\left(\frac{du}{dt}\right)^2$ is given by Batchelor (1951)

$$\left(\frac{du}{dt}\right)^2 = 1.3v^{-1/2} c_d^{1/2} \quad (27)$$

Dispersion of Dust

Skubunov consolidated the results of a number of studies to determine the coefficients of turbulent transfer. A major conclusion of his study is that the coefficients of turbulent transfer agree irrespective of the nature of the flowing fluid or the diffusing coefficient. The empirical formula proposed for longitudinal dispersion was

$$E_x = 15.8UDSc_i^{-0.6} Sc_t \sqrt{\lambda/\lambda_r} \quad (28)$$

The value of the turbulent Schmidt number is taken as 1.1 for dust. The value of Sc_i , the molecular Schmidt number, is 0.72, a generalized value obtained by Skubunov. These values relate to workings with a steady, uniform velocity profile in the transverse direction. Where the velocity profile is not uniform, the coefficient of longitudinal diffusion may be higher.

Numerical Modeling of Dust Flows

The transport and deposition of dust can be modeled using a statistical equation for turbulent diffusion of a parabolic form (Hidy, 1970). For incompressible flows, the equation in generalized form can be expressed as

$$\frac{\partial c}{\partial t} = \frac{\partial}{\partial x} (E_x \frac{\partial c}{\partial x}) + \frac{\partial}{\partial y} (E_y \frac{\partial c}{\partial y}) + \frac{\partial}{\partial z} (E_z \frac{\partial c}{\partial z}) - U(x) \frac{\partial c}{\partial x} - V(y) \frac{\partial c}{\partial y} - W(z) \frac{\partial c}{\partial z} + \text{sources} - \text{sinks} \quad (29)$$

The intense turbulence of mine air precludes significant variation in concentration in the lateral direction, i.e., in the horizontal z direction of an airway cross-section (Figure 1). It has been shown, however, that the concentration of dust varies to some extent in the vertical direction. The concentration in the upper half of an airway is generally higher than that in the lower half (Daves, et al., 1956). This anomaly can, however, be overcome to some extent by assuming an even concentration distribution in the cross-section and basing deposition equations accordingly. These assumptions enable one to adopt a one dimensional population balance equation of the convective-diffusion form for flow in the x-direction:

$$\frac{\partial c}{\partial t} = E_x \frac{\partial^2 c}{\partial x^2} - U \frac{\partial c}{\partial x} + \text{sources} - \text{sinks} \quad (30)$$

This equation has to be solved for different particle size ranges using representative particles diametric for each size range. The behavior of all the size ranges is summed to give the general behavior of the dust cloud.

Initial and Boundary Conditions

The initial condition to solve the equation is of the form

$$c(x,t) = 0 \quad \text{for } t = 0, \quad 0 < x < L$$

where L is the length of the airway under consideration. It is assumed that there is no initial concentration of dust in the mine air at the start of the simulation. The program can be modified, however, to take on some finite value.

The boundary conditions have to be determined depending upon the processes that cause the transfer of the dust particles at the point where the sectional airways meet with the high velocity main return airways. Assuming a dominative convective transfer and that the concentration gradient at the point of mixing does not vary with distance, it can be

$$\frac{dc}{dt} = 0$$

This would mean that at the boundary, the concentration is in the asymptotic region of the

THE RESPIRABLE DUST CENTER

falling concentration curve, an assumption that is reasonable when considering long airways.

Source Term

In any modeling study, characterization of the source is important. In mining, a number of sources for dust generation exist. The primary source is the actual coal cutting process. Room and pillar mining using conventional methods involves coal cutting, drilling, blasting, and loading. Dust is generated during all these processes. The introduction of continuous mining machines has combined the unit operations of cutting, drilling, blasting, and loading into one operation. The actual coal cutting process varies depending on the type of continuous miner employed which may be of the ripping, boring, milling or auger type. Again, depending on the type of miner, the operations involved are sumping, shearing, trimming of bottom, reposition and advance. The dust generation rate depends on the operating mode of the mining machine. For example, in the sumping mode the amount of dust generated is greater than that in the shearing mode. Also, the time the continuous miner is in the sumping mode differs from that in the shearing mode (Figure 2). The dust generation characteristic is typically of the step function type and can be described as:

$$S(t) = A_1 \delta(t - t_1) + A_2 \delta(t - t_2) + \dots \\ + A_i \delta(t - t_i) \quad (31)$$

where $\delta(t - t_i)$ is the direct delta function and A_i is the emission when in mode i of the operation. The particle size distribution is discretized into small intervals, so that the mechanisms acting on the particle can be better represented.

Computer programs are available which simulate the operations of continuous miners. The output of such simulators can be used as input to the dust model to determine average dust exposure levels to which a worker may be exposed over a shift.

Model Solution

The convective diffusion equation is solved using an implicit scheme (Bandopadhyay, 1982) and the model was programmed in WATFIV.

The deposition part of the model was validated with results obtained from deposition studies conducted by the Bituminous Coal Research Inc. (BCR) (Kost, et al., 1981). The BCR experiments were conducted in a continuous mining section consisting of four entries utilizing double split ventilation with two section entries extending over 300 m straight back from the brattice discharge points (Figure 3). In the validation test, due to the absence of data on source strength, it was decided to use a representative constant source strength and compare the results on the basis of relative deposition rates. Also the model assumes average velocity of flow for all the points. The actual velocities in the field study were different at all the measurement points due to the lack of uniformity of airway dimensions. The velocity assumed in the model is the average of the velocities at the five points.

Since the results have been reduced to ratios with respect to the first sampling point, the relative deposition at the various points above the airway will be independent of the source strength. The model output for the deposition pattern for the velocity of flow and airway dimensions of the mine section in which the experimental data was collected is shown in Figure 4. The model output and the experimental data show that the model reasonably duplicates the observed deposition pattern. The input data used in the model as well as the salient experimental data are listed in Table 1.

Sensitivity Analyses

Due to the absence of comprehensive data to validate a model of this type, a sensitivity analysis was made. The model was altered to examine the effect of dispersion coefficient, coagulation and deposition due to turbulent diffusion on deposition and concentration. As a check, another variation attempted was doubling the airway's height and width while maintaining all other values the same as in the original validation run. The results are shown in Figures 5-8.

When turbulent diffusion is ignored as a deposition mechanism, the gravity only model shows a decrease in deposition rate and an increase in ambient concentration. The effect is pronounced for particles in the respirable size range, indicating that turbulent diffusion plays a dominant role in the deposition of finer size particles.

When the dispersion rate is halved, the model showed a steeper fall in deposition showing that a lower dispersion rate results in decreased spread of particles. The result ambient concentration also showed higher values near the source.

Coagulation does not play a dominant role in the system. Runs made with and without coagulation showed insignificant change for the particle size distribution considered for model validation. This does not preclude the possibility of coagulation playing a more dominant role for finer size classes in which case for the same mass the number of particles will be very large. A switch has been provided in the program to activate the coagulation subroutine for finer size distributions.

A doubling of the dimensions of the airway resulted in a decrease in ambient concentration since the same emission amount was dispersed over four times the cross section of the airway. Due to increased surface area, higher deposition was obtained in the respirable range, the range in which turbulent diffusional deposition is dominant. In line with the fact that total ambient concentration was lower than in the original mode, total deposition also showed a decrease.

To examine the effect of particle size distribution and velocity of flow on the concentration and deposition patterns, two sets of runs were made. One set consisted of varying maximum particle diameters. The results showed that as the maximum diameter of the particle size distribution increases, the total concentration and deposition curves tend to be more steeply dipping, indicating that greater amounts of dust are deposited in the first few meters for larger size particles. The effect is less pronounced for particles in the respirable size range (0 - 5 microns).

BEHAVIOR OF DUST CLOUDS

A similar set of runs were made by varying velocities. The velocities used were 0.517 m/s, 0.45 m/s and 0.4 m/s. The results show that the effect is more pronounced in the total size range than in the respirable size range. As the velocity increases the deposition and ambient concentration curves become flatter, indicating increased dispersion and a more uniform deposition along the length of the airway.

Conclusions

A mathematical model for predicting the behavior of dust clouds in mine airways under the action of controlled flow has been described in this paper. The model is designed to evaluate:

1. dust deposition in a straight section of a roadway. Both total dust as well as respirable dust values are output for the various points in the roadway.

2. ambient concentration, including concentration in the respirable range. Time averaged and instantaneous values can be determined.

3. effect of varying source emission rates on the dust exposure values at the various points.

Dust measurements are known to have a high coefficient of variation. One way of complementing experimental data is to use mathematical models, such as the one described here, which attempt to explain the transport characteristics of dust clouds generated by mining machines, predict dust deposition and ambient concentrations.

Acknowledgments

The work reported here is a part of an ongoing research project in the Generic Technology Center for Respirable Dust at The Pennsylvania State University. The Center is supported by a grant from the U.S. Bureau of Mines. Support and assistance from the U.S. Bureau of Mines and The Pennsylvania State University are appreciated.
Grant Number G1135142

References

- Anon., 1975, "An Evaluation on the Accuracy of the Coal Mine Dust Program Administered by the Department of the Interior." Final Report to Senate Committee on Labor and Public Welfare Staff, Institute for Materials Research.
- Anon., 1980, "Report of the Committee on Measurement and Control of Respirable Dust," NMAB-363, National Academy of Sciences.
- Anspbaugh, L. R., Slinn, J. H., Phelps, P. L. and Kennedy, N. C., 1975 "Resuspension and Redistribution of Plutonium in Soils," Health Physics, Vol. 29, pp. 571.
- Bandopadhyay, S., 1982, "Planning with Diesel Powered Equipment in Underground Mines," Ph.D. Thesis, The Pennsylvania State University.
- Batchelor, G. K., 1951, "Pressure Fluctuations in Isotropic Turbulence," Proc. Camb. Phil. Soc., Vol. 47, pp. 359.
- Bradshaw, F., Godbert, A. L. and Leach, F., 1954, "The Deposition of Dust on Conveyor Roads," SHRE Research Report No. 106.
- Browne, L. W. B., 1974, "Deposition of Particles on Rough Surfaces During Turbulent Gas Flow in a Pipe," Atmos. Environ., Vol. 8, pp. 801-816.
- Chock, D., 1982, "The Dispersion Analysis," Mechanical Engineering, Vol. 104, No. 12.
- Chung, H. S., 1981, "Coagulation Processes for Fine Particles," Ph.D. Thesis, The Pennsylvania State University.
- Courtney, W. G., Kost, J. and Colinet, J., 1982, "Dust Deposition in Coal Mine Airways," USBM Technical Progress Report TPR 116, Bituminous Coal Research.
- Davies, C. N., 1945, "Definitive Equations for the Fluid Resistance of Spheres," Proc. Physical Society, Vol. 57, pp. 259.
- Davies, C. N. Ed., 1966, Aerosol Science, Academic.
- Daves, J. G. and Slack, A., 1954, "Deposition of Airborne Dust in a Wind Tunnel," SHRE Research Report No. 105.
- Friedlander, S. K. and H. F. Johnstone, 1957, "Deposition of Suspended Particles from Turbulent Gas Streams," Ind. Engrg. Chem., Vol. 49, p. 1151.
- Friedlander, S. K., 1977, Smoke, Dust and Haze. Fundamentals of Aerosol Behavior, John Wiley and Sons.
- Hamilton, R. J. and Walton, W. H., 1961, The Selective Sampling of Respirable Dust in Inhaled Particles and Vapours, Ed. Davies, C. N., Oxford, Pergamon.
- Hidy, G. M. and J. R. Brock, 1970, Dynamics of Aerocolloidal Systems, Pergamon.
- Hwang, C. C., Geiger, G. E. and Raduovic, P., 1972, "Dust Concentration Simulator for Mine Ventilation Systems for Coal Mines," NTIS PB 213833.
- Kost, J. A., J. F. Colinet and G. A. Shirey, 1981, "Field Survey of Float Dust in Coal Mining Operations," USBM Mineral Research contract report, Contract No. J0308030, Bituminous Coal Research Inc.
- Lin, C. S., Moulton, R. W. and Putnam, G. L., 1953, "Mass Transfer Between Solid Wall and Fluid Streams," Ind. Engrg. Chem., Vol. 45, pp. 636.
- Liu, B. Y. H. and Agarwal, J. K., 1974, "Experimental Observation of Aerosol Deposition," Jl. Aerosol Sci., Vol. 5, No. 2.
- Owen, P. R., 1969, "Pneumatic Transport," Jl. Fluid Mech., Vol. 39.
- Owen, P. R., 1969, "Dust Deposition from a Turbulent airstream," in Aerodynamic Capture of particles, Ed. Richardson.

THE RESPIRABLE DUST CENTER

Persles, E. G., 1958, "Theory of Dust Deposition from Turbulent Airstreams by Several Mechanisms," SHRE Research Report No. 144.

Runca, E., 1977, Transport and Diffusion of Air Pollutants from a Point Source, Modelling, Identification and Control in Environmental Systems, Ed. G. C. Vansteenkiste, North-Holland Publications.

Saffman, P. G. and Turner, J. S., 1956, "On the Collision of Drops in Turbulent Clouds," Jl. Fluid Mech., Vol. 1, pp. 16.

Schmel, G. A., 1971, "Particle Diffusivities and Deposition Velocities over a Horizontal Smooth Surface," Jl. Colloid and Interface Sci., Vol. 37, No. 4.

Schmel, G. A., 1973, "Particle Eddy Diffusivities and Deposition Velocities for Isothermal Flow and Smooth Surfaces," Jl. Aerosol Sci., Vol. 4, No. 2.

Wood, N. B., 1981a, "The Mass Transfer of Particles and Acid Vapor to Cooled Surfaces," Jl. Inst. of Energy.

Wood, N. B., 1981b, "Calculation of Turbulent Deposition to Smooth and Rough Surfaces," Jl. Aerosol Sci., Vol. 12, No. 3.

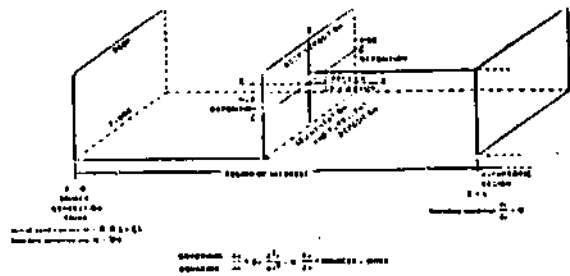


Figure 1. Schematic of dust flow in a mine airway.

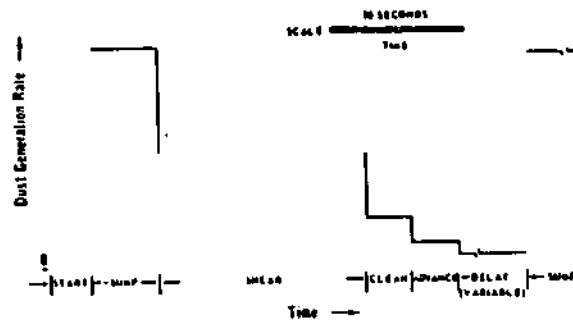


Figure 2. Dust generation rate of a continuous miner.

Table 1. Input Data for Validation Run.

Number of sizes	5
Number of nodes	86
Total simulation time	30 minutes
Time increment	7 seconds
Boltzmann constant	$0.13799992E-22$ J/K
Absolute temperature	291 K
Kinematic viscosity	$0.15E-04$ m ² /s
Absolute viscosity	$0.18269988E-04$ kg/ms
Friction coefficient	0.085
Air density	1.204 kg/m ³
Velocity of flow	0.517 m/s
Distance of airway	340.0 m
Height of airway	3.17 m
Width of airway	6.1 m
Density of particles	1400 kg/m ³
Mean diameter of particles	19.0 microns
Minimum diameter of size distribution	0.6 microns
Maximum diameter of size distribution	28.4 microns
Minimum size class for determination of size classes	0.5 microns

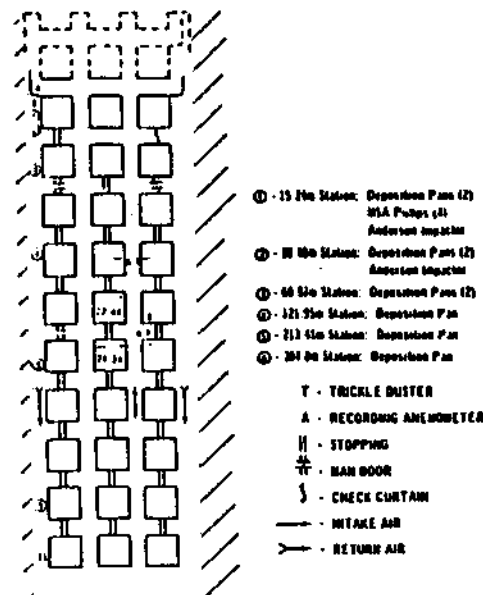


Figure 3. Sampling locations in a mine section return (after Kost, Colinut and Shirey, 1981).

BEHAVIOR OF DUST CLOUDS

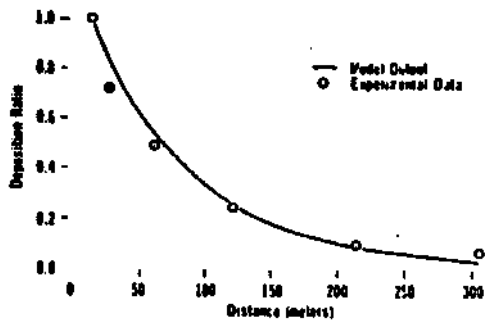


Figure 4. Plot of model output and experimental data.

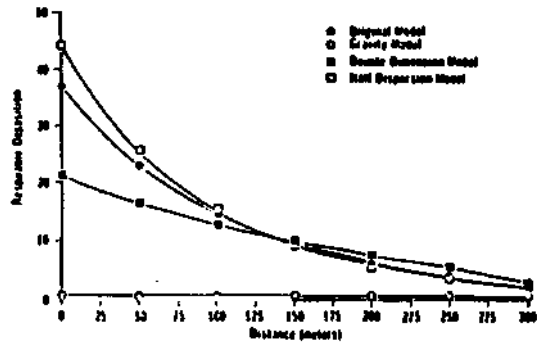


Figure 7. Comparison plots of outputs obtained from original and modified model runs (respirable deposition).

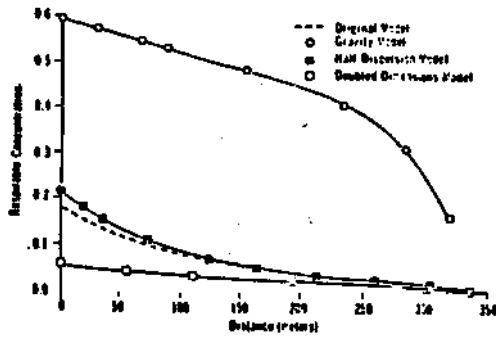


Figure 5. Comparison plots of outputs obtained from original and modified model runs (respirable concentration).

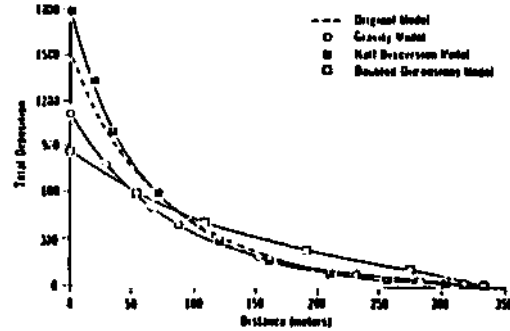


Figure 8. Comparison plots of outputs obtained from original and modified model runs (total deposition).

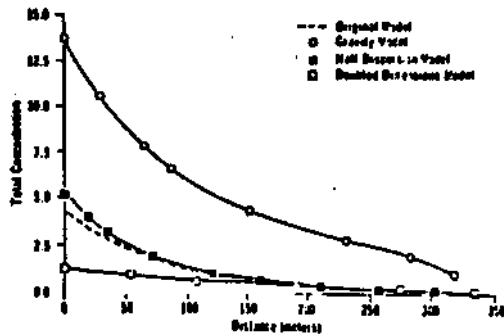


Figure 6. Comparison plots of outputs obtained from original and modified model runs (total concentration).



III

Dust Characterization



1. The first part of the document discusses the importance of maintaining accurate records of all transactions and activities. It emphasizes that this is crucial for ensuring transparency and accountability in the organization's operations.

2. The second part of the document outlines the various methods and tools used to collect and analyze data. It highlights the need for robust data management systems that can handle large volumes of information efficiently.

3. The third part of the document focuses on the role of technology in modern data analysis. It discusses how advanced software and algorithms have revolutionized the way we process and interpret data, allowing for more precise and timely insights.

4. The fourth part of the document addresses the challenges associated with data security and privacy. It stresses the importance of implementing strong security protocols to protect sensitive information from unauthorized access and breaches.

5. The fifth part of the document concludes by summarizing the key findings and recommendations. It reiterates the significance of data-driven decision-making and the need for continuous improvement in data management practices.



SUPPRESSION OF INHALED PARTICLE CYTOTOXICITY BY PULMONARY SURFACTANT
AND RE-TOXIFICATION BY PHOSPHOLIPASE--
DISTINGUISHING PROPERTIES OF QUARTZ AND KAOLIN*

W. E. WALLACE, JR., M. J. KEANE, V. VALLYATHAN,
P. HATHAWAY, E. D. REGAD, V. CASTRANOVA, AND F. H. Y. GREEN

West Virginia University
and
Appalachian Laboratory for Occupational Safety and Health,
Division of Respiratory Disease Studies
National Institute for Occupational Safety and Health

ABSTRACT

Inhaled particle contact with pulmonary surfactant in the hypophase lining pulmonary alveoli was modeled in vitro by exposing two respirable sized dusts, kaolin and silica quartz, to lecithin, a major component of pulmonary surfactant, emulsified in physiologic saline. Lecithin adsorbs to the dusts upon incubation at 37° C and suppresses their cytotoxicity as measured by pulmonary macrophage and erythrocyte assays, suggesting that pulmonary surfactant provides a defense system against prompt cell membrane lysis by inhaled dusts. Subsequent pulmonary macrophage phagocytosis and lysosomal enzyme digestion of the coated dusts was modeled in vitro by incubation with phospholipase A₂ for one hour. With increasing lipase activity, silica hemolytic potential was restored to native silica levels. Kaolin was retoxified to levels far in excess of native kaolin hemolytic potential. Elution, thin layer chromatography and phosphate assay of treated dusts indicate most lecithin on silica is digested to lysolecithin and desorbed, silica retoxification being due to surface and adherent lysolecithin effects. Most lecithin on kaolin is not digested in this same time; that which is results in adherent lysolecithin which is responsible for the kaolin retoxification. Digestion with phospholipases A₂ and C together produces only weakly retoxified kaolin. Results suggest that surface adsorption properties which control the adherence of prophylactic surfactant distinguish the pathogenic potentials of quartz, kaolin and mixed dust.

Inhaled Particles VI - Proceedings of an
International Symposium organized by the
British Occupational Hygiene Society,
Cambridge, England, September 1985.

THE RESPIRABLE DUST CENTER

INTRODUCTION

Erythrocyte hemolysis and pulmonary macrophage enzyme release assays show quantitatively comparable high cytotoxicities for both silica quartz and kaolin respirable sized dusts (BROWN et al., 1980; DANIEL and LE BOUFFANT, 1980). This contrasts with the strong potential for respirable quartz dust to induce pulmonary fibrosis and the much more limited potential of kaolin dust to do the same (MORGAN and SEATON, 1975).

In an attempt to understand this anomalous situation, assays were performed on quartz and kaolin dusts incubated with dipalmitoyl lecithin, emulsified in physiologic saline, to simulate the initial contact of a respired dust with the pulmonary alveolar hypophase. The ability of kaolin dust to adsorb dipalmitoyl lecithin from physiologic saline has been quantified (WALLACE et al., 1975). Such lecithin treatment suppresses the cytotoxicity of both silica and kaolin to background levels (WALLACE et al., 1984).

Surfactant coated de-toxified dusts then should be phagocytised by pulmonary macrophages, incorporated into a macrophage secondary lysosome, and exposed to hydrolytic lysosomal enzymes. Among these is phospholipase A₂, which hydrolyses diacyl lecithin to lysolecithin. This was modeled by incubating lecithin treated dusts with phospholipase A₂ in vitro to determine if the enzyme can digest the dust-adsorbed lecithin, and if the retoxification differs between the two dusts in a manner which might distinguish their pathogenicity.

MATERIALS AND METHODS

The silica used was at least 98.5% pure as determined by x-ray energy spectrometric analysis and was alpha quartz as determined by x-ray diffraction. Its N₂ adsorption specific surface area was 3.97 m²/g. The kaolin used was at least 96% pure, contained no crystalline silica, and had a specific surface area of 13.25 m²/g.

SUPPRESSION OF INHALED PARTICLE CYTOTOXICITY

L- α -dipalmitoyl glycerophosphoryl choline (lecithin) (DPL) was ultrasonically dispersed in 0.165 M NaCl saline to produce an emulsion of 10 mg DPL per ml saline. Dry silica or kaolin dusts were mixed into a concentration of 7.5 mg dust per ml emulsion. Mixtures were incubated for one hour at 37°C in a shaking water bath, centrifuged for ten minutes at 990 xg, and the dusts resuspended in calcium and magnesium free phosphate buffered 0.165 M NaCl saline (PBS). This washing procedure was repeated to remove unadsorbed lecithin, the lecithin coated dusts being suspended finally in PBS.

Aliquots of native or lecithin-treated dusts in PBS with 2.0 mM CaCl₂ were incubated with Phospholipase A₂ (PLA₂), obtained from Crotalus adamanteus venom, at 37° C for one hour. The concentrations used covered a range of activities from that needed to digest from one-tenth to 1000 X the amount of kaolin-adsorbed lecithin (had the digestion been for a homogeneous phase). "Phospholipase activity" is given in terms of "activity equivalents" which are equal to .0817 units of phospholipase. Following digestion, the samples were centrifuged and the dusts resuspended in PBS containing 2.0 mM EDTA to stop the enzymatic digestion. This washing procedure was repeated, with the dusts suspended in PBS alone. All procedures were done under sterile conditions.

Suspensions of 2% by volume sheep erythrocytes and 1.0 mg native or treated dust per ml PBS were incubated in a shaking water bath at 37° C for one or two hours, as indicated, to assay the dusts' hemolytic potential (HARRINGTON et al., 1971). Samples were then centrifuged at 990 xg and the optical density for hemoglobin read at 540 μ m on a spectrophotometer. Hemolysis assays were also performed using kaolin incubated with L- α -lecithin, β palmitoyl (lysolecithin) using the lecithin treatment procedure.

THE RESPIRABLE DUST CENTER

Macrophages lavaged from male Sprague Dawley rats were mixed with native or treated dusts to produce concentrations of 2×10^6 cells per ml and one mg dust per ml. These were incubated for two hours at 37° C in a shaking water bath. Released enzyme activities were determined for lactate dehydrogenase (LDH) (REEVES and FIMIGNARI, 1963), Beta-glucuronidase (B-GLUC) (LOCKART and KENNEDY, 1976), and Beta-N-acetyl glucosaminidase (B-NAC) (SELLINGER et al., 1960). Percentages of enzymes released were calculated relative to Triton X-100 lysed samples.

Parallel samples of dusts were eluted with methanol/chloroform solvent (2:1 vol/vol) following their lecithin and phospholipase treatments. The eluted material was quantitated for lecithin and for lysolecithin by wet phosphate assay of thin layer chromatograph separated materials (BARTLETT, 1959).

Adsorption by silica and by kaolin of lecithin from physiologic saline emulsion at 37° C was measured over a range of final (unadsorbed) supernatant concentrations of 0.02 to 10.0 nanomoles per ml emulsion, as quantitated by wet phosphate assay.

RESULTS

Native quartz and kaolin dusts produce comparable high hemolysis cytotoxic response, as shown in Figure 1. On a surface area basis the two dusts were also comparable with hemolytic strengths of 22.6% for kaolin and 24.4% for silica per square decimeter dust surface area in the dispersion.

Lecithin treatment of dusts suppressed their hemolytic strengths to background levels as shown in Figure 1. This is due principally to lecithin interaction with the dust rather than with the cells (WALLACE et al., 1985). Lecithin treatment also suppresses the cytotoxicity of both silica and kaolin for pulmonary macrophages as shown in Figure 2. The kaolin and silica used in